J.R.M. Muller

A HYBRID SOLUTION FOR THE GALVESTON SEAWALL

Additional thesis

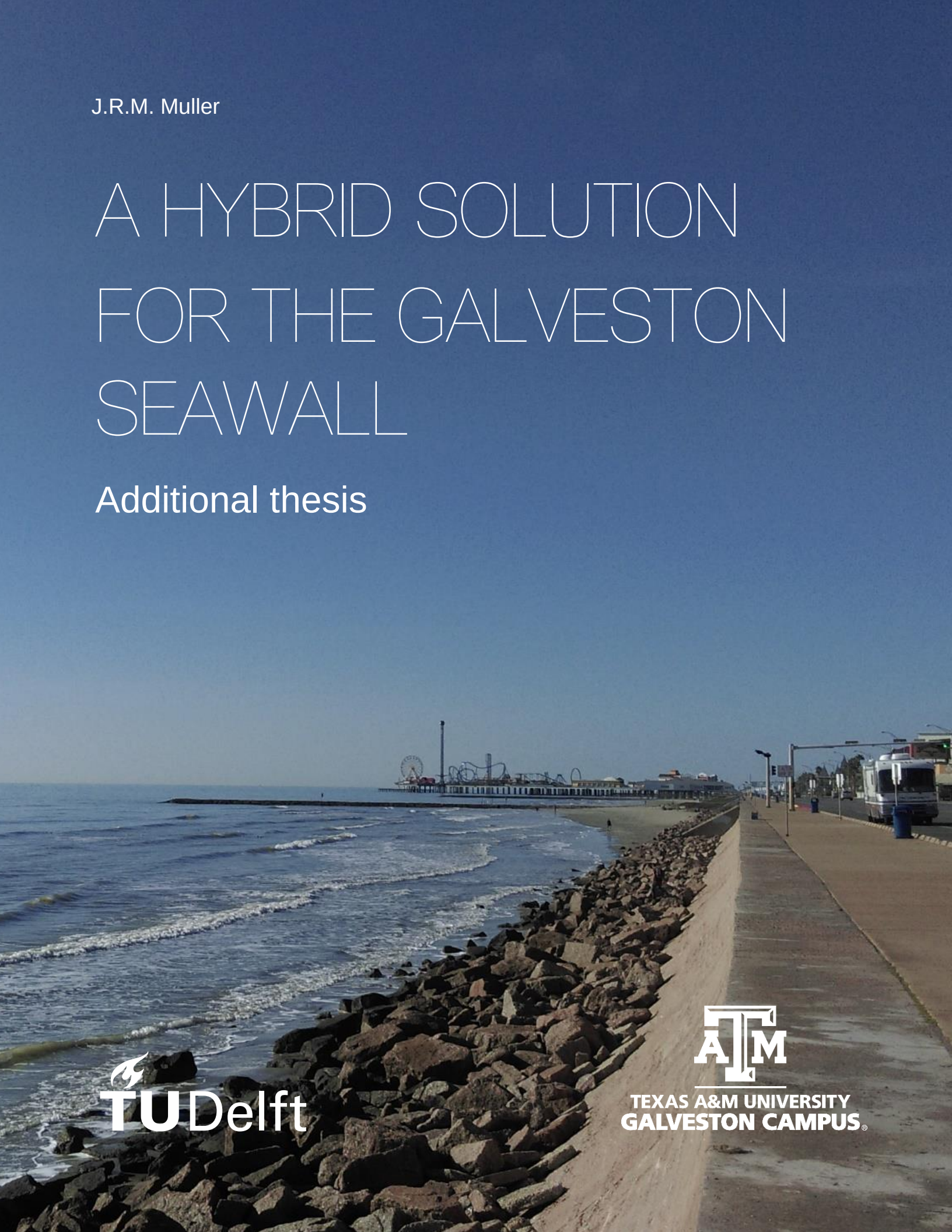

TU Delft

TEXAS A&M UNIVERSITY
GALVESTON CAMPUS

Cover picture, Seawall Blvd with The Pleasure Pier at Galveston, Texas, courtesy J.R.M. Muller

A HYBRID SOLUTION FOR THE GALVESTON SEAWALL

A STUDY ON THE REDUCTION OF THE HYDRAULIC LOADS BY A SAND COVER AT THE GALVESTON SEAWALL WITH THE USE OF XBEACH

ADITIONAL THESIS

by

J.R.M. (JOS) MULLER

Supported by:

Supervivosers | Dr. ir. S. de Vries | Delft University of Technology
Dr. J. Figlus | Texas A&M University – Galveston Campus

Software versions used:
Matlab R2015b (8.6.0.267246)
XBeach v1.22.4867 'Kingsday'
ESRI ArcMap v10.4.1.5685

An electronic version of this thesis is available at https://repository.tudelft.nl

PREFACE

This thesis was part of an elective part of my master track Coastal Engineering at Delft University. It was carried out at the Texas A&M Galveston campus and at Delft University of Technology. This project is part of a larger cooperation between DUT and several Texan Universities and institutes for improving the coastal resilience of the Upper Texas Coast and protection against several coastal and hurricane related hazards.

I would like to thank Dr. Jens Figlus for his hospitality and for all the support I received. There was always time to talk about the course of the research as well as informal talks. I also would like to thank Juan Horrillo for his help in setting up the model and making use of the multi-core computer. I want to thank my colleagues Andrew, Jacob, Katherine, Tariq, Yoon and the people of the research group for all their help.

I also like to thank my parents and all the people who made my stay in Texas really memorable.

ABSTRACT

The Greater Houston Metropolitan Area (GHMA) is located on the Gulf of Mexico coast of the United States and encompasses the city of Houston, Galveston Bay and its six surrounding counties, several ports, as well as the City of Galveston, located on the barrier island of Galveston. The GHMA is of great economic and ecological importance, but is frequently facing threats of hurricanes and accompanying flooding, surge, and wave impact. The City of Galveston is protected from extreme storm impact by a 17-km concrete seawall facing the GoM.

Recent investigations have shown that the seawall may not be sufficient any more to protect against a 1 in 100 year design storm (Jonkman et al., 2015). Since raising the seawall disconnects the city from the beach and may be very costly, a hybrid approach is being discussed in which the existing hard structure is covered by a dune. During storm conditions, the dune that fronts and covers the structure erodes, potentially exposing the seawall. In that process, however, the sand material serves as an extra protection. However, the soft cover contribution to the level of protection is unclear and no design standards for such hybrid solutions exist. This numerical model study investigates the hydro- and morphodynamic effects of adding a sand cover to the Galveston seawall under extreme storm conditions.

A total of 33 different conceptual designs were conceived, that differ in beach height, beach length, dune width and dune slope. Also the shape of the seawall itself was adapted to check for the influence of the core structure. These designs were simulated with a 2DH process-based model, XBeach (Roelvink et al., 2009). This model was developed to simulate storm impacts on coastal morphology. The model set-up was validated by simulating Hurricane Ike at different sections of Galveston Island. The validated set-up was used for the hybrid simulations with an alongshore uniform bathymetry and a synthetic 1 in 100 design storm. The starting position was to keep the current elevation of the Galveston Seawall as low as possible. The variables of interest of each run consisted of the wave induced set-up and the wave height at the breaking point closest to shore.

The validation runs showed satisfactory model performance related to Hurricane Ike impact on island morphology. Erosion volumes were slightly overpredicted, due to simplifications such as not including vegetation and non-erodible surfaces. The results of the simulations showed an overall correlation between the maxima in set-up and wave height in the surf zone close to shore, which was influenced by the dimensions of the sand cover. In general, a larger volume of sand in front of the seawall results in a lower wave height close to shore. This causes a change in the bed level and a modification of the surf zone width. Therefore, the dissipation of energy in the surf zone is more concentrated compared to the situation with no additional sediment, increasing the local wave-induced set-up. This effect can reach to a 40% decrease in wave height in the surf zone and an increase up to 25% in set-up, in comparison to no sand cover. Furthermore, the influence of the slope of the wall was investigated. Several simulations were done with a sloped non-erodible seawall in combination with a sand cover. The results showed a lower wave height in the surf zone close to shore without increasing the local wave-induced set-up. Due the sloped seawall, less scouring occurs at the tow of the structure. Therefore, the local water depth and wave height is smaller. This decreases the bed level change and therefore limits the increase of wind-induced set-up.

This study gave a first insight in the reduction of the hydrodynamic loads due to a sand cover over a seawall. The usage of XBeach for these hybrid cases showed reliable results, without extensive preparations. In order to rehabilitate the Galveston Seawall to provide sufficient protection, a sand cover can have a beneficial effect. Adapting the current seawall into a more conventional sea dike showed to be an effective measure as well. However, the feasibility of applying a hybrid solution has to be researched in more depth. The erosion of dune material during a storm event could result in this type of hybrid coastal protection to be too costly to maintain.

LIST OF ACRONYMS

GSW	Galveston Seawall
DEM	Digital Elevation Model
GHMA	Greater Houston Metropolitan Area
GPS	Global Positioning System
JONSWAP	JOint North Sea WAve Project, a common method of characterizing ocean wave spectra
LAS	LASer, common extension for point cloud data
LATEX	Louisiana and Northern Texas
LiDAR	Light Detection And Ranging of Laser Imaging Detection And Ranging
MHW	Mean High Water
MLW	Mean Low Water
Morfac	Morphological Factor, feature in XBeach to allow for reducing the computational time.
MSL	Mean Sea Level
NAVD88	North American Vertical Datum of 1988
NDBC	National Data Buoy Center
NGS	National Geodetic Survey
NOAA	National Oceanic and Atmospheric Administration
NOS	National Ocean Service
USACE	United States Army Corps of Engineers
USD	United States Dollars
USGS	United States Geological Survey
UTC	Coordinated Universal Time, universal time standard.
WGS84	World Geodetic System 1984

NOMENCLATURE

Δ	Difference operator	[-]
θ	Angle of incidence w.r.t. x	[rad]
ρ	Density of water	[kg·m^{-3}]
γ	Breaking parameter	[-]
ξ	Iribarren number	[-]
η	Surface elevation above still water level	[m]
h_0	Still water level	[m]
h_b	Water depth at breaking	[m]
E	Wave Energy	[J·m^{-2}·s^{-2}]
c_g	Wave group velocity	[m·s^{-1}]
D	Dissipation term for wave energy	[W·m^{-2}]
d	Water depth	[m]
F_x	x-directed wave-induced force	[N·m^{-2}]
g	Gravitational accaleration constant	[m·s^{-2}]
H	Waveheigth	[m]
h	Water level	[m]
H_b	Wave height at breaking	[m]
$H_{b,max}$	Maximum wave height at breaking	[m]
H_{rms}	Root mean square wave height	[m]
H_s	Significant wave height	[m]
L	Wave length	[m]
n	Wave group to the phase celerity ratio	[-]
p_{wave}	Wave-induced pressure	[N·m^{-2}]
S	Source term for waves energy	[W·m^{-2}]
S_{xx}	x-directed momentum flux in the x-direction	[N·m^{-1}]
S_{xy}	x-directed momentum flux in the y-direction	[N·m^{-1}]
t	Time	[s]

u_x	Flow velocity in x-direction	[m·s^{-1}]
x	Cross-shore axis coordinate	[m]
y	Long-shore axis coordinate	[m]
z	Vertical axis coordinate	[m]

TABLE OF CONTENTS

1. INTRODUCTION

1.1. BACKGROUND

The South coast of the United States of America on the Gulf of Mexico is characterized by a system of bays, mud lands, barrier islands and estuaries. One of these systems is the Galveston Bay, located along the upper coast of Texas and south of Houston. This area is known as the Greater Houston Metropolitan Area (GHMA). With a total population of 6.6 million people and a growth of 159.000 people in 2015, it is the fifth largest metropolitan area in the United States (Greater Houston Partnership, 2016). Its economy is mainly driven by the petrochemical and the energy industries and the Galveston Bay houses one of the nation's most important shipping hubs. Together this makes it the 4th biggest economic metropolitan area in the nation (Bureau of Economic Analysis, 2016).(Paine et al., 2012)(Paine, Mathew, and Caudle 2012)(Paine, Mathew, & Caudle, 2012)

Due to its location on the Gulf of Mexico, this area is at significant risk from hurricane-induced flooding. In September 2008, Hurricane Ike crossed the Gulf, hitting The Bahamas, Haiti, Cuba and the United States. When Ike made landfall at Galveston, it had an intensity of a Category 2 hurricane, causing 21 fatalities and a significant damage that is estimated around 29.5 billion USD in Texas, Louisiana, and Arkansas. This makes Ike the second costliest hurricane to affect the United States (Berg, 2009).

In order to prevent these kind of impacts on the GHMA, multiple designs were made to protect the coastal areas and the ports (SSPEED Center, 2015). One of these designs is the proposition of a 'coastal spine' that encloses the entire bay with a barrier, also called the 'Ike Dike' (Merrell, 2010; Merrell and Whalin, 2013). The principle of this design is to prevent or limit the amount of surge that flows into the bay. The overall coastline of the bay is shortened with a combination of movable gates in the channels and land barriers on the barrier islands (Jonkman et al., 2015). The design of the land barrier will have to be integrated into the existing spatial outline on the barrier islands. The most varying land use is present on Bolivar Peninsular and Galveston Island, with the city of Galveston as its the main urban area. A selection of these measures is shown in Figure 1.1.1.

The first development of the city that is now Galveston dates back to 1816, as a simple base of operations for the support of the rebellion of Mexico against the Spanish Empire. At the end of the 19th century, the city served, next to Ellis Island, New York as the second most important entry point for immigrants to the US. It was also one of the important centers of trade in the country. Nowadays, the economy of Galveston is mostly driven by its port and tourism. With an impact of 808 million USD in 2007, it has been acknowledged that the beaches and the tourism industry at the coastline are the important economical drivers for the city (Angelou Economics, 2008). Moreover these beaches form a vital part of the ecological system that is the Galveston Bay (Williams et al., 2009).

In 1900, the city was hit by the most devastating hurricane to date, whipping out big parts of the city and causing approximately 6.000 to 12.000 fatalities. After this event the city council decided to protect the city by constructing a seawall. The Galveston Seawall (GSW) consists of a concrete structure of 17 feet (5 meters) high and was backfilled with sand, creating a gentle slope (U.S. Army Corps of Engineers, 1981).

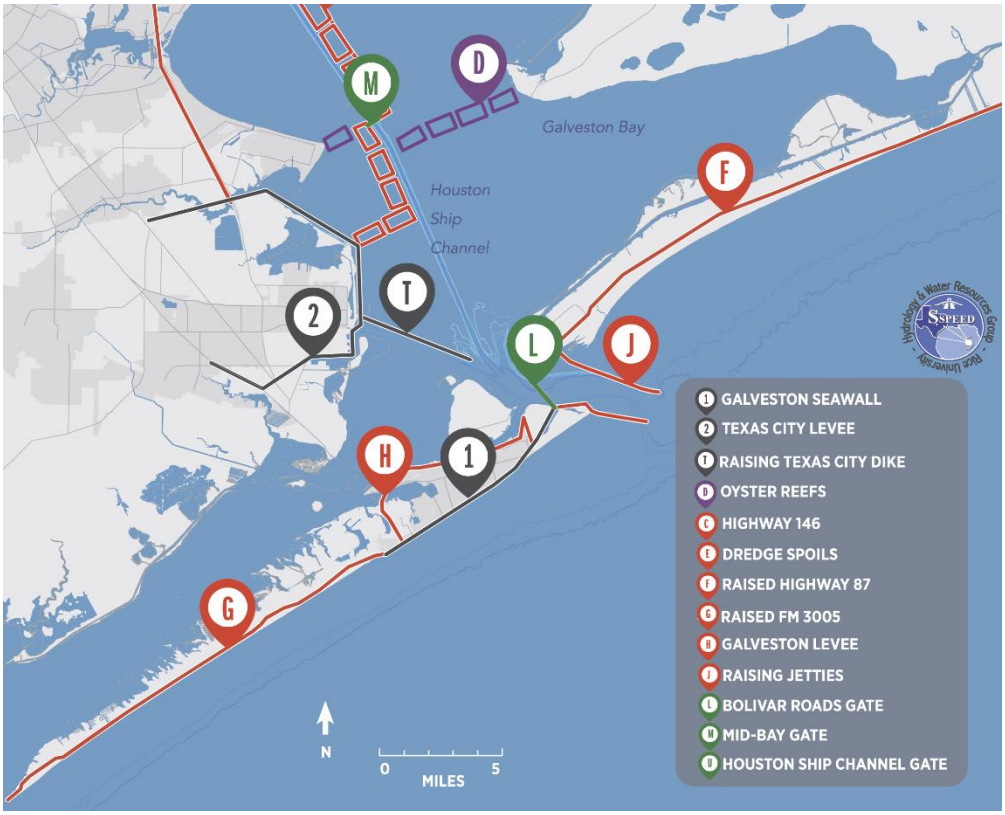

FIGURE 1.1.1. SELECTION OF MEASURES IN THE GALVESTON BAY, ADAPTED FROM SSPEED CENTER 2015

1.2. PROBLEM DESCRIPTION

The Galveston Seawall (GSW) is incorporated in all of the proposed strategies for the coastal protection of the Galveston Bay. However, it is not clear if the seawall is still sufficient to protect the city of Galveston with its current elevation.

The GSW can be strengthened with different options (van Berchum et al., 2016). One of the investigated options are to heighten the current design or reconstructing the GSW into a coastal sea dike. However these options are costly and disconnects the community of Galveston from the beach. Since it has been acknowledged that the beaches play a vital role for the city and its community, raising the seawall is not preferable. A more integrated, 'soft' intervention could offer a solution. By applying the concepts of building with nature, another option would be a so called 'levee-in-dune' or 'dike-in-dune' in which the current seawall is incorporated into a large dune. Big amounts of sediment are placed over the structure, making it a hard structure within a dune as constructed in the Netherlands on multiple locations (Arcadis, 2013, 2008). This hybrid solution creates a natural connection between the beach and the city

However, there is not much known about the physical interaction of a hard structure and a soft cover during a storm. Flume tests and additional research are carried out to examine the processes that occur during a storm and to correlate the strength to different parts of the hybrid (Almarshed, unpublished; Taqi, unpublished; West, 2014). In order to check if a hybrid is a feasible solution for the GSW, the interaction of the sand cover and the seawall with its concave up contour, have to be examined. Since the GSW already exits, the main uncertainty is the effectiveness and related limitations of the sand cover on improving the current level of protection.

1.3. OBJECTIVE

The objective of this research is to gain better understanding on the impact of a hybrid structure with various dimensions for the Galveston Seawall on the reduction of the hydraulic loads during a storm. This will be done with the use of a process-based numerical model and validation with relevant literature.

The secondary objective is to start with the simulation of the complete Galveston Island during hurricane Ike as a starting point for further model efforts for Galveston. (Figlus, 2016).

1.4. RESEARCH QUESTION

In the previous sections an insight in the situation of the Galveston Seawall was given. For the first objective the following research question is formulated:

WHAT IS THE IMPACT OF A HYBRID ON THE HYDRODYNAMIC PROCESSES AT THE GALVESTON SEAWALL?

Within this question the following sub question have been defined:

1. *WHICH HYDRAULIC PROCESSES ARE SIGNIFICANT FOR TESTING THE HYBRID DESIGNS ?*
2. *WHAT IS THE RELATION BETWEEN THE HYBRID STRUCTURE AND THE HYDRAULIC PROCESSES?*
3. *IN WHAT WAY DOES THE DIMENSIONS OF THE SAND COVER INFLUENCE THE HYDRAULIC PROCESSES?*
4. *IN WHAT WAY DOES THE SHAPE OF THE SEAWALL INFLUENCE THE HYDRAULIC PROCESSES?*

1.5. APPROACH AND OUTLINE

The objectives of this research are divided over this report. The main objective is the investigation of the impact of the various hybrid designs, however, in order to asses this a validated model is required. This model set-up and validation is also the secondary objective. Therefore this part is stated in the Appendix D. The report itself focuses itself on the first objective.

First, a literature review will be carried out to examine which processes are of importance for testing the hybrid designs. Additionally, the principles of a hybrid solution and applications in the Netherlands are elaborated. The findings of this literature review can be found in Chapter 2.

Prior to the simulations of the hybrid designs, a data analysis has to be performed and the reliability of the model needs to be validated. This will be done by using Hurricane Ike and comparing the modeled and measured response of Galveston Island during this event. When the model shows reliable results of modeling the erosion of the beach during a hurricane, the hybrid designs can be simulated with a sense of accuracy. This data analysis and validation of the model is needed to address the main research question, but also fulfils the secondary objective of this report. The full elaboration and validation can be found in Appendix D.

The next stage consist of the study on different hybrid designs. A design storm with an appropriate return period is formed based on earlier work. This design storm will be used for all the runs. A first set of hybrid designs with various dimensions are simulated using the validated model. After evaluating the results from each run, a new generation of hybrid designs is composed to look into a specific observed behavior, as displayed in Figure 1.5.1. The methodology of the simulations can be found in Chapter 3.

The end result is a data set with results per hybrid variant. This data will be validated with the earlier found theoretical formulations as reference. The results can be found in Chapter 4.

The found results are then examined for trends or general behavior. This discussion is stated in Chapter 5. Finally the first objective will be fulfilled by answering the corresponding research questions with the findings from the discussion. These conclusions can be found in Chapter 6. In Chapter 7, recommendations for further work are given.

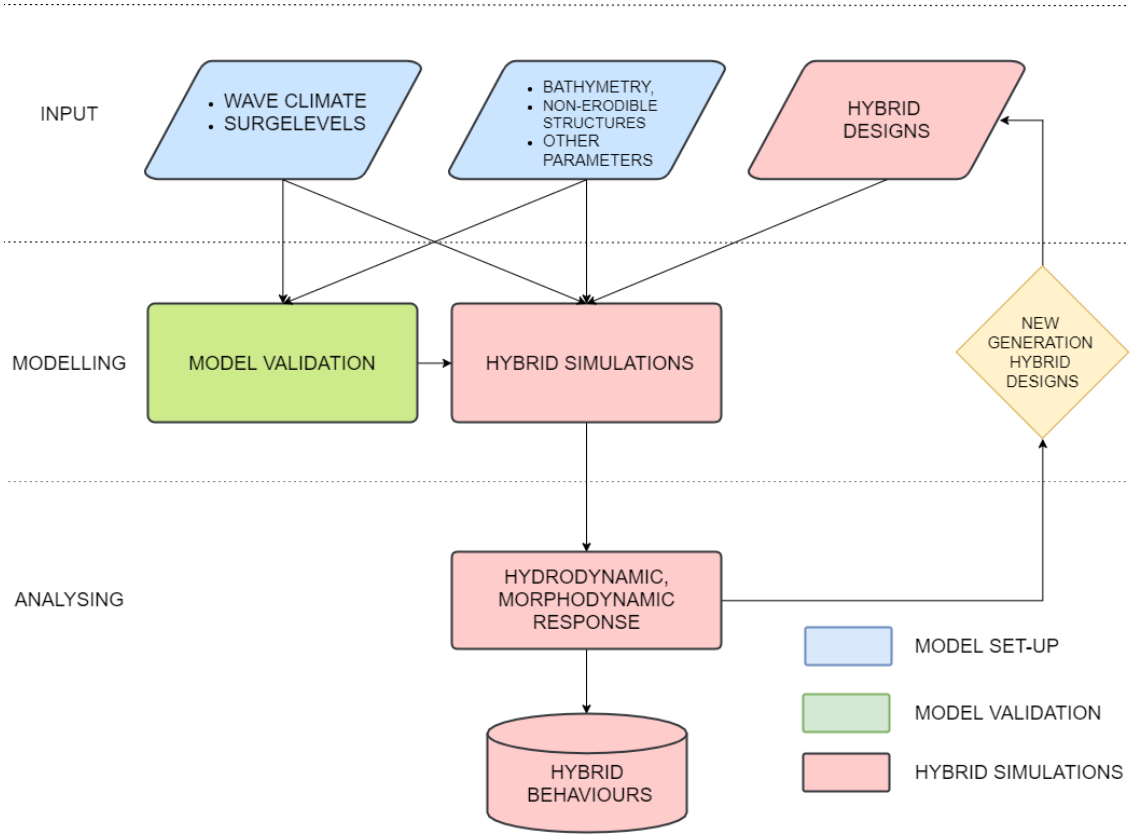

FIGURE 1.5.1. FLOWCHART OF THE PROCESS OF THE HYBRID DESIGNS SIMULATIONS

2. LITERATURE REVIEW

2.1. COASTAL TERMINOLOGY

In the following chapters use will be made of different terminology to specify specific regions or processes within the coastal zone. To clarify this, an overview of some coastal terminology is given in this section and are shown in Figure 2.1.1.

The coastal area in front of Galveston is characterized by relatively narrow and very shallow beaches and nearshores, typically to 20 m deep (Sass, 2011). After the hurricane of 1900, the city of Galveston was raised and the Galveston Seawall was build. The beach in front of the seawall can be divided into two regions; the foreshore and the backshore. The foreshore is the part of the beach that lays under the Mean Sea Level and the backshore lays above this level.

In front of the beach lays the nearshore to the depth of closure, which is the depth at which sediment particles are not picked up anymore and are not part of the active sediment transport. In the nearshore region, waves tend to become more high and steep until they break in the breaker zone. After that the waves decreasingly become smaller in the surf zone. The remaining wave energy can generate run-up or run-down in the swash zone. During storm conditions, these regions and processes can shift.

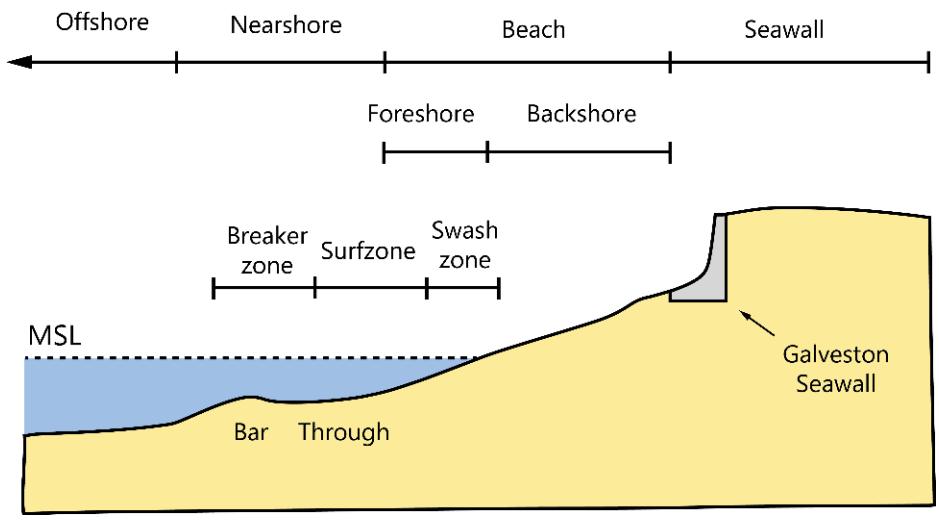

FIGURE 2.1.1: COASTAL REGIONS AND TERMINOLOGY FOR THE GSW, ADAPTED FROM NEDERHOFF, 2014

2.2. HYBRID COASTAL PROTECTION

CONCEPT The last decade, several studies have been carried out on alternative ways of protection coastal regions. It showed that in multiple occasions, natural infrastructure or a combination with existing structures provides not only protection against coastal flooding hazards, but also ecological benefits (Sutton-Grier et al., 2015). The combinations of these two approaches is called a hybrid coastal protection. An existing infrastructure, such as a levee or seawall are combined with more natural coastal systems such as dunes, mangroves, marches, oyster reefs and others. These natural systems not only serve a social and environmental value, but also increases the resilience of the coastal protection. During normal conditions the natural system, such as a salt water march, dune ridge or mangrove thrive and offer a natural habitat for flora and fauna. However, wave action that is being generated in the coastal areas is reduced in these regions. During a storm condition, these reductions are not strong enough, therefore a hard engineered solution serves as the main surge barrier. The natural system, however, is capable of reduction part of the energy during the peak of the storm and therefore reducing the load on the hard solution/ This makes it possible to reduce the dimensions of the hard structure in comparison with a standalone hard solution. However, since both systems have their own behaviors during storm and normal conditions, the behavior of the combination of the two structures is not clear.

Examples of hybrid structures are applied at various places over the world. One of these locations is at the Dutch coastline. After the identification of so called 'weak links' in 2003, the Dutch government and Rijkswaterstaat issued a set of rehabilitations of the primary coastal protection structures (Ministerie van Verkeer en Waterstaat, 2003). These included sea dikes, dunes and other primary surge barriers. A good example of the application of hybrid solutions are at the communities of Katwijk, Noordwijk and Scheveningen, where the integration of the new protection came across opposition of local stakeholders. The main concern was the disconnection with the beach due to the new structures. In collaboration with these local parties a hybrid solution was designed that consisted of a primary sea dike that protected the communities at risk, while a sand cover formed a 'natural' dune on top of the structure. The latter created an open connection with the beach and allowed for recreation and commerce to thrive (Arcadis, 2013, 2008). The main reasoning for the application of a hybrid solution was in these cases mostly for esthetic purposes.

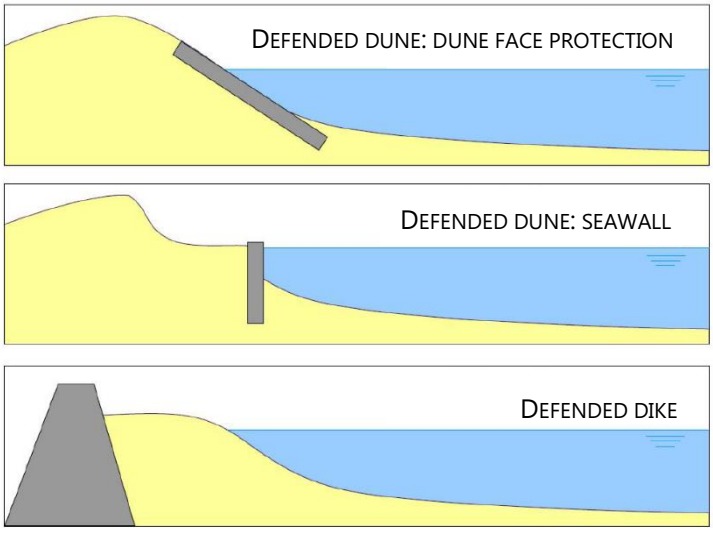

FIGURE 2.2.1. HYBRID EXAMPLES, ADAPTED FROM DELTARES, 2012

ASSESSMENT OF A HYBRID As mentioned, it is hard to assess the combination of hard structure, such as a dike or seawall with a dune covering, since both systems have their own behavior and failure mechanisms. This hybrid structure incorporate both behaviors in one system. Studies have been carried out to prescribe strategies to assess the safety of such hybrid solutions (Deltares, 2012). In these guidelines, distinction is made between two kind of hybrids for coastal protection, namely a **defended dike** or a **defended dune**, as depicted in Figure 2.2.1. The defended dune incorporates a hard structure, such as a seawall or dune face revetment, that protects the dune ridge that lies behind it. The defended dike is a hard structure such as a dike that is protected by a sand nourishment that lays on top of it.

Several methods for the assessment of the required safety of a hybrid surge barrier are described. In case of the defended dike, the safety of the hybrid can be separated for the hard structure and the dune cover that lies in front. The hard structure is regarded the same as in a solution that solely uses a hard structure. Therefore the assessment of the failure mechanisms is done with use specific defined standards and methods for dikes. The safety assessment of the dune cover that lies in on top of it, mainly focuses on determining the amount of erosion with regard for the stability of the inner hard structure, as depicted in Figure 2.2.2. However during the erosion of the dune, this volume deposited in the nearshore. This on its turn has an impact on the waves as they will be reduced by the sand in front of the barrier. There is no direct formulation that gives an relation between this cover and the reduction of the wave height. Hence the current guidelines prescribe a custom assessment for overtopping and erosion rates for each specific case.

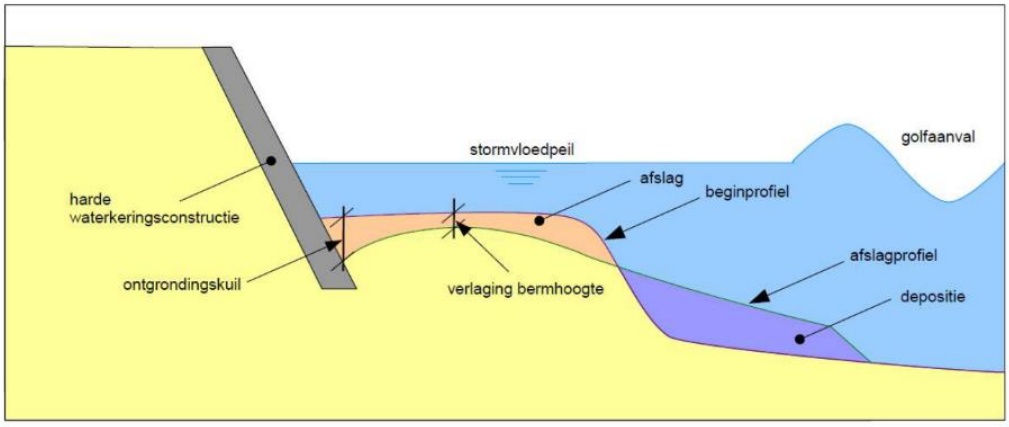

FIGURE 2.2.2. TESTING SCHEMATIC ACCORDING TO THE GUIDELINES. THE SAFETY OF THE HARD INNER CORE (SHOWN AS A GREY SLOPE), IS DONE WITH USE OF SPECIFIC SAFETY ASSESSMENTS THAT ARE DEFINED FOR SEA DIKES. THE METHOD OF DETERMINING THE SAFETY OF THE DUNE IN FRONT OF THE HARD STRUCTURE MAINLY DEALS WITH EROSION AND ACCRETION OF THE SAND VOLUME DURING A STORM, AS THIS MAY CAUSE INSTABILITY OF THE HARD STRUCTURE (DELTARES, 2012).

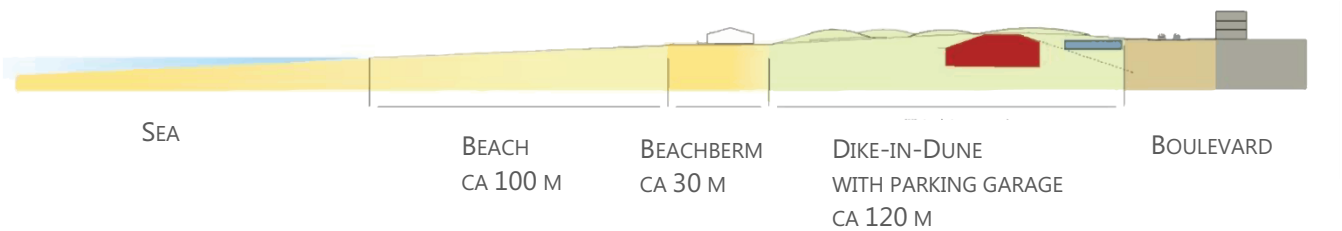

FIGURE 2.2.3. CROSS SECTION OF THE HYBRID DESIGN AT KATWIJK. IN THIS CASE A DIKE WAS CONSTRUCTED IN FRONT OF THE CITY OF KATWIJK. IN ORDER TO KEEP KATWIJK CONNECTED TO THE COAST, A DUNE IS PLACED OVER THE STRUCTURE AND CONNECTS WITH THE BEACH. THE DESIGN ALLOWED FOR A PARKING GARAGE BEING INTEGRATED BEHIND THE DIKE (ADAPTED FROM ARCADIS, 2013).

REFERENCE CASE As a reference, the construction of a hybrid in front of the city of Katwijk, the Netherlands can be observed. The design of the hybrid coastal protection in the cases at Katwijk or Scheveningen is based on the collaboration between a sand cover in the form of a dune and a hard core that is a sea dike. During a storm, the dune cover can be eroded away, exposing the sea dike. The dike is designed as the main surge barrier during the peak of the storm. However, the sand volume that is deposited in front of the dike, reduces the wave energy as it propagates towards the shore. The remaining wave energy is then finally countered by the dike and the revetment. The sand cover is designed in such a way that the maximum rate of overtopping is 1 l/s/m. These rates and the overall safety is assessed with the use of an custom made test/model. (Arcadis, 2013). It must be mentioned that the application of a hybrid at Katwijk and Schevingen is chosen mainly for social and environmental motivations. By covering the main surge barrier with a vast volume of dune ridges, a natural connection with the beach and the communities that lie behind these barriers. Also the design allowed for non-protective structures such as a underground parking garage to be integrated behind the dike. The design of the hybrid at Katwijk can be seen in Figure 2.2.3 and Figure 2.2.4.

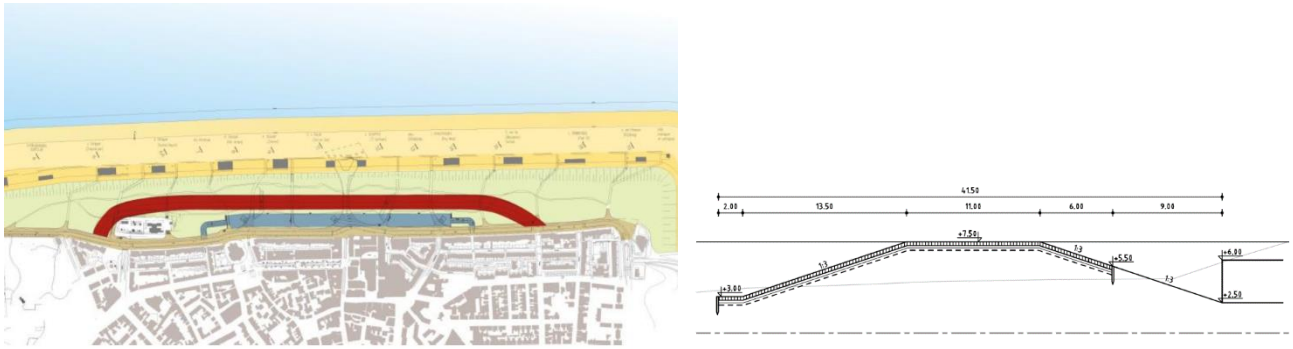

FIGURE 2.2.4. DIKE DESIGN IN THE HYBRID SOLUTION OF PROJECT KATWIJK. THE LEFT PANEL SHOWS THE COURSE OF THE DIKE, ENCIRCLING THE CITY OF KATWIJK. THE RIGHT PANEL SHOWS A CROSS-SECTION OF THE SHAPE OF THE DIKE, RESEMBLING THE DESIGN OF A REGULAR SEA DIKE WITHOUT BERM. (ARCADIS, 2013)

In comparison with the option of applying a hybrid at Galveston, the GSW could form the basis for a hybrid design as the non-erodible structure. However, the seawall is a vertical wall, where as in reality, most of the hybrid designs have a dike with revetment as non-erodible core. As was found, the main function of the hybrids core is to counter the peak of the storm. As these two cores will become exposed during a storm, the reaction will be different. The dike core design consist of a slope with revetment, which is quite effective at dissipating the remaining wave energy. The seawall core design consists of a vertical wall and reflects all the wave energy once it becomes exposed. This implies that large amounts of overtopping can occur compared to a sea dike. Also due to the large turbulent motions, strong scour will occur at the tow of the seawall. (Van der Meer et al., 2016)

2.3. WAVE SETUP, WAVE HEIGTH AND WAVE BREAKING

The application of a sand cover on top of the existing seawall implicates a change of the profile of the beach and to some extend the nearshore. This has an effect on the hydrodynamics that occur in these regions. For testing the impact of different hybrid designs only some of the relevant processes will be treated. In the following paragraphs phenomena such as shoaling and breaking of waves propagating towards the shore, the energy balance, radiation stress and wave induced setup will be discussed.

2.3.1. WAVE ENERGY AND RADIATION STRESSES

Typically short waves are generated due to the energy transfer from wind onto the oceans. This influx of energy can be described by the energy conservation equation:

$$\frac{\partial E}{\partial t} + \frac{\partial}{\partial x}\left(Ec_g cos\theta\right) + \frac{\partial}{\partial y}\left(Ec_g cos\theta\right) = S - D \tag{2.1}$$

Here c_g is the velocity of the wave group, θ is the wave direction with respect to the x-axis (normal to shore), S is the generation term, such as wind energy transferred to the water surface and D the dissipation term, such as bed friction or roller dissipation. E is the total wave energy: $E = 1/8\rho g {H_{rms}}^2$. This balance only holds for a narrow banded spectrum. For this research only normal incident waves are considered, making $\theta = 0$.

The radiation stress is the wave-averaged flux of momentum due to waves. This flux consists of two terms regarded from a plane vertical perpendicular to the wave propagation, as shown in Figure 2.3.1:

- the transfer of momentum ρu_x, through the plane with the particle velocity.
- the wave-induced pressure force acting on the plane due to the wave-induced pressure, p_{wave} in the water.

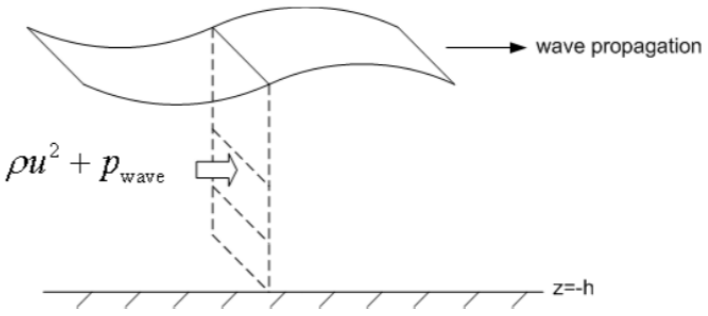

FIGURE 2.3.1. DEFINITION OF THE MOMENTUM FLUX THROUGH A VERTICAL PLANE PERPENDICULAR TO THE WAVE PROPAGATION (BOSBOOM AND STIVE, 2015)

These momentum fluxes behave as a tensor and can be divided into normal and shear stresses. By integrating these fluxes over the depth of the water column and averaging over time, the total wave-averaged transport of x-momentum in the x-direction is obtained. This term is the normal radiation stress S_{xx}.

$$S_{xx} = \overline{\int_{-h_0}^{\eta} (\rho u_x) u_x dz} + \overline{\int_{-h_0}^{\eta} p_{wave} dz} \tag{2.2}$$

The advective and pressure parts of this stress can be expressed in terms of the wave energy E with use of linear wave theory (Holthuijsen, 2010). The full derivation has been left out of this report. The radiation stress in the direction which the wave propagates, is equal to:

$$S_{xx} = \left(n - {}^{1}/_{2}\right)E + n\cos^2\theta\, E \tag{2.3}$$

The first term relates to the pressure part, the second term relates to the advection by the horizontal particle velocity. In this case only normal incident waves are considered, which means the waves are all propagating in the positive x-direction ($\theta = 0$) . Eq. 2.3 then reduces to:

$$S_{xx} = \left(2n - {}^{1}/_{2}\right)E \tag{2.4}$$

From this it can be seen that in deep water regimes, where $n = ½$, the radiation stress in the wave propagation direction S_{xx} becomes $½E$. When waves propagate into shallower waters, n becomes 1 and this term becomes $S_{xx} = 3/2\, E$. When waves travel into to surf zone, they will tend to break and energy will be dissipated by surface rollers and other dissipation terms.

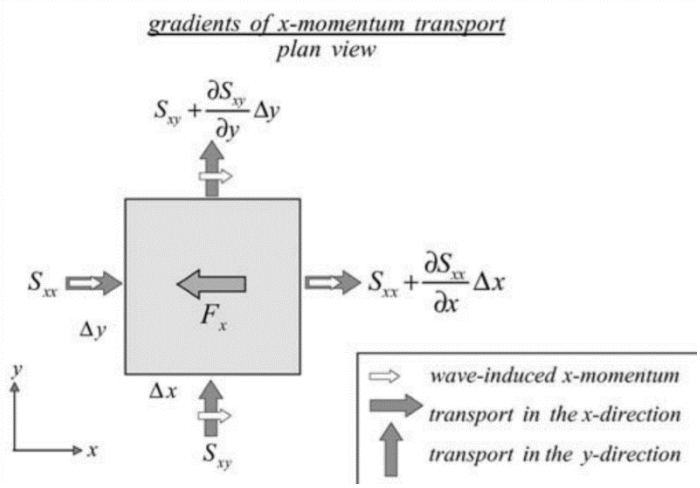

FIGURE 2.3.2. GRADIENTS OF THE WAVE-INDUCED X-MOMENTUM, S_{XX} AND THE WAVE FORCE IN OPPOSITE DIRECTION (HOLTHUIJSEN, 2010)

The radiation stress is determined through a vertical plane perpendicular to the wave propagation, namely the x-direction. If these radiation stresses increase over this direction, e.g. a positive horizontal gradient, a wave induced force is the result. The total force in this x-direction is given as:

$$F_x = -\left(\frac{\partial S_{xx}}{\partial x} + \frac{\partial S_{xy}}{\partial y}\right) \tag{2.5}$$

In this case an alongshore uniform coast is considered and thus the shear terms $\frac{\partial Sxy}{\partial y} = 0$. Therefore the wave-induced force only consists of $F_x = -\left(\frac{\partial S_{xx}}{\partial x}\right)$, as shown in Figure 2.3.2. Variations in wave force can occur due to the change of the wave group number n, the wave energy E or the angle of incidence θ. When waves propagate through deep water, not much deformation or energy transfer takes place. Therefore the wave forces are also low. When these waves propagate towards the nearshore, large wave forces are generated due to big gradients in the bed level and thus the wave energy E, n and the wave direction. It can be translated as a positive gradient of $\partial S_{xx}/\partial x$ and a offshore directed wave force in the shoaling zone. In the surf zone, the deformation of the waves due to breaking and thus the energy dissipation leads to a negative gradient in $\partial S_{xx}/\partial x$ and a net onshore directed wave force. In later section these forces will be discussed further and their role in wave-induced set-up and set-down.

2.3.2. WAVE BREAKING

As waves propagate into intermediate and shallow depths, the celerity of the waves will be affected. Since the energy balance still holds, the wave height will increase, up to the point energy is dissipated due to wave breaking. This is called depth-induced breaking. When the shoaled waves propagate into more shallower water, the water depth will decrease and the wave height will increase. The particles in a wave crest in shallow water have a ellipse shaped orbit; meaning the horizontal axis of the orbit is longer than the vertical axis, as shown in Figure 2.3.3. When a wave shoals, the wave height grows and so does the vertical motion of the particles in the orbit. The horizontal axis subsequently grows in a same manner, meaning the horizontal velocities also increase. This process continues unto the point that the horizontal velocities exceeds the actual wave celerity. This means that water particles in the top of the water column will exceed the wave and the shape of the wave crest will fall apart; the wave starts to break. It is clear that in this state the wave energy is not preserved in the wave anymore, but also in the wave bore that has formed. This can be described as wave energy be converted into roller energy or wave energy being dissipated. Since the wave energy is dissipated, a gradient develop in the radiation stress or momentum flux under the wave crest. Therefore a wave force is being generated when waves are breaking.

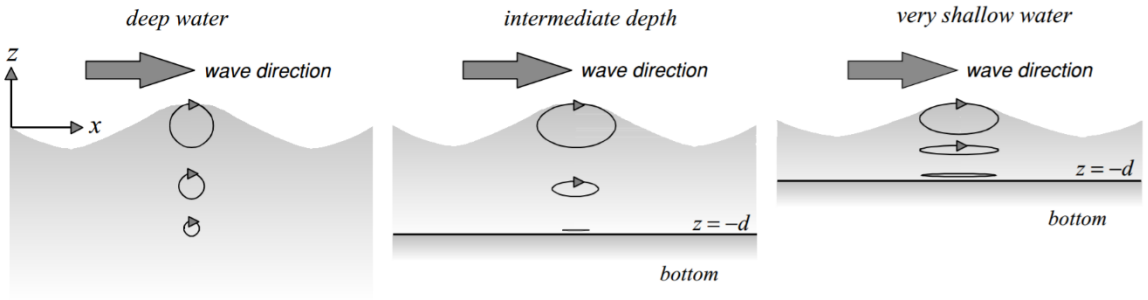

FIGURE 2.3.3. ORBITAL MOTION OF A WATER PARTICLE IN DEEP AND SHALLOW WATER CONDITIONS. WHEN WAVES ARE SHOALING THEY TYPICALLY ARE SITUATED IN THE SHALLOW WATER REGIME (HOLTHUIJSEN, 2010)

Based on the Stokes wave theory, Miche formed a criterion relating wave length to the wave steepness. In shallow waters this reads:

$$\left(\frac{H}{L}\right)_{max} = 0.142\frac{2\pi h}{L} \approx 0.88\frac{h}{L} \tag{2.6}$$

This expression can also be directly be related to the breaking wave height as follows:

$$\gamma = \left(\frac{H_b}{h_b}\right) \approx 0.88 \tag{2.7}$$

With γ the breaker index, H_b is the breaking wave height and h_b is the water depth at the breaking point. These derivations were made for a horizontal bed. Maximum values were found with $\left(\frac{H_b}{h_b}\right)_{max} \approx 0.9$ (Sorensen, 2006).

However in reality, coastal areas have a sloping bed. This has an effect on the breaker index and the process how wave break on shores (Weggel, 1973). Battjes showed that this process is described by the Iribarren number ξ (Battjes, 1974). The Iribarren number is the ratio between the steepness of the beach slope and the steepness of the wave. Breaking waves can be divided into certain types of breaking, based on the Iribarren number. These distinctions are surging, collapsing, plunging and spilling waves, as shown in Figure 2.3.4.

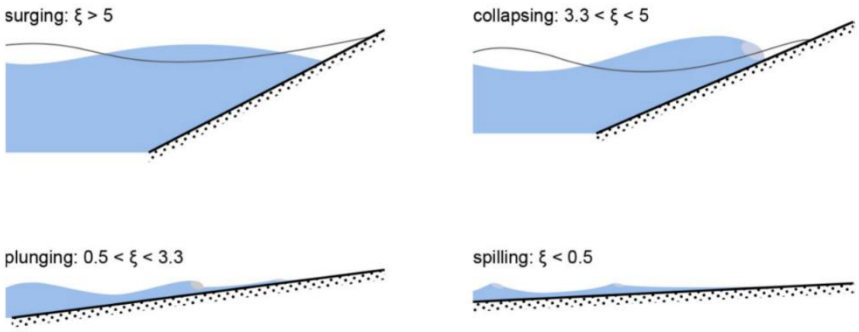

FIGURE 2.3.4: BREAKER TYPES (BOSBOOM AND STIVE, 2015)

Experimental research has shown that the breaking of waves needs time. Hence on a steeper slope, a wave will break at smaller water depths. This means that the breaker index γ depends on the bottom slope of the beach. (Tsai et al., 2005). The breaker index is therefore depended on the Iribarren number. For a horizontal bed the breaker index is around 0.8 (Miche criterion), for spilling breakers 0.6-0.8 to 0.8-1.2 for plunging breakers (Bosboom and Stive, 2015). To account the influence of the bottom slope on the breaker index, adaptations of the Miche equation have been made (Battjes and Janssen, 1978).

2.3.3. WAVE SETUP

As waves travel towards the shore, the water depth decreases. Therefore, the radiation stress increases and the wave force F_x is directed seaward and decreases. This imbalance of forces on the water column is countered by a gradient in the still water level, with a lower water level at the shore side. This negative water level gradient is also referred to as wave-induced set-down and is shown in Figure 2.3.5. This process continues up to the breaker zone.

In the breaker zone, the waves break by the depth, resulting in a negative gradient in the radiation stress. This decrease of the radiation stress is stronger than the, earlier discussed, increase of the radiation stress due to the continuous decrease of the water depth. The wave force is then positive directed towards the shore. As a response, a positive water level gradient is generated to balance this force. This positive gradient in the still water level is called a wave-induced set-up and is shown in Figure 2.3.5.

The wave-induced set-up is therefore thus related to the wave force. This dependency is given in Eq. 2.8 and Eq. 2.9.

$$F_x = -\frac{\partial S_{xx}}{\partial x} = \rho g h \frac{\partial \bar{\eta}}{\partial x} = \rho g (h_0 + \bar{\eta}) \frac{\partial \bar{\eta}}{\partial x} \tag{2.8}$$

Thus:

$$F_x \propto h \frac{\partial \bar{\eta}}{\partial x} \tag{2.9}$$

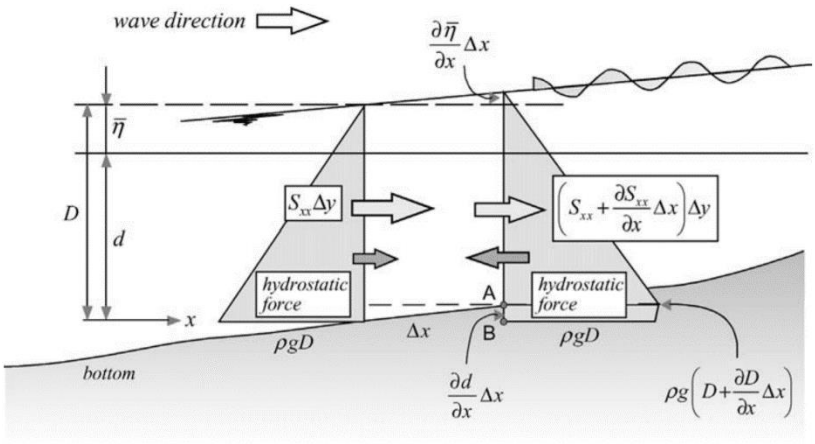

FIGURE 2.3.5. BALANCE OF THE RADIATION STRESS AND HYDROSTATIC PRESSURE ON A VERTICAL COLUMN UNDER WAVES PROPAGATING AT NORMAL INCIDENCE TO THE SHORE (HOLTHUIJSEN, 2010).

2.4. XBEACH

After the destructive hurricanes in 2004 and 2005 there was need to assess the vulnerability of the US coastal areas. In an initiative by the USACE and the Dutch dune safety assessment at the same time initiated the development of an open source program, XBeach, which focusses on the nearshore response to hurricane impacts and storms. The models approach is describing different formulations for the storm impact regimes in the coastal zone as described by Sallenger (Sallenger, 2000).

The model consist of formulations for short wave envelop propagation, nonstationary 2DH shallow water equations, sediment transport and bed update. These modules are shown in Figure 2.4.1.

The wave actions consists of a 2DH formulation of wave groups in combination with infra-gravity waves. The model is able to formulate time varying wave action, including refraction, shoaling, current refraction and wave breaking. The model also include a roller formulation, which represent the momentum stored in surface rollers, wave-current interactions and a wave dissipation model.

The model also uses a 2DH description of the shallow water equations. This includes a time varying wave forcing terms and depth averaged undertow.

The model is able to describe the complex surf- and swash zone sediment transport after careful elaborations with the relative simple Soulsby-Van Rijn relations. The model uses these relations to solve a depth-averaged advection-diffusion equation to calculate the suspended sediment transport. Furthermore, the model uses an avalanching formulation during the collision regime, which describes the avalanching of dune faces due to the exceeding of the critical wet and dry slope of the dune face. This leads to the dune erosion over time. XBeach allows options to include multiple sediment fractions and hard structures that are not available for erosion.

The model has been able to solve for a variety of analytical, laboratory and field tests. These validations were carried out with a set of standard parameters for which the model describe the different storm impact regimes very well.

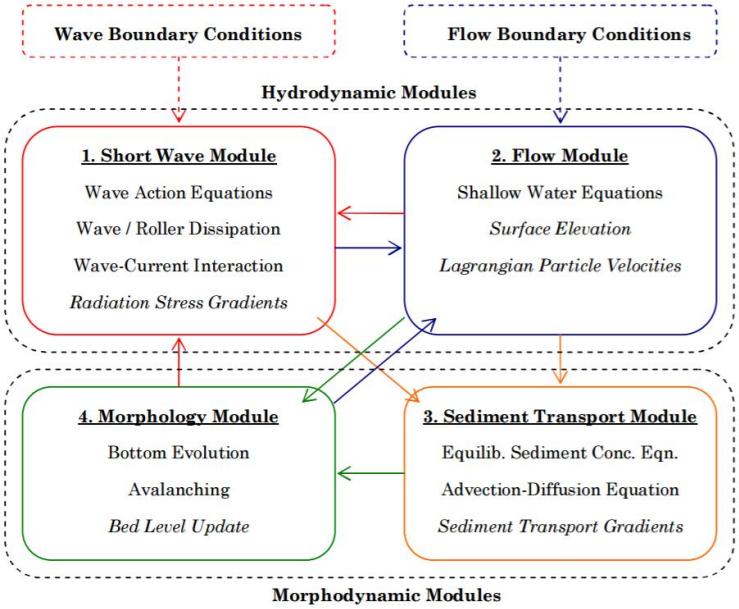

FIGURE 2.4.1. COMPONENT MODULES IN XBEACH. THE DASHED BOXES SHOW THE HYDRODYNAMIC AND THE MORPHODYNAMIC MODULES. THE ARROWS INDICATE THE INFORMATION EXCHANGE BETWEEN FORMULATIONS AND THE ITALIC TERMS SHOW THE RELEVANT OUTPUT PARAMETERS. THE GIVEN BOUNDARY CONDITIONS ARE USED FOR THE FIRST ITERATION. (DALY, 2009)

2.5. CONCLUSIONS

The hybrid concept is based on the building with nature concept, where natural processes are utilized for the goal of additional protection against flooding or other hazards. In case of the Galveston seawall, a sand cover offers a possibility of reducing the loads of waves before they hit the seawall itself. However, there is no direct formulation that gives an relation between this cover and the reduction of the wave height, overtopping or other design parameters. Hence, the current guidelines prescribe a custom assessment of these parameters for each specific case.

In the literature review, two significant processes have been identified that will be affected by the construction of a sand cover. These are the wave height at breaking closest to shore and the wave-induced set-up, which both are linked to the diffusion of wave energy as they propagate towards shore. Xbeach is a numerical model that is capable of measuring the interaction of an eroding coast and the hydrodynamics e.g. the diffusion of the wave energy and the wave setup and height.

3. METHOD

In this chapter, the methodology of the testing of the hybrid designs at the GSW is elaborated. First, the variation in hybrid designs is described. Then, the used input and boundary conditions are elaborated. Finally, the model set-up is discussed. The model set-up is made at a characteristic section of the GSW. In order to incorporate all the relevant structures and specifics of the area, an elaboration was made into the Galveston Bay, the Galveston Seawall and other structures. The result of this analysis can be found in Appendix B.

3.1. HYBRID DESIGNS

3.1.1. DESIGN PARAMETERS

Starting point of the hybrid designs are two requirements. The first is regarding the total elevation of the structure. This has to be as low as possible, since raising the seawall will result in high costs and disconnects Galveston and the beach, as disused in section 1.2. . The second requirement is to keep the sand cover volume small, due to the limited sand mining locations in the Gulf of Mexico and the following costs (U.S. Army Corps of Engineers, 2014).

The hybrid structure consist of the combination of a 'hard' structure or core and a 'soft' coverage. In this research the hybrid concept is specifically applied at the GSW. This makes the GSW the constant starting point on which a soft layer is simulated. This cover can be simulated in every preferred shape. The design of this cover is therefore defined in several parameters which can be varied per design, as shown in Figure 3.1.1. The design is divided in a **beach** and **dune part**. The dune is the section that covers the seawall and starts were the elevation of the cover layer increases with a certain **dune slope**. This slope is significantly steeper than the beach slope. The dune continues up to a certain elevation or **dune height**. At this point the maximum elevation of the cover is reached and the dune maintains on this elevation. The horizontal extend of this point towards the face of the seawall is considered the **dune width**.

The beach is defined as the part that starts from the end of the dune slope to a point at MSL. The horizontal distance between these two points is considered the beach length. The total elevation or vertical distance between these points is the beach elevation or **beach height**.

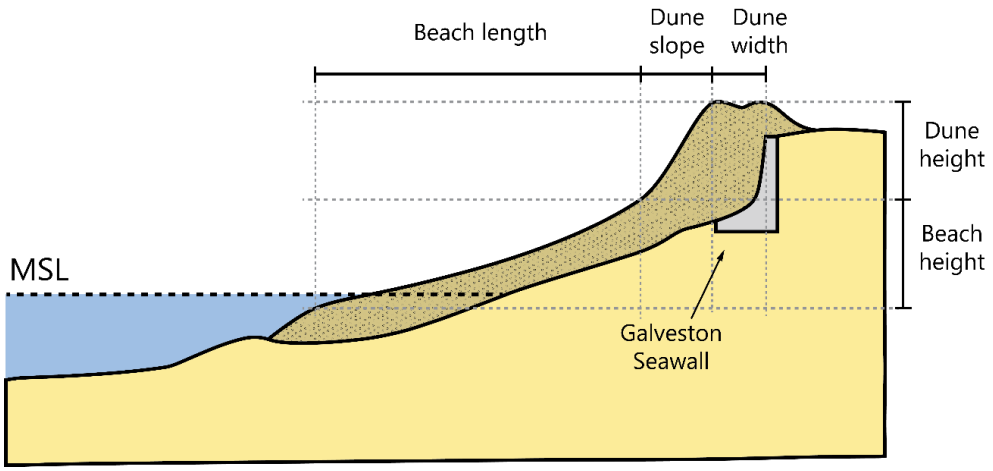

FIGURE 3.1.1. DEFINITION OF DESIGN PARAMETERS OF THE COVER LAYER, ADAPTED FROM NEDERHOFF, 2014

In total 33 different designs were simulated. In these designs the parameters as mentioned earlier were variated, to study what the effect is per variable. Additionally, 6 designs had special designs to look into a specific detail. These included:

- A case in which the seawall has been extended and no sand was placed. This case was introduced to check the effect of extending the seawall instead of the hybrid concept.
- Several cases with the introduction of a beach berm.
- Several cases where the GSW, which is modeled as a vertical wall, was replaced by a dike profile. This dike was simulated as a non-erodible structure with a smooth slope. The effect of revetment or dike protection is not incorporated. It can be expected that this will dissipate the wave energy even more as it hits the structure.

An overview of the dimensions of all the designs can be found in Appendix E, Table E.1.1.

3.2. MODEL SET-UP

3.2.1. PREPARATORY MODEL VALIDATION

The hybrid designs are tested with use of the XBeach model. This model can simulate hydrodynamic and morphodynamic processes in the nearshore which are important for beach and dune erosion. In order to simulate with a level of certainty, the model has been validated prior to the testing of the hybrid design. This validation looked at capability of the model to reproduce the hydrodynamics and the erosion/aggregation in the nearshore during a historical event, namely Hurricane Ike.

The results of the validation showed that the model managed to simulate the surge during the storm pretty well. The morphodynamic response of the model showed an overestimation of the erosion volumes on the beach face and on the island itself. It was found that this mainly contributes due to the fact that XBeach only considered to be sediment with a certain distribution in grainsize and non-erodible structures were present in the input. The reinforced effect of dune vegetation and overall vegetation on the island was not taken into account. Also several cases showed a divergent result from the output of XBeach compared to the measured data, due to existing structures that were not taken into account or errors in the initial input. The full process of the validation of the simulation of Hurricane Ike at the Galveston coast with XBeach model can be found in Appendix D.

3.2.2. BATHYMETRY

The bathymetry used in the model is derived from the DEM of the Galveston bay area, Table 5.3., Figure A.1.2. The bathymetry used for the validation of the model is also used for the simulation of the hybrid variants. In this case a smaller selection of the total DEM has been made, being an area of 6 km offshore and 5 km in the along shore. The coastal bathymetry was maintained while the shore bathymetry and the hinterland was smoothen out. This was done in order to easily construct different hybrid designs and save computational time, as shown in Figure 3.2.1.

3.2.3. GRID

To model all the significant processes with sufficient accuracy, a grid must have sufficient grid points. However, a grid with a high resolution will lead to large computational time. Therefore, a tradeoff has to be made in the definition of the grid. A set of tools and scripts were developed in order to prepare and process data for the XBeach model (Deltares, 2016). The grid is created by combining a cross- and alongshore discretization. The cross shore grid is defined based on i.a. the slope of the bed, the courant number and other manual parameters. The alongshore grid is created based on a certain band in the middle of the domain, where the cell size in y-direction becomes finer. This is done to keep the areas near the alongshore boundaries coarse, but the area of interest fine. The grid of the hybrid test model has a grid resolution of $dx = 5\ to\ 15\ m$ and $dy = 10\ to\ 20\ m$. In Figure 3.2.2. the used grid is shown.

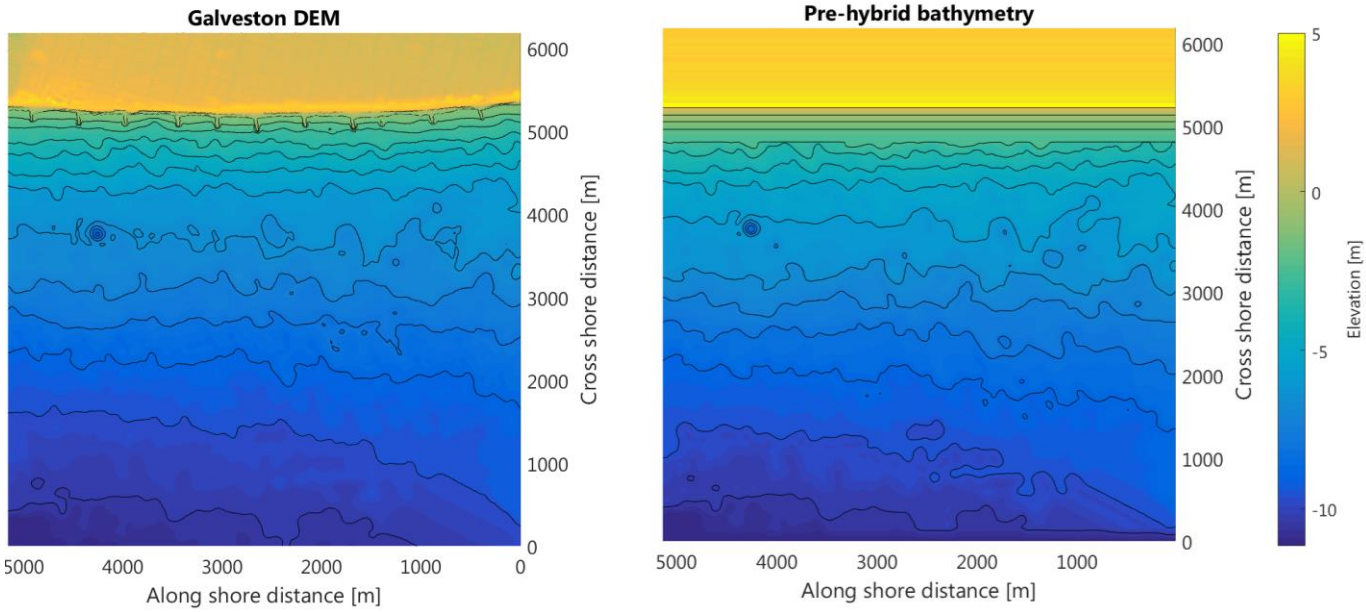

FIGURE 3.2.1. SELECTED BATHYMETRY BEFORE AND AFTER THE ADAPTATION. THE OFFSHORE BED PROFILE WAS MAINTAIN, WHERE THE ACTUAL BEACH/DUNE FRONT WAS ALTERED IN ORDER TO SIMULATE CONSISTENT HYBRID DESIGNS.

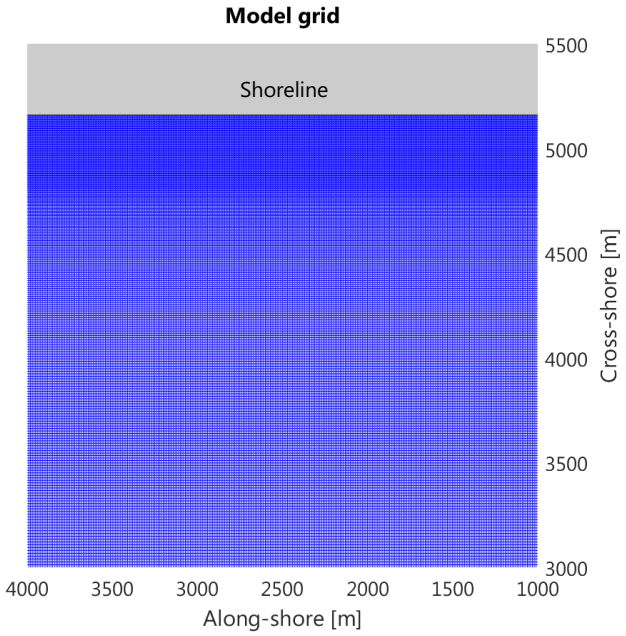

FIGURE 3.2.2. APPLIED GRID, THE TOTAL GRID SIZE WAS REDUCED FROM 1501 X 1400 TO 635 X 414

3.2.4. NON-ERODIBLE STRUCTURES

XBeach offers a possibility to include structures, which are not vulnerable for erosion. The way this is defined in the numerical model is a certain value of erodible material per grid point. The non-erodible layer is defined as a certain elevation beneath the actual bathymetry, e.g. a revetment beneath a dune. At this location the elevation of this non-erodible layer is extracted from the bathymetry's elevation, resulting in a certain depth of erodible material. Once this depth has been eroded away due to the wave and current motions, the non-erodible layer becomes exposed and no morphological change is further modeled at this point. The hydrodynamics however are still being modeled, since motions still occur over a revetment once it is exposed. In Figure 3.2.3, the non-erodible layer for run 2.12 is shown. The creation of the non-erodible layer for the simulations is further discussed in Appendix D.2.1.

3.2.5. PARAMETERS AND PROCESSES

PROCESSES XBeach contains several modules for hydro- and morphodynamic processes, as shown in Figure 2.4.1. Overall no significant processes have be turned off with respect to the normal configuration. However some processes that were chosen, are elaborated.

One of the important formulations in the hydrodynamic module, is the wave breaking formula. For this research the Baldock function has been chosen to model the wave breaking. Due to the fact that the design test model wave input is composed of stationary sea states which vary in time, the Baldock formulation is the appropriate way of computing wave breaking (Roelvink et al., 2010). The breaker index γ, is set on 0.7 as this value is in agreement with other elaborations on breaking conditions (Battjes and Janssen, 1978; Bosboom and Stive, 2015; Weggel, 1973).

In the design tests no vegetation was defined and this option was not included in the formulations. The same holds for the input of wind forcing and groundwater flow. These processes were not included and therefore the corresponding formulations were not elaborated during the runs.

The output from XBeach for each run consisted of 10 minute interval time series of several hydro- and morphodynamic variables. The variables are stated in Table 3.2.1. Some of these variables are not used in the final conclusions as the focus of the research shifted during the process.

TABLE 3.2.1. OUTPUT PARAMETERS OF THE DESIGN TEST MODEL AND ITS DEFINITION

H	H_{rms} wave height based on instantaneous wave energy	[m]
hh	Water depth	[m]
zs	Water level	[m]
zb	Bed level	[m]
u	GLM (Generalized Lagrangian Mean) velocity in cell center, x-component	[$m \cdot s^{-1}$]
D	Dissipation	[$W \cdot m^{-2}$]
DR	Roller energy dissipation	[$W \cdot m^{-2}$]
Dc	Diffusion coefficient	[$m^2 \cdot s^{-1}$]
E	Wave energy	[$Nm \cdot m^{-2}$]
Fx	Wave force, x-component	[$N \cdot m^{-2}$]
Subg	Bed sediment transport (excluding pores), x-component	[$m^2 \cdot s^{-1}$]
Susg	Suspended sediment transport (excluding pores), x-component	[$m^2 \cdot s^{-1}$]
Sutot	Sediment transport integrated over bed and suspended load, x-component	[$m^2 \cdot s^{-1}$]

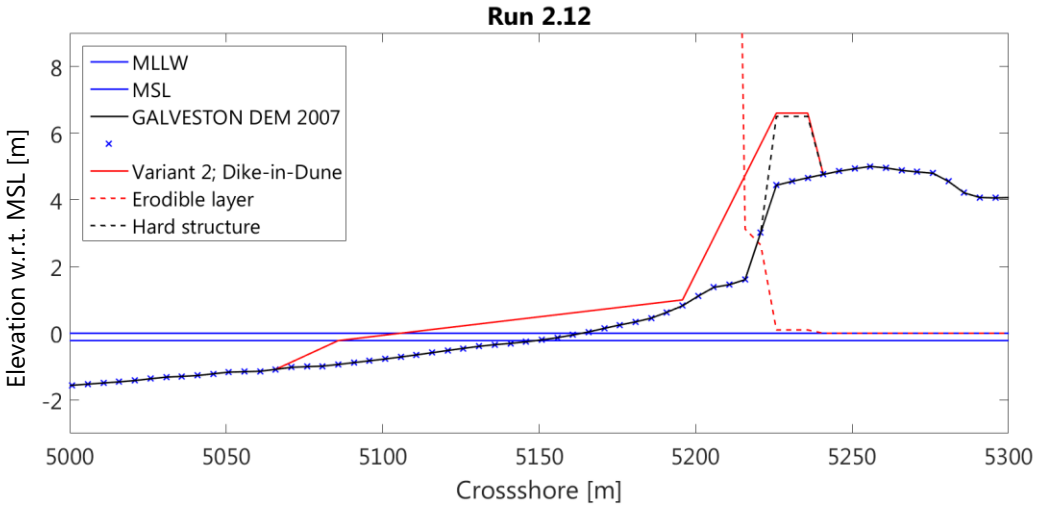

FIGURE 3.2.3. CROSS SHORE PROFILE OF VARIANT 2.12. THE NON-ERODIBLE SEAWALL IS EXTENDED AS INDICATED BY THE BLACK DASHED LINE, THE RED SOLID LINE REPRESENTS THE SANDY COVER. THE DASHED RED LINE SHOWS THE ERODIBLE LAYER WHICH IS AVAILABLE FOR MORPHODYNAMIC CHANGES. ONCE THIS LAYER HAS BEEN ERODED AWAY THE NON-ERODIBLE LAYER IS EXPOSED AND THUS NO SEDIMENT IS AVAILABLE FOR TRANSPORTATION.

PARAMETERS XBeach offers several options to fine-tune the model with certain parameters. These parameters can be adapted depending on results during the validation process. Due to time constrains, a full elaboration on these parameters has not been executed. Instead the results of earlier work has been examined (Daly, 2009; Harter, 2015; McCall, 2008; Nederhoff, 2014; Roelvink et al., 2009). In these studies, parameters such as the morfac, courant number, bottom friction e.g. the Chezy value etc. have been assessed. These parameters have been adopted. The full input file with all the specific parameters (params.txt) can be found in Appendix F.

BOUNDARIES For each model run wave and flow conditions are imposed at the offshore boundary. In order to let obliquely-incident and obliquely-reflected waves and currents exit the domain without reflection, a weakly reflective-absorbing type of boundary was included. The two lateral boundaries, perpendicular to the coast were described as Neumann boundaries, which allows to let the flow exit the two lateral boundaries without reflecting it. XBeach offers different locations for the tide or surge to be specified (Roelvink et al., 2010). An overview of the models boundaries are shown in Figure 3.2.4.

SEDIMENT DISTRIBUTION Studies of the sediment size along the Galveston Island coastline showed a mean sediment grainsize between 100 and 150 µm. A single sediment size distribution was adopted in the model with a D_{50} of 150 µm and a D_{90} of 187 µm (Harter, 2015; Texas General Land Office, 2016; U.S. Army Corps of Engineers, 2014). However, it is known that the Upper Texas Coast is characterized by thick muddy layers that cover the sand layers (Anderson, 2007). This makes the nearshore sediment transport more complex and challenging to model. Therefore, a single sediment distribution is used in this research.

3.2.6. APPLIED BOUNDARY CONDITIONS

The input conditions consists of a time-varying wave input and a time-varying tide/surge input. This design storm was composed from different values of earlier work on design surge levels and wavelengths at the Galveston coast. In this section, the resulting input data is given. The full elaboration of the design storm and references to the corresponding work can be found in Appendix C.

SURGE The surge elevation for the design storm is compiled with found values from earlier elaborations. The main surge elevation for a 1/100 year^{-1} event has been adopted from an extreme value analysis (Almarshed, 2015). Other work has been carried out on determining the 1/100 surge level (Lendering et al., 2014; Rippi, 2014; Stoeten, 2013). These values corresponded well with used findings. The surge input is described as a surge level from offshore, including a fore runner surge and a peak surge. There is no bay side in the models domain , so no bayside boundary is needed. The incoming surge is specified as a single surge level along the entire offshore boundary. An overview of the models boundaries are shown in Figure 3.2.4. The design surge levels and the profile of the time series is shown in Figure 3.2.5.

WAVES For the design wave height, use has been made by the most recent work. This contains a brief study by analyzing time series from an offshore buoy with an extreme value analysis. These offshore wave heights were simulated towards shore, including hydrodynamic processes (Almarshed, 2015; van Berchum et al., 2016). Referencing these values with other work shows similar results and correspond with a category 3 storm. (Jin et al., 2010; NOAA, 2016a). The peak wave period was also derived by Almarshed and is used in this study. The angle of incidence of the waves can change during a storm. In this study the angle of incidence is chosen normal to the shore as no energy is lost due to refraction and along shore processes. This will form the strongest possible forcing on the shore. The used wave height and period are shown in Figure 3.2.6.

FLOW The focus in this study lies on the cross shore effect of a storm on different hybrid designs. Therefore only a relative short storm is simulated. Astronomical constituents or other currents or flows are not included in the input. As described are the boundaries open, so any generated flow can leave the model domain without causing disruptions.

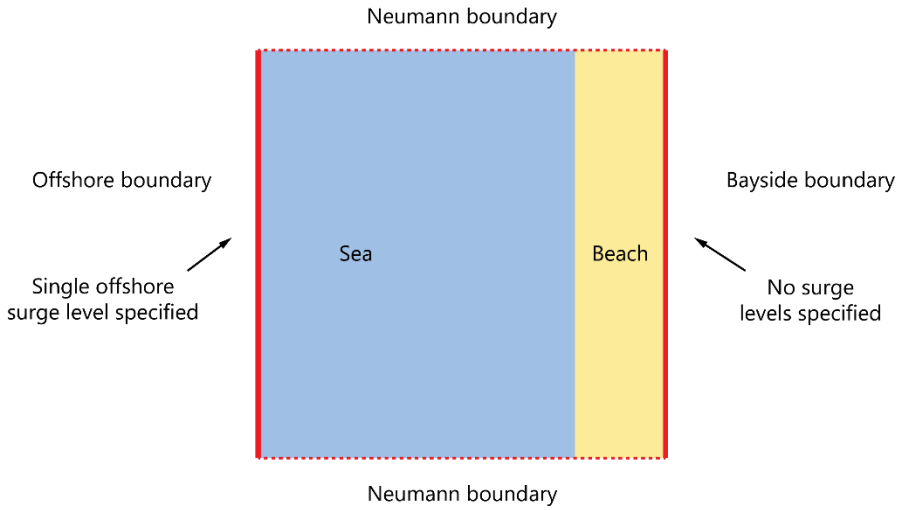

FIGURE 3.2.4. SCHEMATIC OVERVIEW OF THE BOUNDARY DEFINITIONS OF THE MODELS DOMAIN. AT THE OFFSHORE BOUNDARY (LEFT) A SINGLE SURGE TIME SERIES IS APPLIED TO THE ENTIRE BOUNDARY. ON THE ONSHORE/BAYSIDE BOUNDARY (RIGHT), NO BAY OR WATER BODY IS PRESENT, THUS NO SURGE TIME SERIES IS REQUIRED. THE TWO LATERAL BOUNDARIES (UP AND DOWN) ARE DEFINED AS NEUMAN BOUNDARIES.

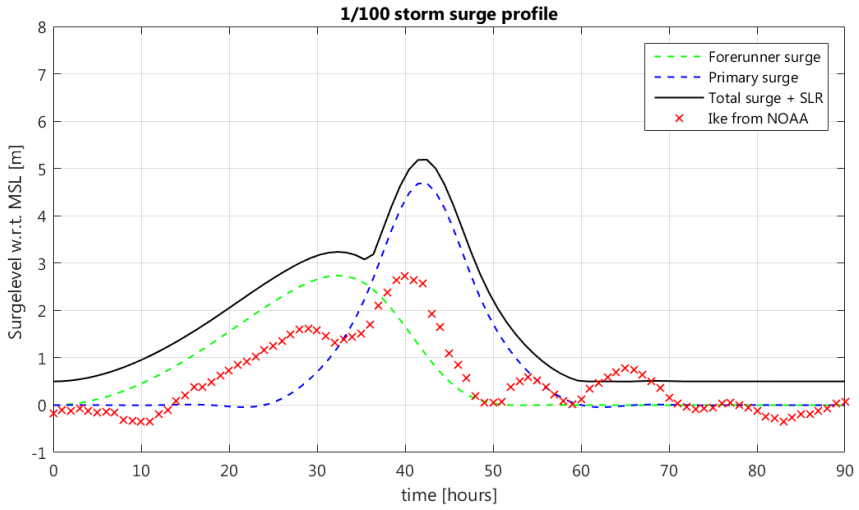

FIGURE 3.2.5. DESIGN STORM SURGE PROFILE AS USED IN ALL THE SIMULATIONS. THE TOTAL SURGE LEVEL CONSISTS OF THE ADDITION OF A FORERUNNER SURGE, PRIMARY SURGE AND AN ADDITION TO ACCOUNT FOR SEA LEVEL RISE AND SUBSIDENCE. REFERENCE IS MADE TO THE SURGE PROFILE OF HISTORIC EVENT OF HURRICANE IKE, AS MEASURED BY STATION 42035 (NOAA, 2013). THE STORM PROFILE OF IKE WAS USED AS A BASE FOR THE TIME SERIES OF THE DESIGN STORM.

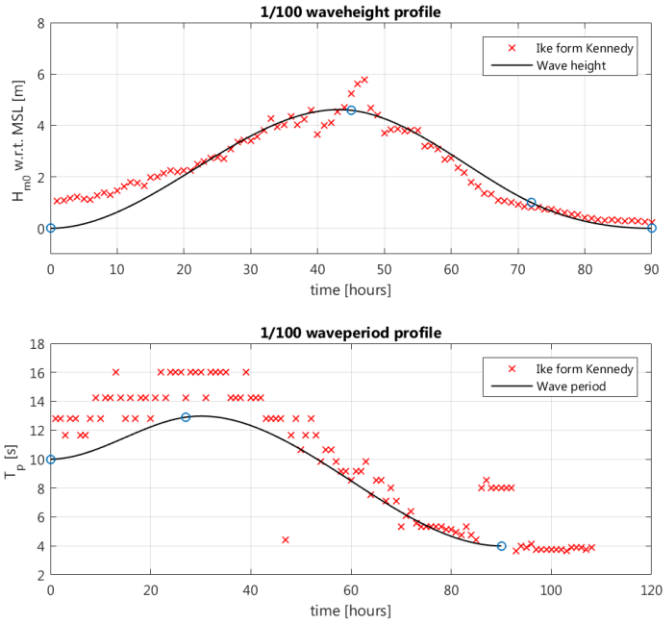

FIGURE 3.2.6. DESIGN WAVE HEIGHT AND PERIOD AS USED IN ALL THE SIMULATIONS. REFERENCE IS MADE TO THE WAVE HEIGHT AND WAVE PERIOD OF HISTORIC EVENT OF HURRICANE IKE, AS MEASURED BY KENNEDY (KENNEDY, 2011A).

4. RESULTS

4.1. MEASURING QUANTITIES OF INTEREST

The focus of the research is the effect of different designs of the sandy cover at the current GSW. As elaborated in section 2.3.2, due to the different dimensions of the beach and/or dune, the wave height is being reduced as waves propagate towards the shore. The more effective this reduction is, the less high the wave height when it hits the exposed seawall. This wave height is the first quantity of interest, since it serves as an indication of the forces and overtopping rates at the seawall. The literature also has shown that due to the wave breaking more energy is being transferred to a water level gradient e.g. the wave-induced setup. This is the second quantity of interest, since it applies to the mean water level. This could potentially lead to overflow of the seawall if this is not accounted for in the design.

The wave height is measured at the point of breaking closest to the shore. As earlier established, depth induced wave-breaking transfers wave energy to roller energy and other dissipation terms. This can be seen in a decrease in wave energy, E or radiation stress over the cross shore, $\frac{dS_{xx}}{dx}$ ($\cong 3/2\ E$ in the nearshore) and thus an increase in wave force, F_x. If this wave force is examined over the cross shore, this increase can be observed at the breaker lines, as can be seen in an arbitrary output of a run in Figure 4.1.1. Therefore the used value for the wave height at breaking is the wave height at the breaker line closest to shore. This value is found at the location and time where the wave force is at its maximum, $t_{F_x,max}$.

The wave-induced setup is measured as the total increase of the mean water level at the shoreline. Since the wave height breaks multiple times over the cross shore, the increasing wave-force requires an increasing water level gradient towards the shore. All these contributions are accounted by taking the water level at the breaker line closest to shore and calculate the overall gradient with respect to the still water level, as shown in Figure 4.1.2.

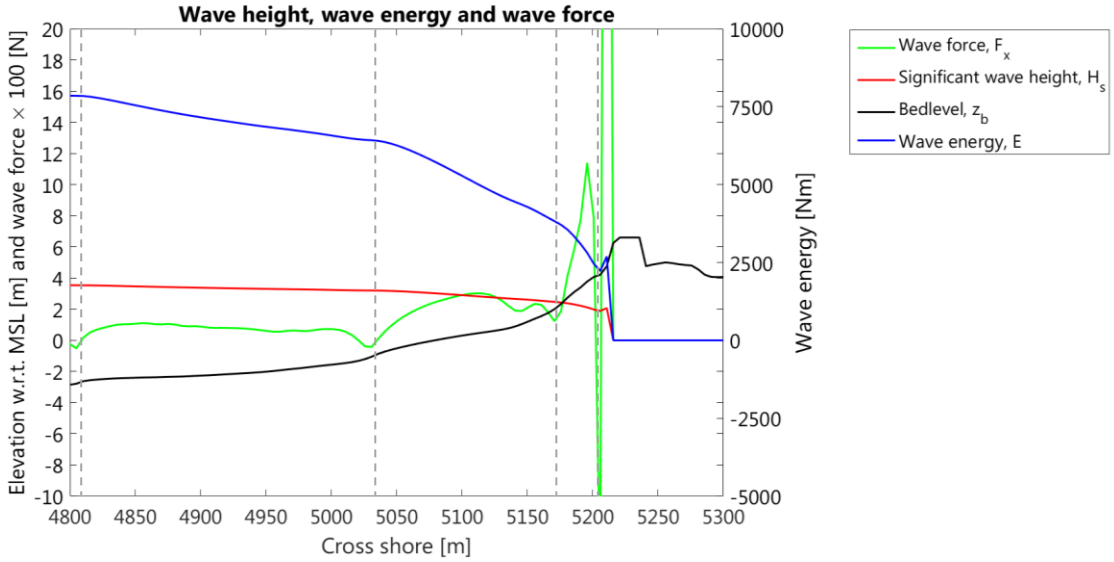

FIGURE 4.1.1. OVERVIEW OF THE RELATION BETWEEN WAVE HEIGHT, WAVE ENERGY AND WAVE FORCE AT THE MOMENT THE WAVE FORCE REACHES A MAXIMUM, $T_{FX,MAX}$ IN AN ARBITRARY RUN. INDICATED WITH THE DASHED LINES ARE ROUGHLY THE ADDITIONAL BREAKER LINES WHERE THE WAVE HEIGHT IS BEING REDUCED, WAVE ENERGY IS DISSIPATED AND THE WAVE FORCE INCREASES.

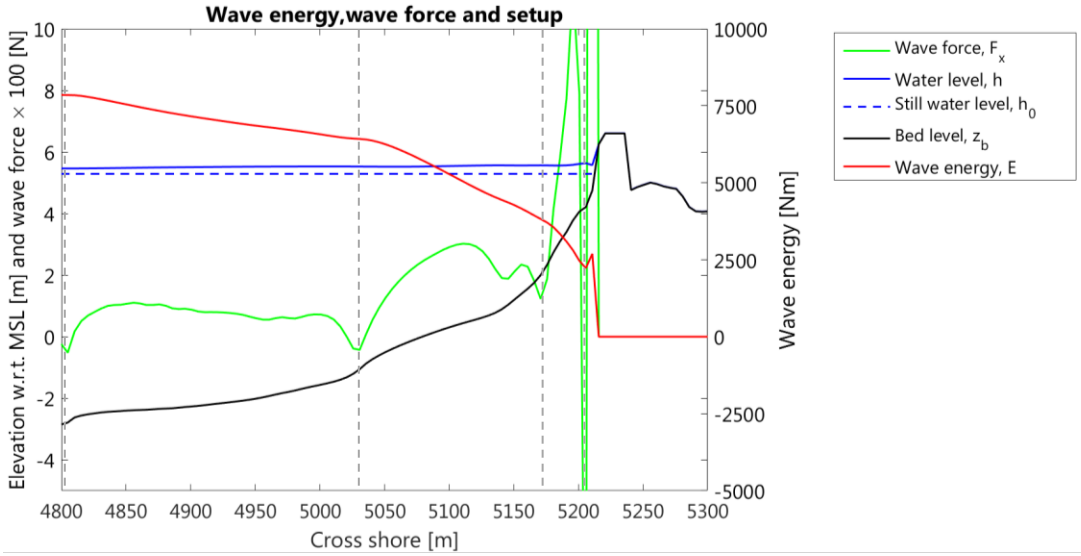

FIGURE 4.1.2. OVERVIEW OF THE RELATION BETWEEN WAVE ENERGY, WAVE FORCE AND THE WAVE-INDUCED SETUP AT THE MOMENT THE WAVE FORCE REACHES A MAXIMUM, $T_{Fx,MAX}$ IN AN ARBITRARY RUN. AGAIN THE DASHED LINES ARE THE ADDITIONAL BREAKER LINES WHERE THE WAVE HEIGHT IS BEING REDUCED, WAVE FORCES INCREASES AND A WATER LEVEL GRADIENT IS REQUIRED.

The design storm is defined as a wave and water level input changing over time. This implies that no characteristic wave-setup or wave height at the shoreline can be found, since these also change over time. However, it is possible to identify a maximum for both the wave height at breaking and the set-up, as depicted in Figure 4.2.2. These values change given the effectiveness of the hybrid designs and thus serve as an indication of the effectiveness per variant. The results of all the runs can then be represented in a single plot, showing the maximum wave height at the nearest breakpoint at the shore and the wave-induced setup of each run. It is then possible to compare the runs with each other and identify certain trends. This will be further elaborated in section 5.1.

4.2. INITIAL CASE

First, an initial case is tested. This is carried out with the original bed profile and seawall elevation without any sand cover. The results of the model shows that substantial overflow occurs during the peak of the design storm, as shown in Figure 4.2.3. This means that waves can propagate over the seawall. As a result, the wave height and wave-induced setup is not well represented any more. Since this research focuses on the ability of the hybrid to reduce the load parameters on the structure, these overflow cases can therefore not be used. In order to solve this problem a necessary increase of the concrete seawall is added to the non-erodible layer, as shown in Figure 4.2.1. The results of the altered run serves as the null case, since all the wave energy is contained in front of the seawall and its effect on the wave height and setup is contained. The result of the null case, run 1.1 is shown in Figure 4.2.2.

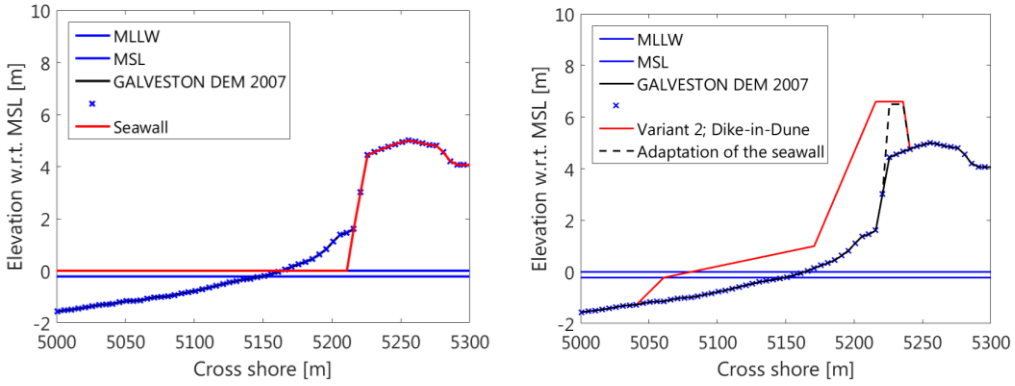

FIGURE 4.2.1. NECESSARY ADAPTATION OF THE SEAWALL. IN ORDER TO BLOCK THE MAIN SURGE HEIGHT, THE SEAWALL IS HEIGHTENED TO A MINIMAL ELEVATION. THE LEFT PANEL SHOWS THE PRE-HYBRID CASE, THE RIGHT PANEL SHOWS RUN 2.16 WITH THE EXTENDED SEAWALL.

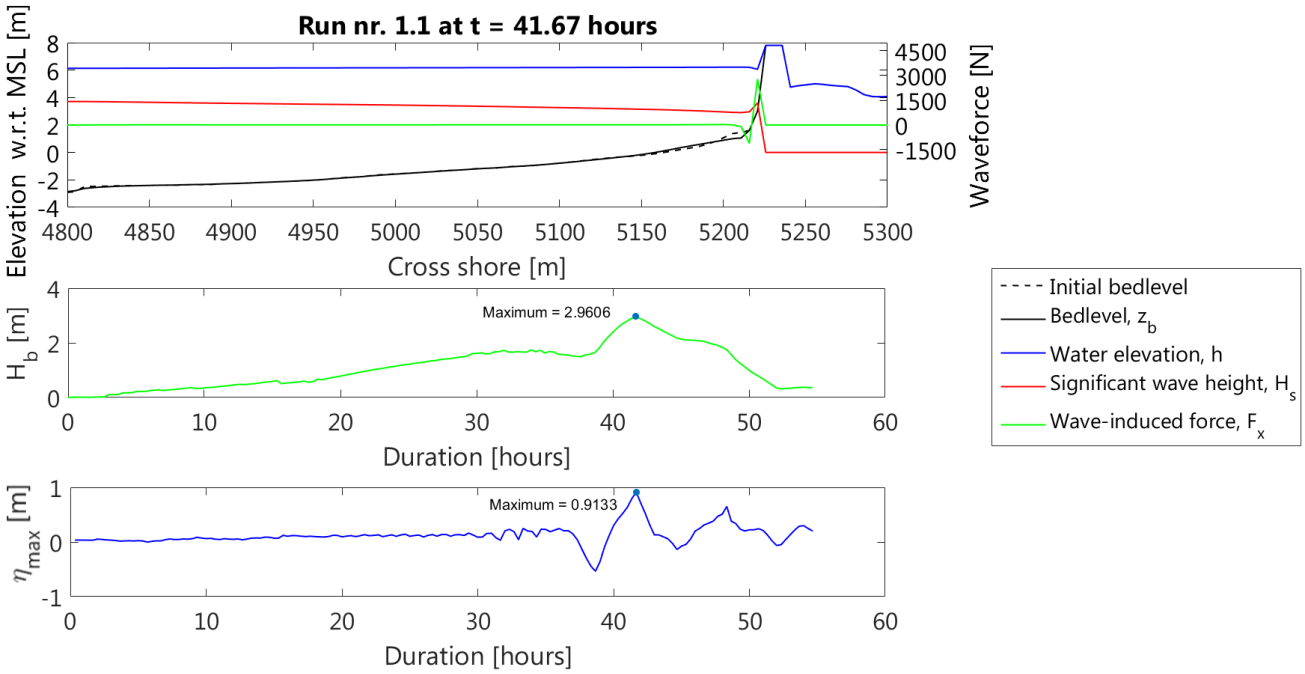

FIGURE 4.2.2. OUTPUT OF RUN 1.1. THE TOP PANEL SHOWS THE WATER LEVEL AND WAVE HEIGHT IN THE CROSS SHORE AT THE MOMENT F_X IS AT ITS MAXIMUM ($T_{Fx, MAX}$). THE MIDDLE PANEL SHOWS THE DEVELOPMENT OF THE WAVE HEIGHT AT THE BREAKER LINE IN TIME. THE BOTTOM PANEL SHOWS THE DEVELOPMENT OF THE WAVE-INDUCED SETUP WITH RESPECT TO THE MEAN WATER LEVEL. IN THE LATTER TIME SERIES A MAXIMUM CAN BE FOUND. THESE VALUES SERVE AS THE REPRESENTATIVE NUMBERS FOR EACH RUN.

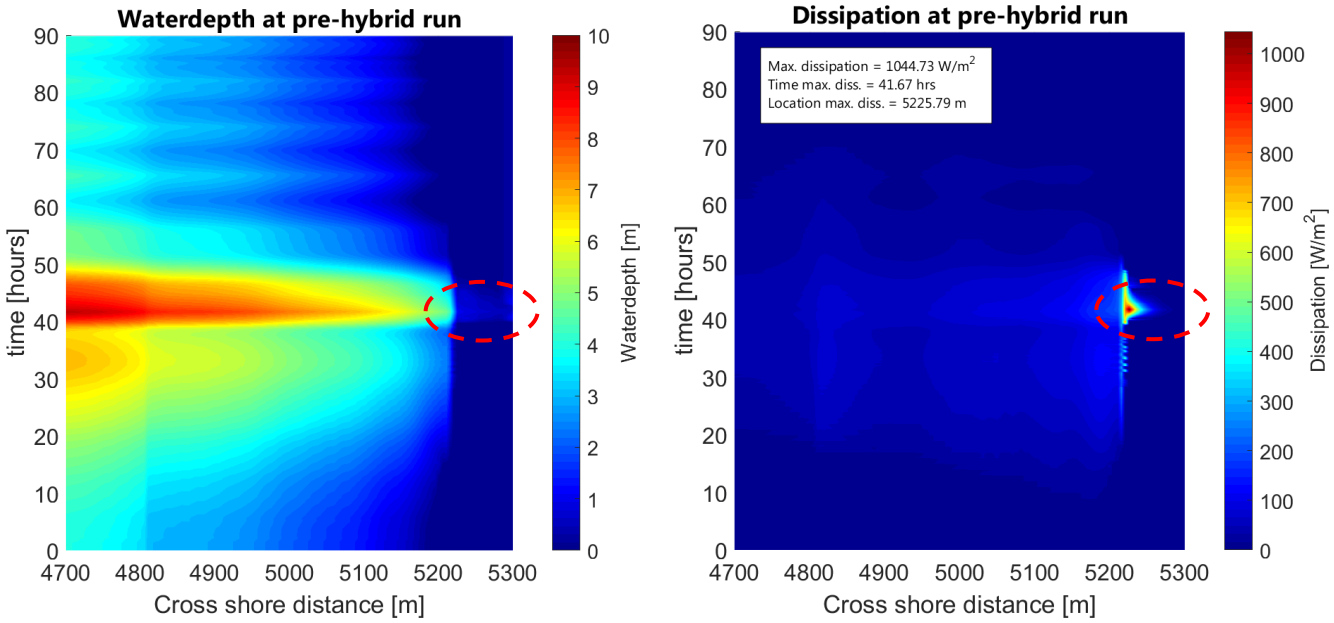

FIGURE 4.2.3. WATER DEPTH AND DISSIPATION IN TIME AT A CHARACTERISTIC TRANSECT FOR THE PRE-HYBRID SITUATION. INDICATED IN THE RED CIRCLE IS OVERFLOW AT THE MAXIMUM SURGE. THIS OVERFLOW MEANS A DISSIPATION OF WATER AND ENERGY OVER THE SEAWALL AND THUS 'LOST' ENERGY.

4.3. ALL USABLE RUNS

As explained in the previous section, every run can be represented with a value for the maximum wave height at breaking closest to shore and the maximum wave-induced setup with respect to the still water level. In Figure 4.3.1 all the usable runs, e.g. no overflow occurs, are given.

A general trend can be observed that shows a relation between the maximum wave height and the wave-induced setup. This trend starts with the null case run 1.1, which shows relative high maximum wave height and a low wave induced setup, as shown earlier in Figure 4.2.3. This can be expected since no artificial cover was applied to the non-erodible, concrete wall. Therefore the waves traveling towards the seawall tend to break less until they hit the seawall itself, leading to a large wave height near the seawall and hardly any extra setup. In the following runs the hybrid models were composed with different designs of a sandy cover. It can be seen that in these runs $H_{b,max}$ decreases and the maximum setup, $\frac{d\eta}{dx}$ increases. This can be explained by looking into the designs of the tested hybrid models and will be done in the next sections.

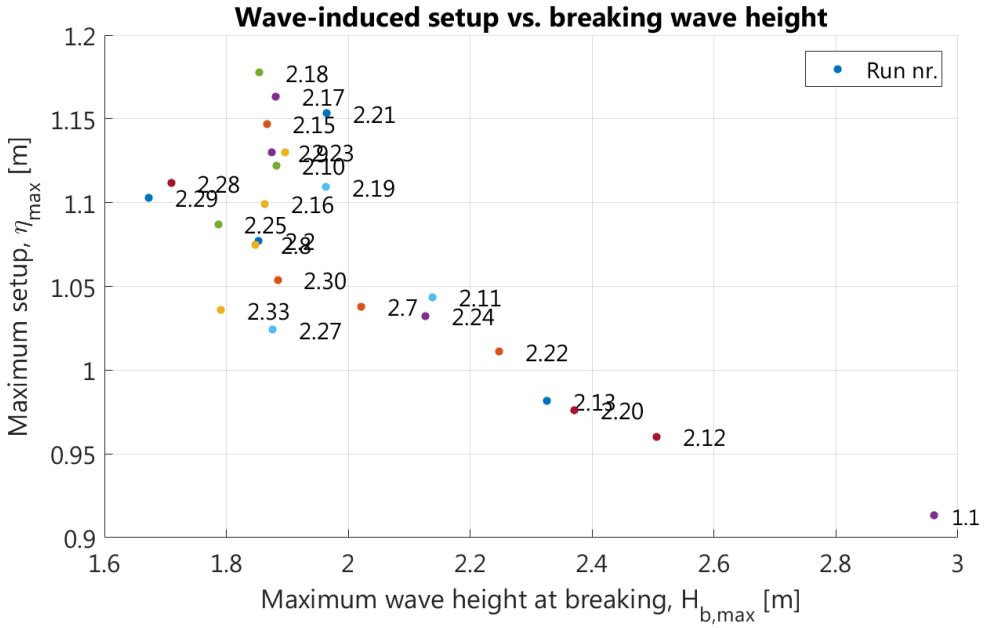

FIGURE 4.3.1. OVERVIEW OF ALL THE RUNS WITHOUT OVERFLOW.

4.4. VALIDATION OF THE RESULTS

As found in earlier sections, the behavior of the breaking of the waves and the wave-induced setup can be related to the wave energy balance and the wave forcing. Since these processes are the main driver behind the found values of each model, the corresponding formulations should hold for these results. This is done by looking into the relation of the essential parameters for the process of wave breaking and wave setup.

The wave set-up is the response of the mean water level due to the forcing of the waves. The found relation of the wave forcing and the wave set-up gradient in the x-direction, can be described as $F_x \propto h \cdot \frac{\partial \bar{\eta}}{\partial x}$. If the found values of the wave set-up are plotted versus this maximum wave force of the same run, a trend can be observed as shown in the left panel of Figure 4.4.2. This does not show a clear linear dependency. However, if the product of the local water depth and the gradient of the wave set-up in the x-direction is plotted against the corresponding wave force, a much distinct relation can be observed, as shown in the right panel of Figure 4.4.2. It is therefore concluded that the wave forcing and the coinciding wave set-up show an expected behavior.

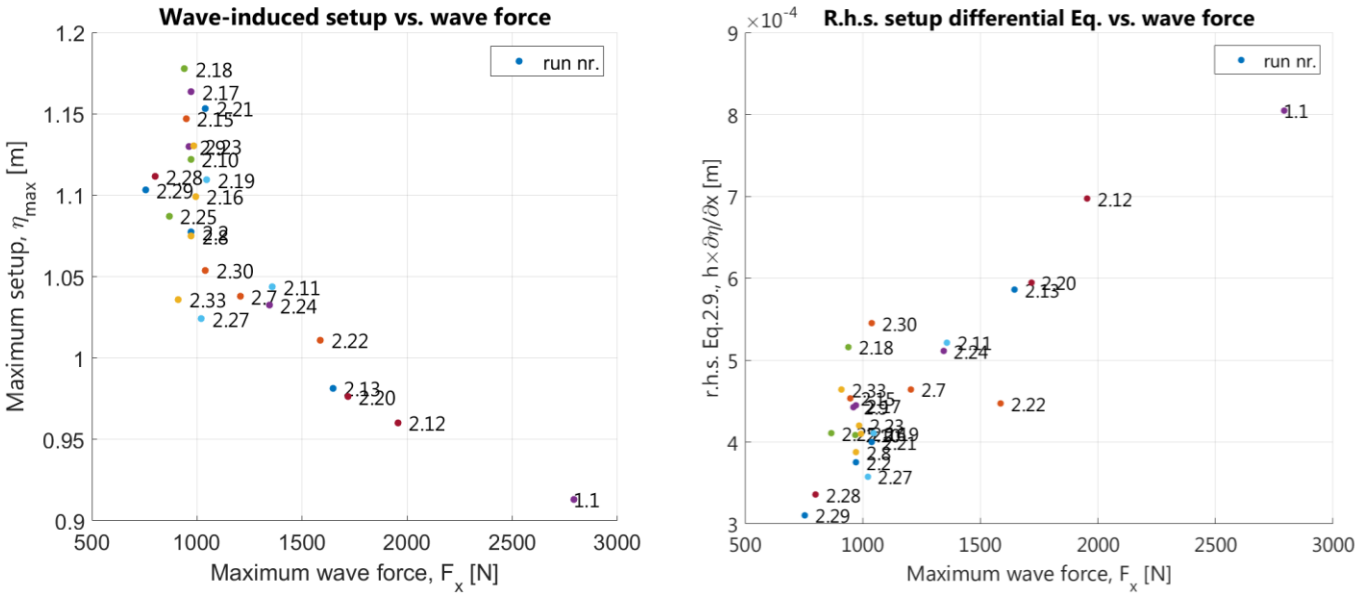

FIGURE 4.4.1. THE LEFT PANEL SHOWS THE RELATION BETWEEN THE MAXIMUM WAVE FORCE AND THE MAXIMUM SET-UP FOUND FOR EACH RUN. THIS HOWEVER DOES NOT SHOW A LINEAR DEPENDENCY. IF THE RIGHT HANDS SIDE OF THE SET-UP FORMULATION, AS FOUND IN SECTION 2.3.3 IS TAKEN INTO ACCOUNT, A MUCH CLEARER LINEAR RELATION CAN BE SEEN. THIS IS IN LINE WITH EXPECTATIONS AS A BIGGER WAVE FORCE WOULD REQUIRE A NET BIGGER WAVE SET-UP.

Similar to the wave set-up, the found wave heights at breaking for each run can be validated using the wave breaking theory as found in the literature review. Here it has been elaborated that the breaking of waves transfers wave energy into roller energy and other dissipation terms. This reduction of wave energy means a reduction in radiationstress and thus an increase in wave force. If the found values of the maximum wave height at breaking and the corresponding maximum wave force for each run are plotted versus each other, a clear dependency can be found, as shown in the left panel of Figure 4.4.1.

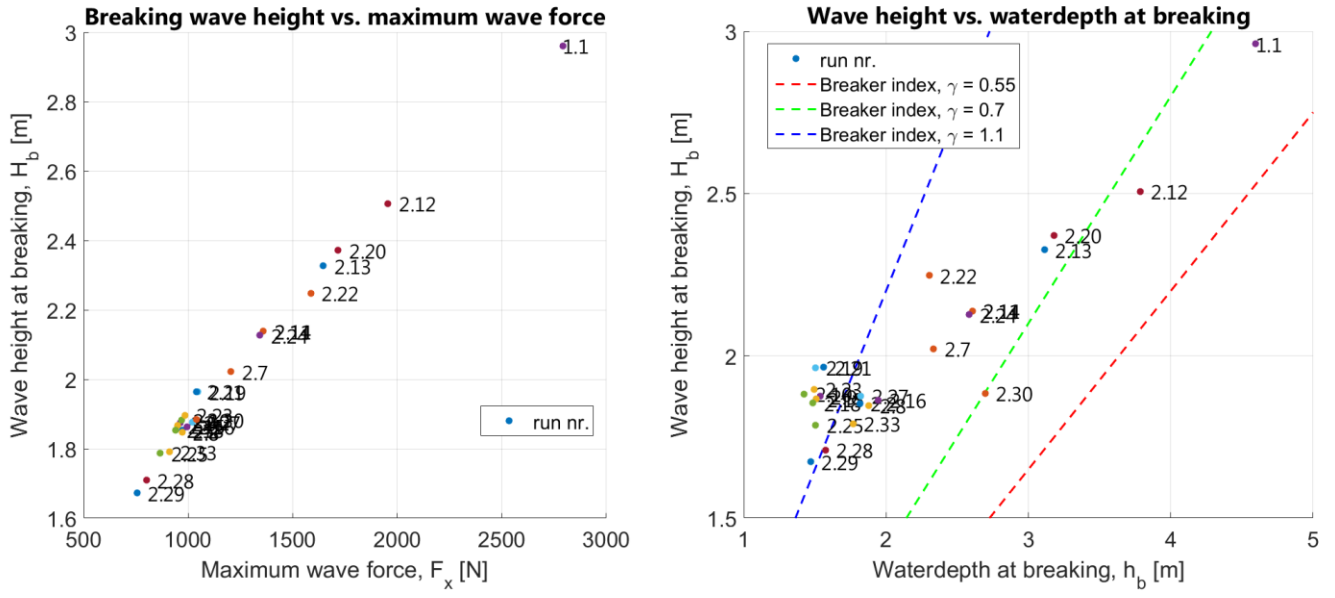

FIGURE 4.4.2. THE LEFT PANEL SHOWS THE RELATION BETWEEN THE MAXIMUM WAVE HEIGHT AT BREAKING VERSUS THE WAVE FORCE. THIS IS IN WELL CONFIRMATION WITH EACH OTHER, VALIDATING THE FOUND WAVE HEIGHTS WITH THE THEORY. THE RIGHT PANEL SHOWS THE BREAKING WAVE HEIGHT VERSUS THE WATER DEPTH AT THAT LOCATION. THE SPECIFIED BREAKER INDEX IS PLOTTED IN THE SAME FIGURE.

Additional to this the wave heigth at breaking, $H_{b,max}$, is dependend on the waterdepht at this location, d_b. The model has been setup with a breaker index of $\gamma = 0.55$, as elaborated in section 2.3.2. If the wave height at breaking and the waterdepth are plotted versus one another, some confirmation can be seen, as shown in the right panel of Figure 4.4.3. However the data is still quite scattered. Additionaly, the inputted breaker index is plotted in the same figure. It can be seen that the data does not match the theoretical relation at the location near the seawall. However if different breaker indices are plotted, some of the data folows the relation of $\gamma = 1.1$. This can be explained due the different sloped beaches and its influence on the breaking types as elaborated in section 2.3.2. If the designs are looked up it can be seen that the designs matching the $\gamma = 1.1$ still have a lot of sand cover during the peak of the storm. Therefore, the breaking process matches that of the plunging behaviour. However, once the seawall becomes exposed during a run, as is the case for run 2.12, 2.13, 2.14, 2.20 a.o., the breaking occurs partly due to the sand cover and finaly by the seawall itself. The corresponding breaking index of that run clearly diverges from the earlier match. This effect is illustrated by some crossections from representative runs in Figure 4.4.3.

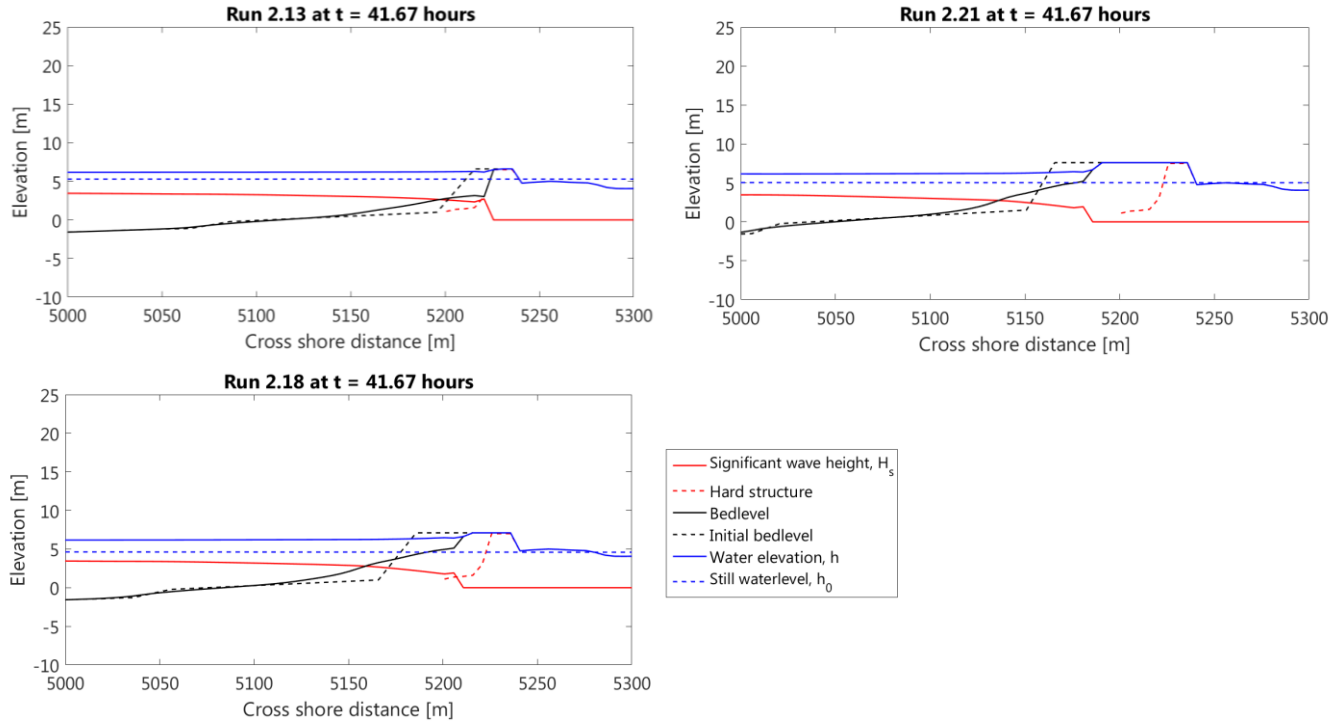

FIGURE 4.4.3. CROSS SECTION OF RUNS WITH EXPOSED AND COVERED SEAWALLS AT THE MOMENT OF MAXIMUM WAVE BREAKING CLOSEST TO THE SHORE, $T_{HB,MAX}$. IT CAN BE SEEN THAT THE SEAWALL IS EXPOSED IN RUN 2.13, WHERE IN RUN 2.21 AND 2.18 THE SEAWALL IS STILL COVERED. IN THE LATTER CASES THE BEACH SLOPE IS MORE GRADUAL AND THE WAVES BREAK IN A SAME MANNER. IN RUN 2.13 THE WAVE BREAKING OCCURS LESS DUE TO THE WATER DEPTH BUT DUE TO THE SEAWALL, WHICH CAUSES HEAVY BREAKING.

5. DISCUSSION

From the found results, several observations can be made. In the following sections, overall trends are being elaborated and discussed in more depth.

5.1. GENERAL TREND

The overall results are shown in Figure 4.3.1. It can be seen that from the null case, run 1.1., the maximum wave height and maximum set-up changes, depending on the specific hybrid design. As mentioned in section 3.1, the designs were composed by varying different dimensional parameters. In Figure 5.1.1, the energy dissipation in the nearshore for run 1.1 (null case) and run 2.10 are shown. The null case shows a very narrow and high dissipation zone at the seawall. This confirms that most of the waves break against the seawall. Due to this rapid transfer of wave energy at the seawall itself, there is almost no energy dissipation in front of the seawall. Therefore, the waveforce, F_x, is low and thus the wave-induced set-up is low as well.

The opposite can be said about run 2.10, which is a design with a sand cover on top of the seawall. Due to this sand cover, waves will 'feel' the bottom at an earlier stage. More wave energy dissipation takes place over a wider area, which is further offshore. The more continuous energy dissipation in the surf zone leads to a higher waveforce and requires a higher compensating set-up. As a result, more wave-induced set-up is being generated.

Form Figure 4.3.1. it can be seen that the most extreme differences in $H_{b,max}$ and η_{max} occur between run 1.1 and around run 2.18. Comparing these values give approximately $\sim 3.0\,m \rightarrow \sim 1.9\,m \approx 40\,\%$ reduction of the wave height near the structure and a $\sim 0.9\,m \rightarrow \sim 1.15\,m \approx 20\,\%$ increase of the wave-induced set-up, due to the application of a sand cover. However, these runs give the most extreme differences. In the next section the contribution of the different dimensional parameters on this effect is being examined.

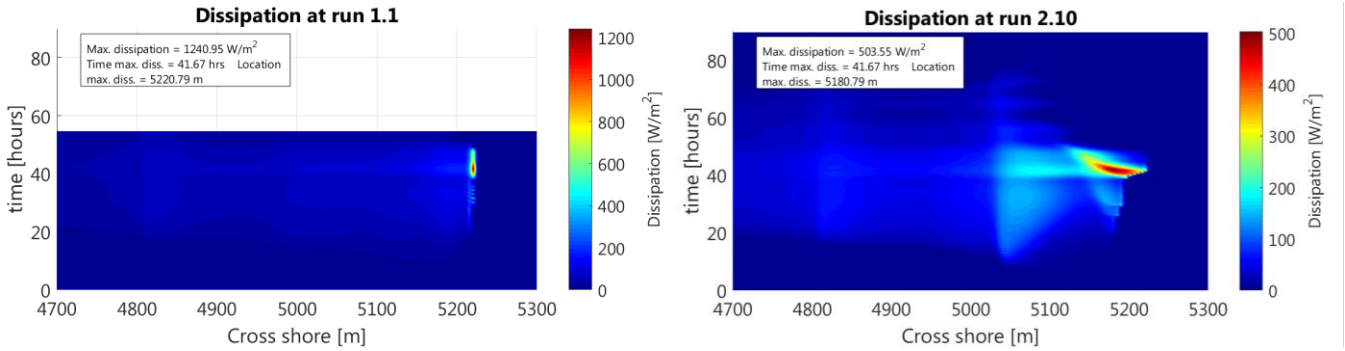

FIGURE 5.1.1. DISSIPATION DURING RUN 1.1 AND RUN 2.10. IT CAN BE SEEN THAT THE HEIGHT AND DENSITY OF THE DISSIPATION REGIONS DIFFER FOR CASE OF THE SEAWALL AND THE HYBRID VARIANT.

DUNE WIDTH The influence of the dune width is tested with 4 specific runs. The configuration of these run are displayed in Table 5.1.1. In Figure 5.1.2, the overall results are shown with the 4 runs for the dune width highlighted. Starting from run 2.20, it can be seen that by increasing the dune width, the maximum wave height at breaking decreases and the wave-induced set-up increases. By increasing the volume of the dune, wave energy will be dissipated more offshore, thereby reducing the wave height. This leads to less bedlevel change and a relative narrow surf zone. As a result, the energy dissipation becomes concentrated within this narrower surf zone and leads to a higher local wave force. This is then balanced with a higher set-up. Run 2.21 diverges a bit from the trend compared, however it still follows the line of expectation compared to the design of run 2.20.

TABLE 5.1.1. DESIGN PARAMETERS FOR THE DUNE WIDTH INFLUENCE MODEL SETUP

Run	Dune width [m]	Dune slope	Beach height w.r.t. MSL [m]	Beach length [m]
2.20	10	1 : 3.5	1	110
2.19	20	1 : 3.5	1	110
2.18	40	1 : 3.5	1	110
2.21	60	1 : 3.5	1	130

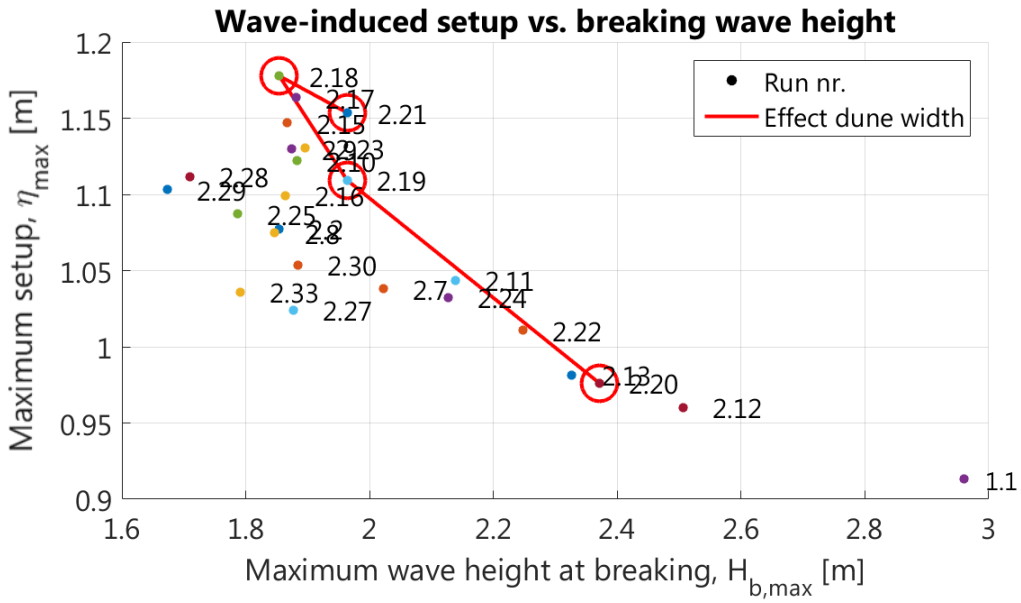

FIGURE 5.1.2. RESULTS FOR ALL THE RUNS WITH THE DUNE WIDTH INFLUENCE MODELS HIGHLIGHTED. IT CAN BE SEEN THAT STARTING FROM RUN 2.20, WHICH HAD THE SMALLEST DUNE WIDTH THE WAVE HEIGHT DECREASES AND THE SET-UP INCREASES.

DUNE SLOPE The influence of the dune slope is tested with 3 runs, which only varied in dune slope. The configuration of these designs can be seen in

Table 5.1.2. As in the case of the dune width, it can be seen that with an increase in dune slope and thus more volume on top of the seawall, the maximum wave height in the surf zone decreases and the maximum wave-induced set-up increases. This is shown in Figure 5.1.3.

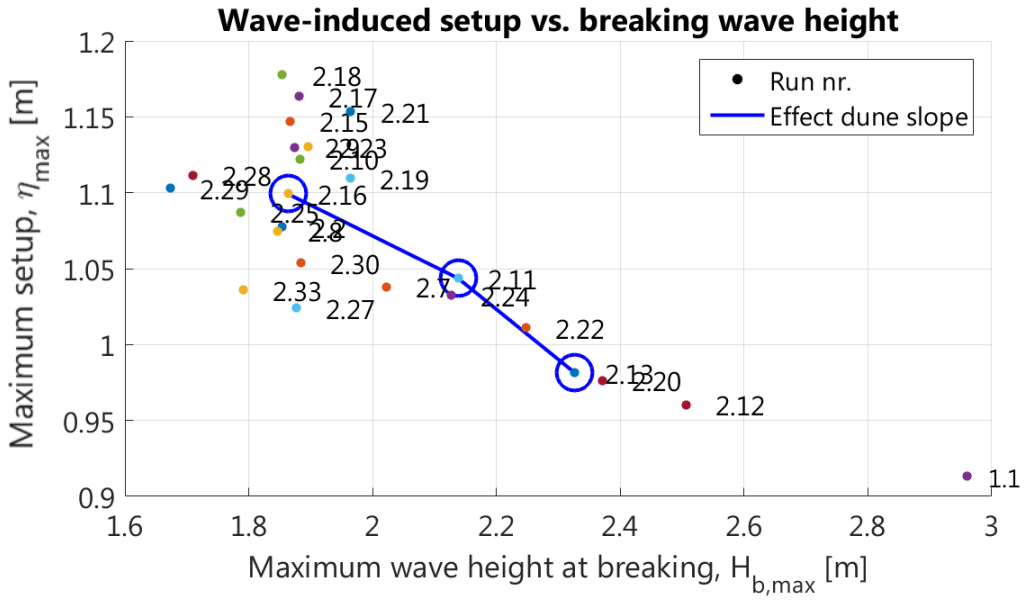

FIGURE 5.1.3. RESULTS FOR ALL THE RUNS WITH THE DUNE SLOPE INFLUENCE RUNS HIGHLIGHTED. IT CAN BE SEEN THAT STARTING FROM RUN 2.13, WHICH HAD THE SHALLOWEST SLOPE, THE WAVE HEIGHT DECREASES AND THE SET-UP INCREASES.

TABLE 5.1.2. DESIGN PARAMETERS FOR THE DUNE SLOPE INFLUENCE MODEL SETUP

Run	Dune width [m]	Dune slope	Beach height w.r.t. MSL [m]	Beach length [m]
2.13	10	1 : 3.5	1	110
2.11	10	1 : 5.5	1	110
2.16	10	1 : 8	1	110

BEACH HEIGHT The influence of the height of the beach is tested with 6 specific runs, which are divided in 3 sets of a run, with and without beach heightening. The configuration of these runs are stated in Table 5.1.3. It is clear that the increase of the beach height leads to an increase in the maximum set-up and a decrease in maximum wave height for each of these 3 comparisons, as shown in Figure 5.1.4. Due to raising of the beach, the beach slope consequently also becomes more steep. This implies that relatively more wave energy dissipates in a narrower area. Therefore the wave height is reduced and more set-up is being developed.

TABLE 5.1.3. DESIGN PARAMETERS FOR THE BEACH HEIGHT INFLUENCE MODEL SETUP

Run	Dune width [m]	Dune slope	Beach height w.r.t. MSL [m]	Beach length [m]
2.13	10	1 : 3.5	1	110
2.24	10	1 : 3.5	2.5	95
2.11	10	1 : 5.5	1	110
2.25	10	1 : 5.5	3	130
2.16	10	1 : 8	1	110
2.28	5	1 : 8	3.5	130

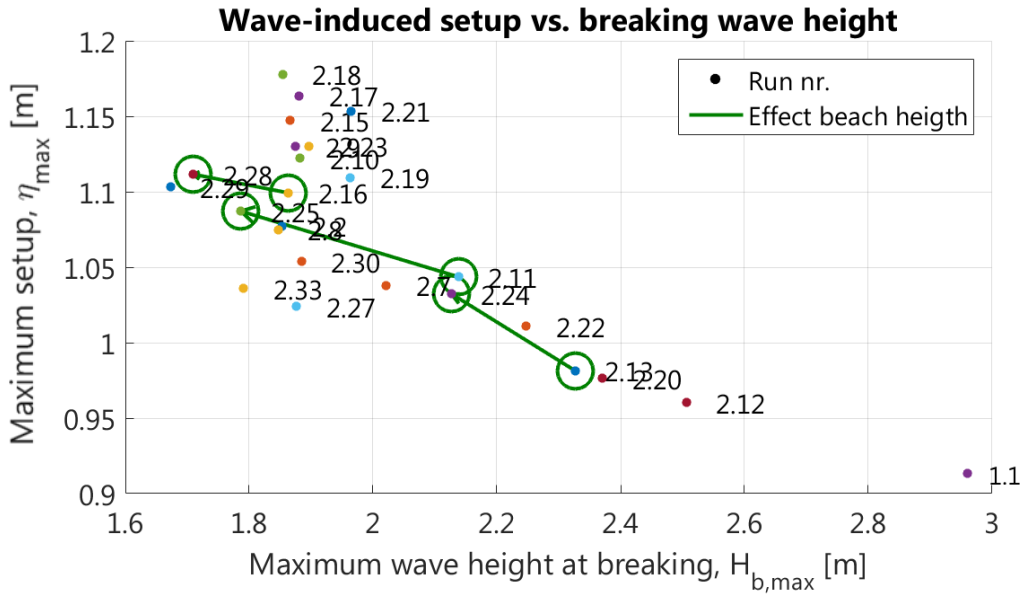

FIGURE 5.1.4. RESULT FOR ALL THE RUNS WITH THE BEACH HEIGHT INFLUENCE RUNS HIGHLIGHTED. 3 CASES HAVE BEEN CARRIED OUT, WHICH CONSISTED OF A RUN WITH AN INCREASED BEACH HEIGHT AND ONE WITHOUT. IT CAN BE SEEN THAT ALL THE CASES SHOW A SHIFT FROM THE RUN WITHOUT BEACH HEIGHTENING TO THE RUN WITH BEACH HEIGHTENING, WHICH HAS A HIGHER WAVE SET-UP AND LOWER WAVE HEIGHT.

CONCLUSION In this section, the effect of the hybrid design was elaborated and the influence of different design parameters was examined. As shown in the overall results of all the runs, it can be seen that, starting from the null case, which is just an extended version of the current seawall and no sand cover, the wave height is barely reduced and relative little wave-induced set-up occurred. Offshore of the seawall, little dissipation takes place, thereby generating small wave-induced set-up.

This process changes when a sand cover is placed over the seawall. As the waves erode the dune face of the structure, the dissipation of wave energy shifts towards a location more offshore and takes place over a larger area. Due to this stronger dissipation, a higher local waveforce is being generated, which is balanced by a higher wave-induced set-up. This effect can lead up to an overall reduction of the wave height in the surf zone by approximately 40 % and an increase in wave-induced set-up by approximately 25 %.

In the examination of all the isolated cases that focuses on the impact of each design parameter, it can be shown that more volume of sand that covers the seawall leads to a shift towards lower wave height in the surf zone and higher wave-induced setup.

5.2. EXPOSURE OF THE SEAWALL

In the last section, the overall trend in the scatter of all the runs was elaborated. However, after closer inspection and model simulations, it became clear that a significant amount of runs did not reduced the wave height, but kept increasing in maximum wave-induced set-up, as encircled in Figure 5.2.1. To look into this effect, 3 runs were selected. These are runs are run 2.13, 2.16, 2.15 and 2.18 as shown in Figure 5.2.2. and Table 5.2.1. Each profile was taken at the moment the maximum wave height at breaking occurred, $t_{H_b,max}$.

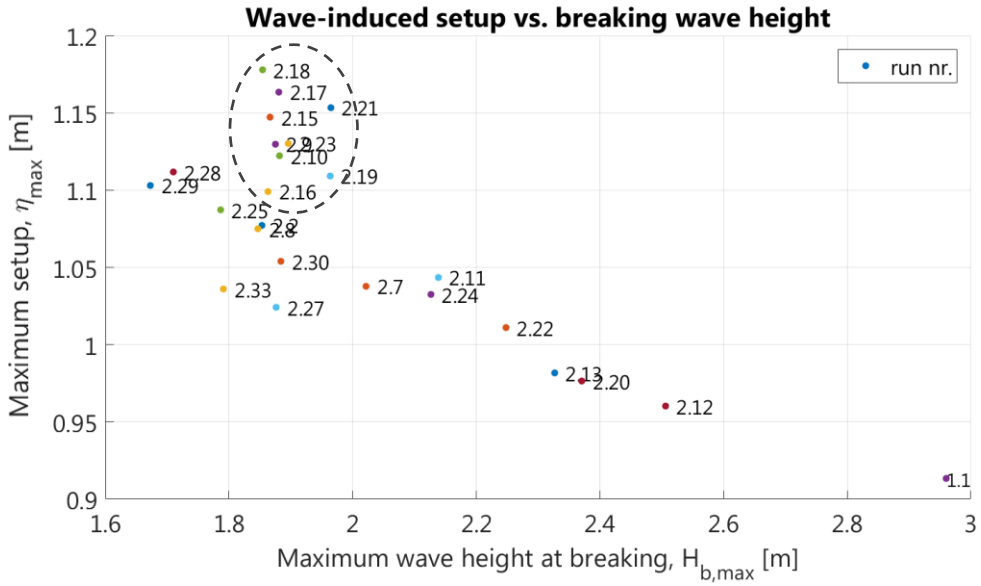

FIGURE 5.2.1. RESULTS OF ALL THE RUNS WITH THE DEVIATING RESULTS ENCIRCLED. IN THESE DESIGNS THE WAVE HEIGHT DID NOT DECREASED ANY MORE, HOWEVER THE SET-UP HYBRID INCREASE.

Run 2.13 shows the behavior as established in the previous section. From Figure 5.2.2, it can be seen that a significant part of the total dissipation takes place on the beach and the dune face, which is eroded away over time. However at the peak of the storm, the seawall becomes exposed and most part of the dissipation takes place at the seawall. Therefore, very little set-up is being generated, which is similar to the null case as seen in section 5.1. . Once the seawall becomes exposed, scour will occur in front of the structure. This turbulent region speeds up the process of erosion of the sand cover in front of the seawall and exposing it even more.

From run 2.16 it becomes clear that the seawall is also exposed at $t_{H_b,max}$. However, due to the design of the sand cover, more dissipation takes place on the beach and the dune face as the storm develops. The resulting ratio of the wave height and the wave set-up is also in the line of expectations. However from this point, some runs are not effectively reducing the wave height anymore.

In run 2.15, it can be seen that at $t_{H_b,max}$ the seawall is still not exposed, due to the vast volume of sand cover in this design. Therefore, as the dune face erodes, a gradual profile develops, starting from the beach up to the eroded dune face. Due to the limited water depth, nearly all the dissipation takes place in this wider area. This results in a higher total set-up.

This effect becomes even more clear in run 2.18 where the dune is still present at $t_{H_b,max}$. Due to the resulting shallow surf zone, all of the dissipation takes place in this region. This gives rise to a higher wave-induced set-up, without decreasing the wave height significantly compared to the previous cases. In case of run 2.18, the seawall was raised with an additionally 0.5 m. Some cases without this increment led to overflow due to this extra set-up.

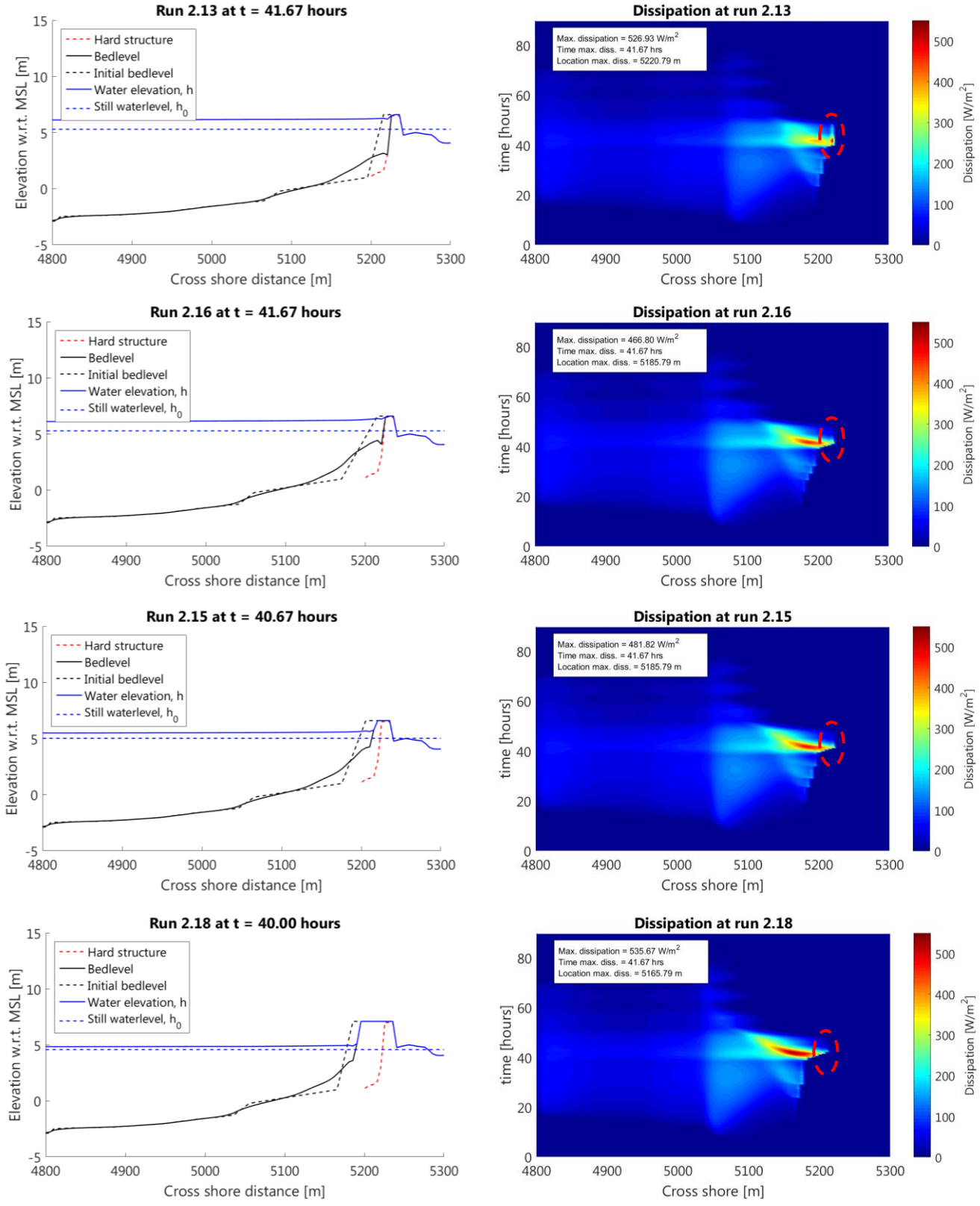

FIGURE 5.2.2. STATE OF THE HYBRID AT $T_{HB,MAX}$ AND THE DISSIPATION ALONG THE CROSS SHORE OVER TIME. INDICATED IN THE RED CIRCLES IS THE DISSIPATION AT THE EXPOSED SEAWALL. IN RUN 2.15 AND 2.18 THIS REGION DISAPPEARS

TABLE 5.2.1. DESIGN PARAMETERS FOR THE MODEL SETUP OF THE DIVERGING RUNS

Run	Dune width [m]	Dune slope	Beach height w.r.t. MSL [m]	Beach length [m]	Height seawall
2.13	10	1 : 3.5	1	110	6.5
2.15	20	1 : 5.5	1	110	6.5
2.16	10	1 : 8	1	110	6.5
2.18	40	1 : 3.5	1	130	7

CONCLUSION With a general trend observed in the previous section, the conclusion made was that the ratio of maximum wave height in the surf zone and the wave-induced set-up, depends on the dimensions and total volume of the sand cover. However some runs diverge from this result by not further decreasing the wave height, but did show an increase in set-up. By examining the cross sections and dissipation rates during these runs, it was found that this is due to the extensive volume of the sand cover on top of the seawall during the peak of the storm. Explanation could be that due to the eroding of the dune face without exposing the seawall, a gradual slope from the beach and the dune develops. This creates a wide and shallow surf zone in which all the wave energy dissipation takes place. This results into a higher total wave-induced set-up.

5.3. INFLUENCE OF SEAWALL CORE

The difference between a vertical seawall and a dike core is examined by simulating several hybrid designs with a vertical wall with a sand cover and performing the exact same case with a dike as core structure. To test this effect, 3 cases have been performed, as shown in Figure 5.3.1. This dike structure is modeled as a smooth non-erodible layer, so any effects such wave reduction by revetments are not taken into account in these simulations.

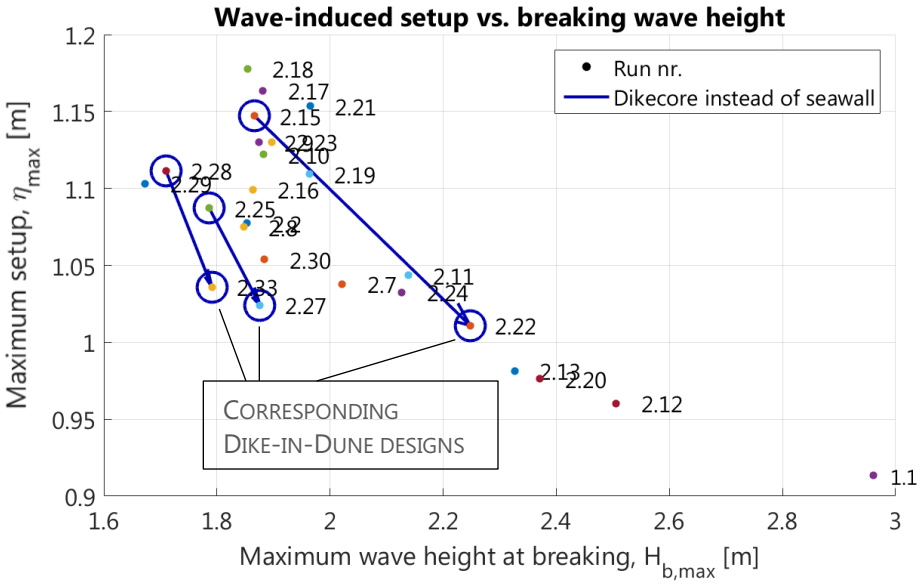

FIGURE 5.3.1. RESULTS OF ALL THE RUNS WITH THE SEAWALL CORE HYBRID AND THE CORRESPONDING DIKE-IN-DUNE DESIGN.

It can be seen that for each of the 3 cases, the transition of the non-erodible core from a seawall variant to a dike variant results in a slightly higher maximum wave height at breaking and a lower maximum set-up. This effect is examined with the use of run 2.28 and run 2.33, as shown in Figure 5.3.2 and

Table 5.3.1.

Run 2.28 is the case with a vertical wall as non-erodible core in combination with a sand cover. The results match the expectation, as the dissipation takes place on the beach and eroded dune face in the beginning of the storm. In this emerged shallow surf zone, the wave height is lower compared to the case without a sand cover. However, this gradual dissipation results into a higher wave-induced set-up. Less volume of sand on top of the vertical wall will result in an earlier exposed seawall and larger water depth in front of the wall. This will result in a higher wave height and less dissipation in the surf zone, therefore a lower wave-induced set-up, as found in the cases in section 5.1.

If the vertical wall core is replaced by a dike (e.g. a non-erodible layer with a slope), the footprint of the core becomes bigger compared to the seawall, as can be seen in Figure 5.3.2. It can also be seen that less sand cover volume is needed to achieve the same barrier width, compared to run 2.28. Figure 5.3.2. also shows the wave energy dissipation during the peak of the storm. Most of the dissipation pattern, both spatially and in time, stays the same compared to run 2.28. However, due the sloped seawall, less scouring takes place at the tow of the structure. Once the seawall is exposed during the peak of the storm, less material has been scoured and lays in front of the structure. Therefore, the maximum dissipation takes place on the slope of the dike instead of at the foreshore. This results in a lower wave-induced set-up, but a slightly higher wave height in the surf zone. However, this higher wave energy finally dissipates on the sloped dike.

TABLE 5.3.1. DESIGN PARAMETERS FOR THE MODEL SETUP OF THE DIVERGING RUNS

Run	Dune width [m]	Dune slope	Beach height w.r.t. MSL [m]	Beach length [m]	Non-erod. core structure
2.28	5	1 : 8	3.5	130	Vertical wall
2.33	5	1 : 8	4	110	Dike (1 : 5)

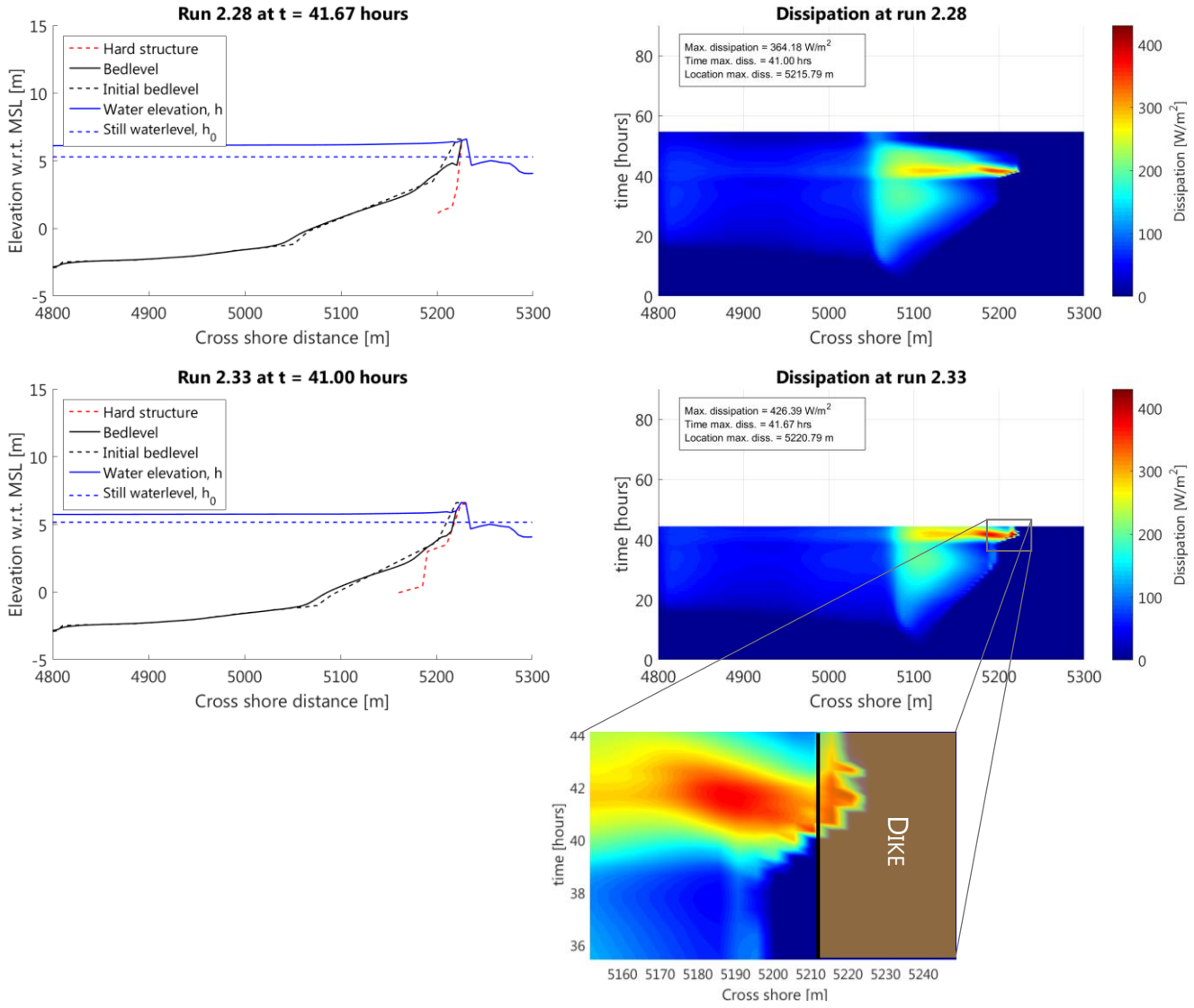

FIGURE 5.3.2. CROSS SECTION OF RUN 2.28 AND 2.30 AT $T_{Hb,MAX}$ AND THE DISSIPATION ALONG THE CROSS SHORE OVER TIME. THE TOP PANELS SHOW THE RESULTS OF RUN 2.28, WHICH BEHAVIOR IS IN LINE WITH EXPECTATIONS. THE LOWER PANELS SHOW THE RESULTS FOR THE DIKE-IN-DUNE MODEL. THE DIKE IS SHOWN IN THE DASHED RED LINE WITH THE COMBINATION OF A TOW PROTECTION IN FRONT OF IT, WHICH IS CONSIDERED NON-ERODIBLE AS WELL.

CONCLUSION

Changing the non-erodible layer from a vertical wall to a sea dike or sloped core, has a positive effect. In case of a sloped non-erodible structure, the wave-induced set-up can be decreased. By changing the shape of the sea wall into a sea dike, the structure attains a larger footprint. During a storm, the sea dike with a sand cover becomes exposed at an earlier stage. Due to the relative smaller volume of scoured material in front of the structure, less dissipation takes place in this region and less set-up is being generated. However, due to this lower dissipation in the foreshore, the wave height remains relative high. This remaining wave energy is finally dissipated along the fixed slope of the exposed sea dike, which gradually reduces the wave height.

In the model set-up, the dike core was modeled as a smooth non-erodible slope. In reality dike slopes are constructed with a revetment that is designed to reduce the load of waves on the dike. Therefore, it is expected that a hybrid design with a sea dike with revetment as a core can effectively reduce the wave height even more, once exposed. This is a big advantage in comparison with variants with vertical seawalls as a core.

6. CONCLUSIONS

In this research the effect of hybrid solution for the Galveston Seawall is examined. This is done by modeling the seawall with different sand cover designs in a process-based numerical model, XBeach. The model was validated with use of the historic event Ike and then applied to simulate different hybrid designs in a design storm. The starting position for applying the concept of a hybrid solution is to keep the solution as low as possible, not to disconnect the city of Galveston with the beachfront. The results of these simulations were validated using theoretical formulations and examined for general behavior or trends. To conclude this report, the stated research questions will be stated once more.

The main research question was:

WHAT IS THE IMPACT OF A SAND COVER AT THE GALVESTON SEAWALL ON THE HYDRAULIC LOADS?

Within this research questions several sub questions were formulated. These sub questions will be stated and then answered accordingly to the findings of this research.

WHICH HYDRAULIC PROCESSES ARE SIGNIFICANT FOR TESTING THE HYBRID DESIGNS ?

In the literature review, several processes were discussed that are of importance as waves propagate towards the shore. These processes mainly deal with the relation between wave energy and the effect of the water depth and the bed. Important processes for the testing of the hybrid designs are the wave height in the surf zone and the wave-induced set-up.

WHAT IS THE RELATION BETWEEN THE HYBRID STRUCTURE AND THE HYDRAULIC PROCESSES?

In the initial case, where there is no sand cover on top of the seawall, nearly all the wave energy dissipates at the seawall during the design storm. It was found that the wave height is barely reduced and a relative small wave-induced set-up is formed. This process changes when a sand cover is applied on top of the seawall. The dissipation of the wave energy shifts offshore and spreads over a larger length. The wave height is being reduced as it progresses towards shore and simultaneously the dissipation of the wave energy drives a wave-induced set-up in the surf zone.

IN WHAT WAY DOES THE DIMENSIONS OF THE SAND COVER INFLUENCE THE HYDRAULIC PROCESSES?

Changing the dimensions of the sand cover within the hybrid design shows a general trend. It was found that more volume of material that covers the seawall leads to a lower wave height in the surf zone and a higher wave-induced setup. As the dune face is being eroded, more material is being deposited in front of the structure. This creates a shallow surf zone, in which the most of the wave energy dissipation takes place. This generates larger wave forces, which are balanced by a higher wave-induced set-up. This can even lead to a situation with overflow, if these volumes becomes too big and the elevation of the structure is kept at a minimum.

IN WHAT WAY DOES THE SHAPE OF THE SEAWALL INFLUENCE THE HYDRAULIC PROCESSES?

The Galveston seawall is a vertical seawall, which can be incorporated into the hybrid design. However, it was found that by changing the vertical wall into a sea dike as a core, the wave-induced set-up can be decreased. In case of a sea dike core, the structure attains a larger footprint with a relative smaller volume of sand cover. The sea dike becomes exposed more earlier and less eroded material is present in front of the structure. This causes less dissipation in the foreshore and generates less wave-induced set-up. The wave energy, however, is being dissipated on the slope of the exposed sea dike, where also the maximum energy dissipation takes place. Due to the slope of the dike, the waves are being dissipated more gradual, reducing the wave height effectively compared to case of a vertical sea wall. It is expected that a hybrid design with a dike core in combination with revetment reduce the wave height even more, once the dike becomes exposed.

7. RECOMMENDATIONS

In this research, several conclusions are made. However, some assumptions were made that require additional investigation in order to determine the effect of these schematizations.

- The hybrid designs, that are used in this study, were conceived with the requirements of a limited sand cover volume and keeping the total elevation of the barrier as low as possible. However, hybrid designs with higher elevations or bigger sand cover volumes, may lead to more desirable results that outweigh the costs.
- The simulations were carried out with a single grain size distribution. However, multiple grain sizes are present at the Upper Texas Coast, resulting in a more complex morphology as has been assumed. Also the stabilizing effect of vegetation in dunes or the sand cover are not considered. These aspects has to be taken into account for future design assessments as well as for future efforts of modeling Galveston Island for others purposes.
- The determination of the non-erodible layer was done via a relative simple procedure. The groins that are present at the Galveston seawall, are also not incorporated. It is recommended to improve the schematization of the Galveston coastline and include other structures to acquire more accurate results.
- The used bathymetry was based on a single DEM. As a result, the resolution of the bathymetry and the grid at the nearshore and the seawall was relative course. In order to accurately simulate the impact of a hybrid in this region, as well for future modeling of Galveston Island, this resolution has to be improved by merging different bathymetry with finer resolutions.
- The hybrid designs were judged on the reduction of the wave height at breaking closest to shore and the reduction of the wave-induced set-up. Other design parameters, such as the amount of overtopping and the required freeboard are not considered. Also the amounts of erosion of the sand cover and the stability of the seawall as an consequence are not looked into. Future design assessments have to incorporate these processes as well as an cost-benefit analysis of the amount of erosion and upkeep of the sand cover, to prove if a hybrid is a feasible solution at the Galveston seawall.
- To test the hybrid designs, a design storm was compiled from earlier work. The used data consisted out of the maximum wave height and set-up during the development of the storm. As a consequence, no characteristic value could be determined, nor is it possible to determine a interval of confidence of these values. It is recommended to run test with design storms with significant values.

8. BIBLIOGRAPHY

Almarshed, B.F., 2015. Hydrodynamic design conditions from measured data. Texas A&M University, Galveston, TX.

Almarshed, B.F., unpublished. Phd. research. Texas A&M University, Galveston, TX.

Anderson, J.B., 2007. The Formation and Future of the Upper Texas Coast: A Geologist Answers Questions about Sand, Storms, and Living by the Sea. Texas A&M University Press.

Angelou Economics, 2008. Tourim Economic Impact Analysis, Galveston Island.

Arcadis, 2013. Projectplan Kustversterking Katwijk. Arcadis Nederland BV.

Arcadis, 2008. Verbeteringsplan Versterking zeewering Scheveningen. Arcadis Ruimte & Milieu BV, Alkyon Hydraulic Consultancy & Research BV.

Atlantic Oceanographic & Meteorological Laboratory, 2014. Hurricane Research Division, FAQ [WWW Document]. Atl. Oceanogr. Meteorol. Lab. NOAA. URL http://www.aoml.noaa.gov/hrd/tcfaq/G16.html (accessed 12.13.16).

Battjes, J.A., 1974. Surf similarity, in: Proc. 14th Int. Conf.Coastal Engineering. pp. 466–480.

Battjes, J.A., Janssen, J., 1978. Energy loss and set-up due to breaking of random waves, in: Proc. of 16th Int. Conf. Coastal Engineering. ACSE, pp. 569–587.

Berg, R., 2009. Tropical Cyclone Report Hurricane Ike (No. AL092008). National Hurricane Center.

Bosboom, J., Stive, M.J.F., 2015. Coastal Dynamics I, lecture notes CIE4305, 0.5. ed. Delft Academic Press, Delft.

Bureau of Economic Analysis, 2016. Gross Domestic Product by Metropolitan Area, 2015 (No. BEA 16-49). Bureau of Economic Analysis.

Daly, C., 2009. Low frequency waves in the shoaling and nearshore zone. Delft University of Technology, Delft.

de Vries, P.A.L., 2014. The Bolivar Roads Surge Barrier: A conceptual design for the environmental section. Delft University of Technology, Delft.

Deltares, 2016. OpenEarth [WWW Document]. URL https://publicwiki.deltares.nl/display/OET (accessed 9.20.16).

Deltares, 2012. Technisch Rapport Duinwaterkeringen en Hybride Keringen (No. 1206018-1-NaN-9). Deltares, Delft.

Figlus, J., 2016. Personal communication.

Greater Houston Partnership, 2016. Population update, Greater Houston Partnership Research. Greater Houston Partnership.

Harter, C., 2015. The impact of Hurricane Ike on the geomorphology of Follett's Island, Texas - Short and long term effects. Texas A&M University.

Holthuijsen, L.H., 2010. Waves in oceanic and coastal waters, 2nd ed. Cambridge University Press, New York.

Hu, K., Chen, Q., 2011. Directional spectra of hurricane-generated waves in the Gulf of Mexico. Geophys. Res. Lett. 38, L19608. doi:10.1029/2011GL049145

Jin, J., Jeong, C., Chang, K.-A., Song, Y.K., Irish, Edge, 2010. Site specific wave parameters for texas coastal bridges: Final report (No. FHWA/TX-10/0-6063-1). Texas A&M University at Galveston, Galveston, TX.

Jonkman, S.N., Lendering, K.T., van Berchum, E.C., Nillesen, A., Mooyaart, L., de Vries, P., Ledden, M. van, 2015. Coastal spine system-interim design report. TUDelft, IV-infra, Royal HaskoningDHV, Texas A&M University, Defacto.

Keim, B.D., Muller, R.A., Stone, G.W., 2007. Spatiotemporal Patterns and Return Periods of Tropical Storm and Hurricane Strikes from Texas to Maine. J. Clim. 20, 3498–3509. doi:10.1175/JCLI4187.1

Kennedy, A.B., Gravois, U., Zachry, B., 2011a. Observations of landfalling wave spectra during Hurricane Ike. J. Waterw. Port Coast. Ocean Eng. 137, 142–145.

Kennedy, A.B., Gravois, U., Zachry, B.C., Westerink, J.J., Hope, M.E., Dietrich, J.C., Powell, M.D., Cox, A.T., Luettich, R.A., Dean, R.G., 2011b. Origin of the Hurricane Ike forerunner surge. Geophys. Res. Lett. 38, L08608. doi:10.1029/2011GL047090

Lendering, K.T., van der Toorn, A., de Vries, P., Mooyaart, L., van Ledden, M., Willems, A., Jonkman, S.N., 2014. Report Galveston Bay: Barge barrier design: phase 3. TUDelft, IV-infra, Royal HaskoningDHV.

McCall, R.T., 2008. The longshore dimension in dune overwash modelling: development, verification and validation of XBeach. Delft University of Technology, Delft.

McCall, R.T., Van Thiel de Vries, J.S.M., Plant, N.G., Van Dongeren, A.R., Roelvink, J.A., Thompson, D.M., Reniers, A.J.H.M., 2010. Two-dimensional time dependent hurricane overwash and erosion modeling at Santa Rosa Island. Coast. Eng. 57, 668–683. doi:10.1016/j.coastaleng.2010.02.006

Merrell, W., 2010. Let's Build the Ike Dike.

Merrell, W., Whalin, R.W., 2013. The Ike Dike: A Coastal Barrier Protecting the Houston/Galveston Region from Hurricane Storm Surge. Presented at the THC-IT-2013 Conference & Exhibition.

Ministerie van Verkeer en Waterstaat, 2003. Procesplan zwakke schakels in de Nederlandse kust, Bestuurlijk overleg kust.

Nederhoff, C.M., 2014. Modeling the effects of hard structures on dune erosion and overwash. Delft University of Technology, Delft.

NOAA, 2016a. Extreme Water Levels [WWW Document]. URL http://tidesandcurrents.noaa.gov/est/ (accessed 11.17.16).

NOAA, 2016b. Extreme Water Levels - Galveston Pleasure Pier, TX [WWW Document]. URL https://tidesandcurrents.noaa.gov/est/est_station.shtml?stnid=8771450 (accessed 4.5.17).

NOAA, 2016c. NDBC Station Page [WWW Document]. URL http://www.ndbc.noaa.gov/station_page.php?station=42035 (accessed 12.2.16).

NOAA, 2016d. Sea Level Trends: Galveston Pleasure Pier [WWW Document]. URL https://www.tidesandcurrents.noaa.gov/sltrends/sltrends_station.shtml?stnid=8771510 (accessed 12.2.16).

NOAA, 2008. Digital elevation model of Galveston, Texas: Procedures, data sources and analysis (No. Technical Memorandum NESDIS NGDC-12). NOAA.

NOAA, 2006. Pre-Ike LiDAR survey from Galveston County [WWW Document]. URL https://coast.noaa.gov/dataviewer/#/lidar/search/ (accessed 3.27.17).

NOAA, NGS, 2017. National Spatial Reference System, Geodetic control map [WWW Document]. URL https://www.ngs.noaa.gov/NGSDataExplorer/ (accessed 3.7.17).

NOAA, USACE, 2009. Post-Ike LiDAR survey from Galveston County [WWW Document]. URL https://coast.noaa.gov/dataviewer/#/lidar/search/ (accessed 3.27.17).

Paine, J.G., 1993. Subsidence of the Texas coast: inferences from historical and late Pleistocene sea levels. Tectonophysics, Tectonophysics 222, 445–458.

Paine, J.G., Mathew, S., Caudle, T., 2012. Historical shoreline change through 2007, Texas Gulf Coast: rates, contributing causes, and Holocene context. GCAGS J. V 1 2012 13–26.

Rippi, K., 2014. Bolivar Roads Surge Barrier: How to estimate the optimal barrier height after a risk assessment. IV group, Delft University of Technology, Delft.

Roelvink, D., Reniers, A., van Dongeren, A., van Thiel de Vries, J., McCall, R., Lescinski, J., 2010. XBeach Model Description and Manual. Unesco-IHE Institute for Water Education, Deltares and Delft University of Technology.

Roelvink, D., Reniers, A., van Dongeren, A., van Thiel de Vries, J., McCall, R., Lescinski, J., 2009. Modelling storm impacts on beaches, dunes and barrier islands. Coast. Eng. 56, 1133–1152. doi:10.1016/j.coastaleng.2009.08.006

Sallenger, A.H., 2000. Storm Impact Scale for barrier islands. J. Coast. Res. 3, 890–895.

Sass, R.L., 2011. Water currents and the protection of Upper Texas coastal marshes, bays and estuaries from oil spills in the Gulf of Mexico. James A. Baker III Institute for Public Policy, Rice University, Houston, TX.

Sorensen, R.M., 2006. Basic coastal engineering, 3rd ed. ed. Springer Science+Business Media, New York.

SSPEED Center, 2015. Houston-Galveston Area Protection System (No. 2015 Annual Report). Severe Storm Prediction, Education and Evacuation from Disasters Center.

SSPEED Center, 2010. Learning the lessons of Hurricane Ike. SSPEED Center, Houston, TX.

Stoeten, K.J., 2013. Hurricane surge risk reduction for Galveston Bay. Delft University of Technology, Delft.

Sutton-Grier, A.E., Wowk, K., Bamford, H., 2015. Future of our coasts: The potential for natural and hybrid infrastructure to enhance the resilience of our coastal communities, economies and ecosystems. Environ. Sci. Policy 51, 137–148. doi:10.1016/j.envsci.2015.04.006

Taqi, A., unpublished. Wave overtopping and runup of a hybrid coastal structure under oblique wave attack. Texas A&M University at Galveston, Galveston, TX.

Texas General Land Office, 2016. Texas Coastal Sediments Geodatabase [WWW Document]. URL http://gisweb.glo.texas.gov/txsed/index.html (accessed 12.6.16).
Tsai, C.-P., Chen, H.-B., Hwung, H.-H., Huang, M.-J., 2005. Examination of empirical formulas for wave shoaling and breaking on steep slopes. Ocean Eng. 32, 469–483. doi:10.1016/j.oceaneng.2004.05.010
U.S. Army Corps of Engineers, 2014. Galveston Island, Texas, Sand Management Strategies. U.S. Army Corps of Engineers.
U.S. Army Corps of Engineers, 1981. Galveston's bulwark against the sea; History of the Galveston Seawall.
USGS, 2009. Hurricane Ike: Observations and Analysis of Coastal Change (No. 2009–1061). USGS.
USGS, 2008. Pressure and surface elevation gauges as part of Hurricane Ike storm surge project [WWW Document]. URL https://pubs.usgs.gov/of/2008/1365/downloads/ike_SSS-TX-GAL-008.txt (accessed 12.4.16).
van Berchum, E.C., de Vries, P.A.L., de Kort, R.P.J., 2016. Galveston Bay Area. TUDelft, Royal HaskoningDHV, Defacto, Delft.
Van der Meer, J.W., Allsop, N.W.H., Bruce, T., De Rouck, J., Kortenhaus, A., Pullen, Schüttrumpf, H., Troch, P., Zanuttigh, B., 2016. EurOtop, 2016. Manual on wave overtopping of sea defences and related structures.
Weggel, J.R., 1973. Maximum breaker height for design, in: Coastal Engineering 1972. pp. 419–432.
West, N.A., 2014. Conceptual Design and Physical Model Tests of a Levee-in-Dune Hurricane Barrier. Texas A&M University.
Williams, A.M., Feagin, R.A., Smith, W.K., Jackson, N.L., 2009. Ecosystem impacts of Hurricane Ike on Galveston Island and Bolivar Peninsula: perspectives of the coastal barrier island network (CBIN). Shore Beach 77, 71.
Young, I.R., 2006. Directional spectra of hurricane wind waves. J. Geophys. Res. Oceans 111, C08020. doi:10.1029/2006JC003540
Young, I.R., 1998. Observations of the spectra of hurricane generated waves. Ocean Eng. 25, 261–276. doi:10.1016/S0029-8018(97)00011-5

APPENDIX A DATA ANALYSIS

A data analysis is preformed to obtain information of the bathymetry, hydraulic boundary conditions and the historic coastline changes. Different surveys and stations have been evaluated, as shown in Figure A.1.1. In this section these data sources are briefly handled.

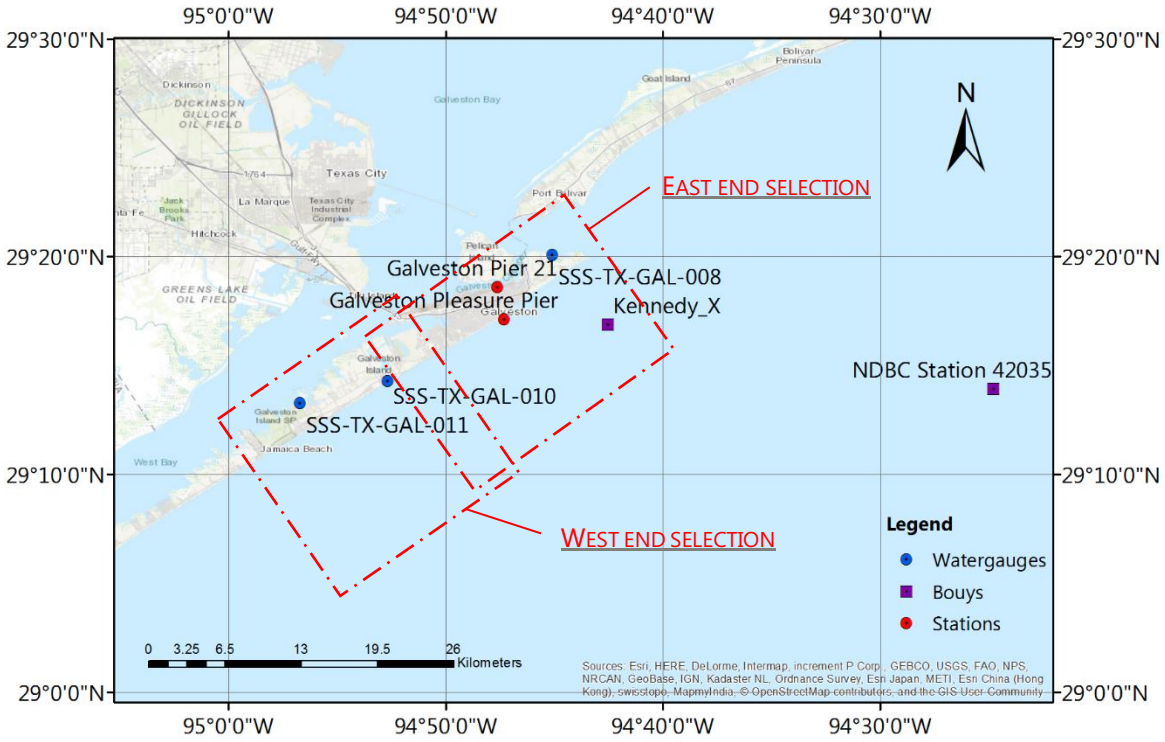

FIGURE A.1.1. OVERVIEW OF THE LOCATIONS OF ALL THE USED DATA SOURCES. INDICATED IN THE RED DASHED SQUARES ARE THE SELECTED AREAS FOR THE VALIDATION PROCESS.

A.1. DIGITAL ELEVALTION MODEL

The modeling requires a fine resolution bathymetry in order to capture all the nearshore processes. Use has been made of a digital elevation model (DEM) of the Galveston bay area. This 3D representation of a terrain's surface is constructed with data from several US federal, state and local entities and contains bathymetry, shoreline and land surveys (NOAA, 2008). This data represents the surface elevation, by combining the topography, hydrographic surveys and bathymetry of the dredged channels. Buildings and high rise structures are excluded from the data.

The DEM has a grid spacing of 1/3 arc second (~10.0 m). The bathymetry in front of Galveston Island was mainly measured around 1980 to 2002. An overview of the specifics of the DEM are stated in Table 5.3., and is shown in Figure 5.3.2.

Three selections were made of the DEM to form the bathymetry in the models. The first selection is used for the testing of the hybrid designs. More of this selection is found in section 3.2. The other two selections were used for the validation of the model itself. More on the selections for the validation of the model in section D.1.

TABLE 5.3.1. SPECIFICS OF THE GALVESTON DEM, USED AS BASE FOR THE MODELS BATHYMETRIES.

Grid Area	Galveston, Texas
Coverage Area	94.3º to 95.25º W; 28.85º to 29.8º N
Coordinate System	Geographic decimal degrees
Horizontal Datum	World Geodetic System 1984 (WGS84)
Vertical Datum	Mean High Water (MHW)
Vertical Units	Meters
Grid Spacing	1/3 arc-second

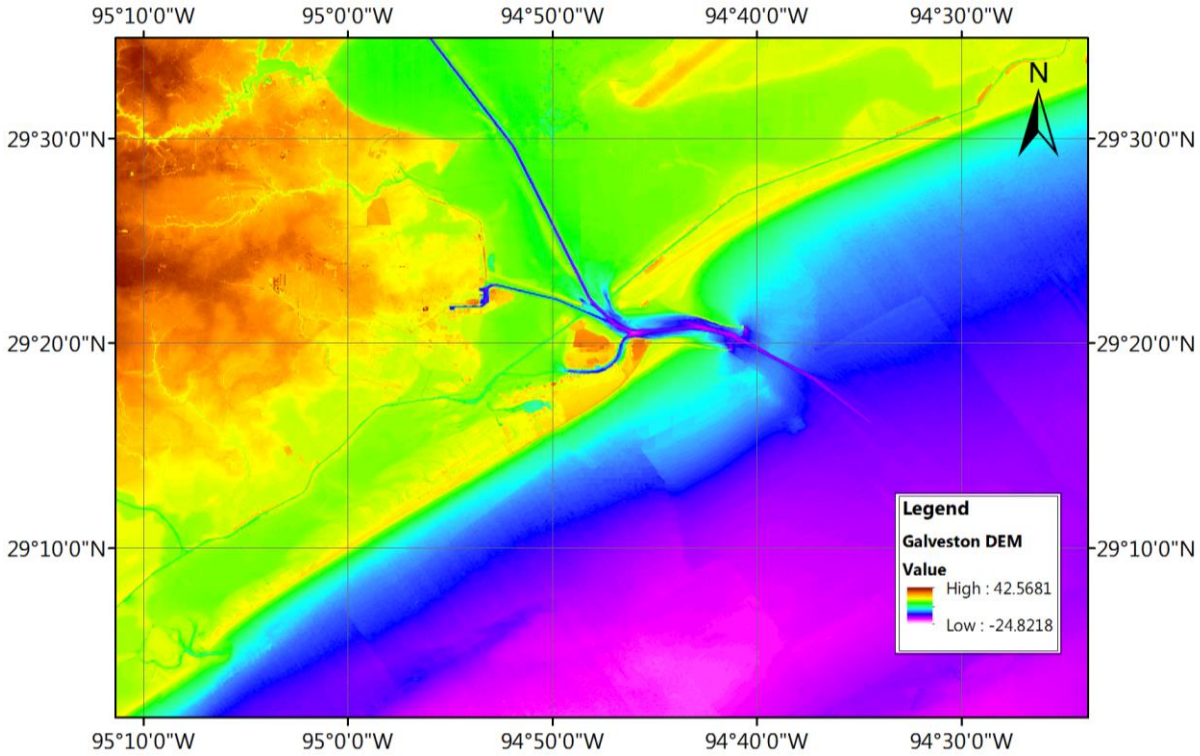

FIGURE 5.3.2. GALVESTON DEM USED AS BASE FOR THE MODELS BATHYMETRIES. INDICATED WITH A COLOR SCALE IS THE ELEVATION WITH RESPECT TO MEAN HIGH WATER.

A.2. BUOYS AND WATERLEVEL GAUGES/STATIONS

There are several permanent buoys and stations around Galveston that have been used. The locations of these stations are shown in Figure A.1.1. In this section an overview of the specifics about these stations is given.

Besides the permanent stations, some temporarily stations have been deployed in order to measure different quantities during Hurricane Ike in September 2013. The measurements that have been used are eight temporary gauges that measured hydrodynamics in front of Galveston during Ike and three on land gauges that measured pressure and water levels. The temporary gauges were deployed in front of the Upper Texas Coast, a couple days before Ike made landfall. These buoys produced 1Hz time series of the wave height, water depth and peak frequency versus yearday. (Kennedy et al., 2011a). The data of "station X" is used for the wave characteristics in the model. The United States Geological Survey (USGS) had set up three on-land gauges as part of the Hurricane Ike storm surge project. These gauges measured barometric pressure and the water level at key locations around Galveston (USGS, 2008). The water levels during the inundation stage of Ike at the lower parts of the island are used to validate the hydrodynamics in the output of the models. An overview of the used data sources is shown in Table A.2.1.

TABLE 5.3.1. OVERVIEW OF THE DATA SOURCES USED.

Name	**Station ID**	**From**	**Measures:**
Galveston Pleasure Pier	8771510	NOAA	Acoustic WL, air temp., water temp., barometric pressure
Galveston Pier 21	8771450	NOAA	Acoustic WL, air temp., water temp., barometric pressure
Offshore buoy	S42035	NDBC	Wind speed/direction, wave height/period, barometric pressure, temperature a.o.
Rapid deployed buoys	Buoy X	A. Kennedy	Wave height, water depth, peak freq.
On-land water gauges	SSS TX GAL 008/010/011	USGS	Barometric pressure, WL

A.3. SURVEYS

The key quantity in the output of the models is the coastline change and the cross shore coastal profile after a storm. The models are therefore validated with the use of a hurricane Ike case. The response of the model on the coastline change was referenced with pre- and post-Ike surveys of the coast and Galveston island.

In October 2006, NOAA, NOS and other entities published a data set with the surface elevation of the coastal islands. Using Light Detection And Ranging (LiDAR) systems, an multiple run mass points data set were obtained and processed to a useable LAS data set. Since the LiDAR uses laser pulses to register the surface elevation, waterbodies are an obstacle to map properly. Therefore, this dataset is contained to the land surface elevation in a situation prior to Ike (NOAA, 2006).

In April 2009, the US Army Corps of Engineers (USACE) performed a similar survey commissioned by NOAA and other entities. The goal was to establish a post hurricane Ike and Gustav topographic survey. Again LiDAR techniques were used and waterbodies were left out (NOAA and USACE, 2009).

These two data sets are used to represent a rough pre- and post-situation of Galveston Island. Since the post-Ike survey was produced a significant time after Ike actual made landfall, new coastal formations such as dunes and other accumulations of sediment had to be taken into account. Selections of these LiDAR sets are shown in Figure 5.3.1.

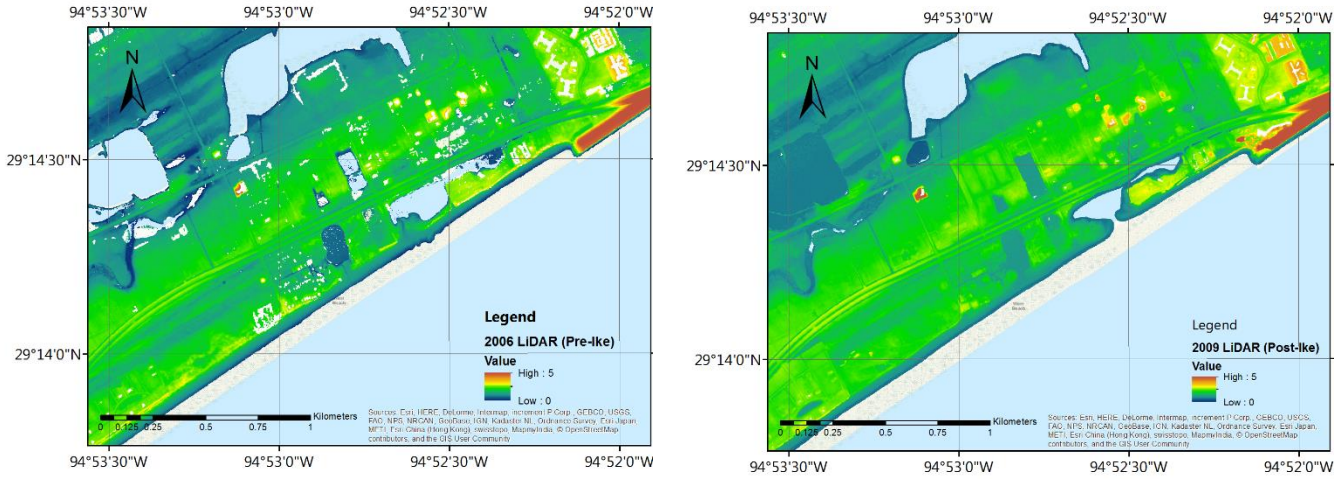

FIGURE 5.3.1. SELECTION OF THE PRE (LEFT PANEL) AND POST-IKE (RIGHT PANEL) LIDAR SURVEYS, USED IN THE VALIDATION PROCESS OF THE MODEL (NOAA, 2006, 2009).

A.4. DATUM

All the elevation data and water levels are referenced using the most recent datum reference (NOAA, 2016b).

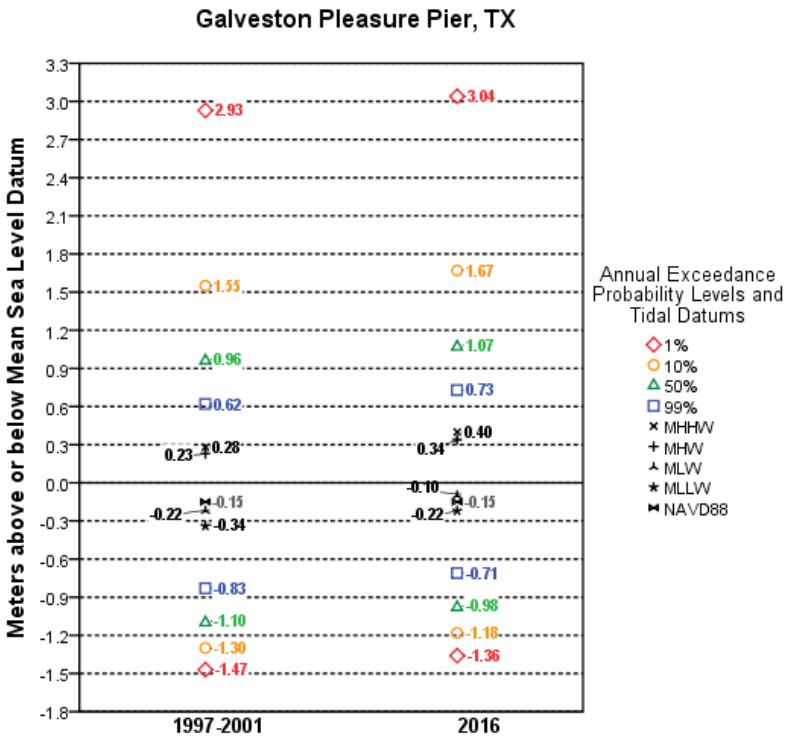

FIGURE A.4.1. TIDAL DATUMS AND EXCEEDANCE PROBABILITY LEVELS RELATIVE TO MEAN SEA LEVEL NOAA, 2016A

APPENDIX B GALVESTON BAY AND THE GALVESTON SEAWALL

B.1. GALVESTON BAY

The south coast of the United States lies on the Gulf of Mexico and is characterized by a system of estuaries, mud lands and a number of bays with barrier islands and peninsulas. The Galveston Bay is one of these areas and is situated at the Upper Texas Coast, south of Houston, as depicted in Figure B.1.1. The bay covers an area of approximately 1.150 square kilometers and is shielded by Follet's Island, Galveston Island and Bolivar peninsular. The barrier islands are not densely populated with the exception of some private own properties and the city of Galveston itself.

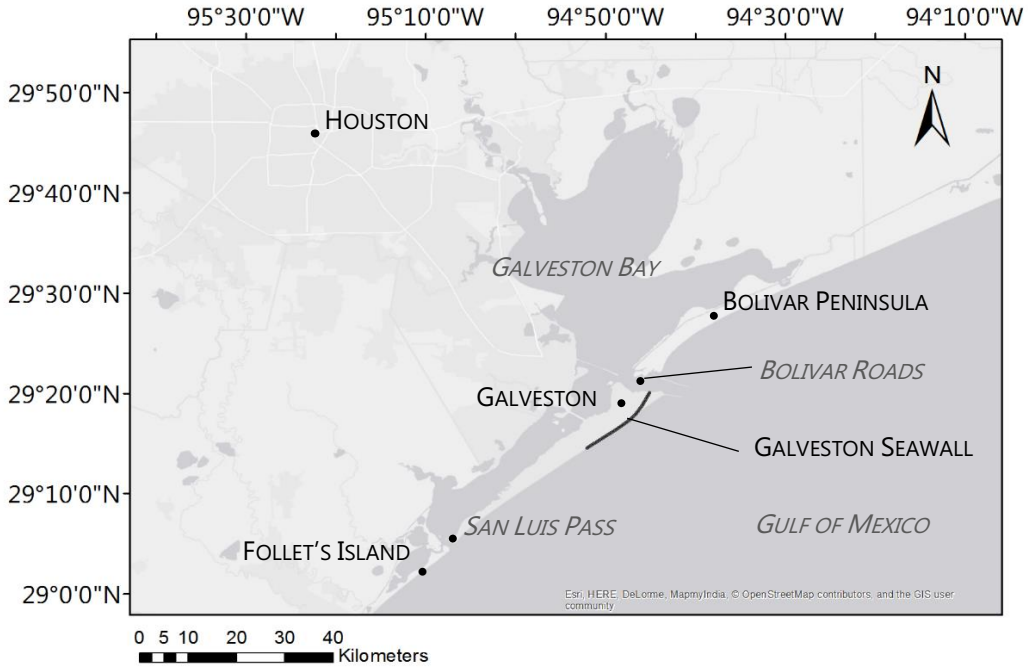

FIGURE B.1.1. GALVESTON BAY AREA

A big part of the upper Texan coastal region mainly originates from inundated marshes and deltas, the first layers on top of the Pleistocene layers are made up of clay and fine silts. When sea levels rose and offshore sandy deposits were washed towards the coast, sandy layers were created on top of the clay layers. This process continued when waves could actively move available the sand particles. Therefore, with the retreating coastline, these sandy deposits can only be found in the highly dynamic, wave dominated, nearshore zone about 5 to 6 meters of water depth. Below this so called depth of closure, sand cannot be effectively be picked up. During significant storm events sand particles are delivered to the more lower shore face. Here, these particles mixes with the muddy layers around 8 to 10 meters of depth. With the current trend of coastal retreat of the upper Texas coast, mud covers the mixed layers in the lower shore face. Beyond these depths lays the continental shelf (Anderson, 2007). The buildup of the layers can be seen in Figure 5.3.2.

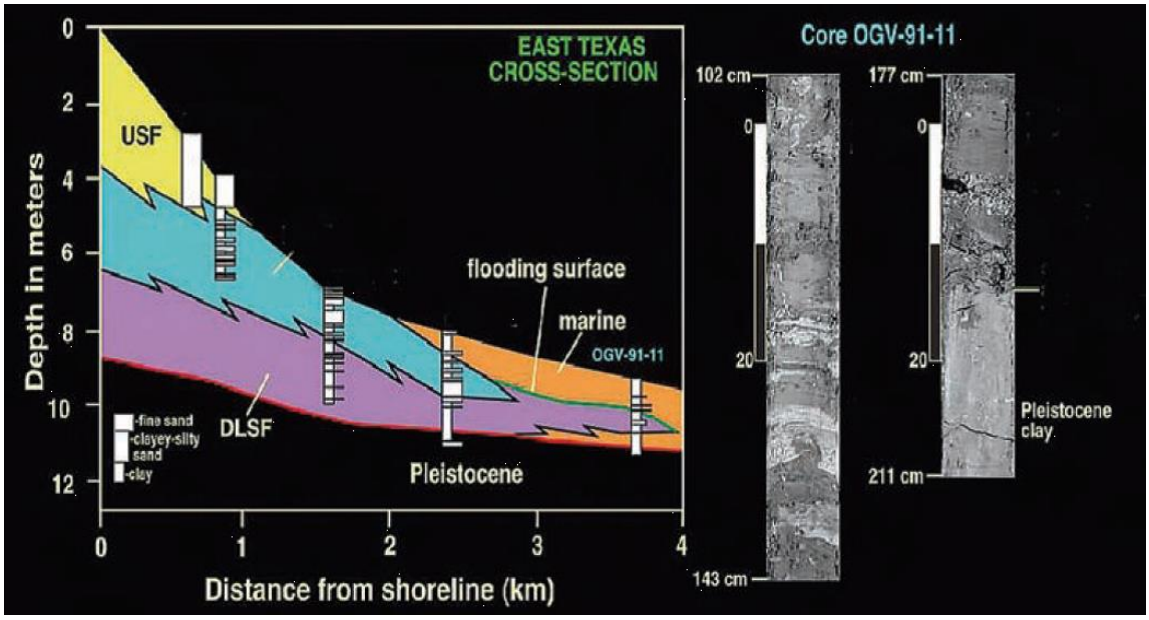

FIGURE 5.3.2. SEDIMENT CORES IN FRONT OF GALVESTON ISLAND. MOVING OFFSHORE, THE BED COMPOSITION CHANGES FROM SAND TO MUD DOMINATE. MUD LAYERS (ORANGE) COVER THE SAND AS A SIGN OF COASTAL REGRESSION (ANDERSON, 2007).

DEVELOPMENTS

The city of Galveston is protected by a large seawall and other artificial structures. After the big hurricane in 1900, the City Commission of Galveston and the County Commissioners Court of Galveston order a board of engineers to construct a defense structure against the sea. The board of engineers designed a solid concrete wall and filled at the back with excavated material from the backside of the island (Offatts Bayou).

At the end of the 19th century, the shipping channel between Bolivar Peninsula and Galveston island has been deepened several times. In order to protect the ships and to prevent the silting up of the channel the North and South jetty was constructed. These jetties implied a big change in the sediment transport along the Galveston coast. Big accumulation of sediment occurred just downstream of the South jetty forming the East Beach area, as shown in Figure B.1.3. (Anderson, 2007).

Since this seawall formed a serious impact on the sediment transport along the coast, the beach in front of the wall started to erode. In order to prevent this, a series of 13 cross shore were constructed in 1936. These consisted of timber wales and support piles. In 1970 the total groin field was rehabilitated to a total of 15 rubble mound groins. (U.S. Army Corps of Engineers, 1981).

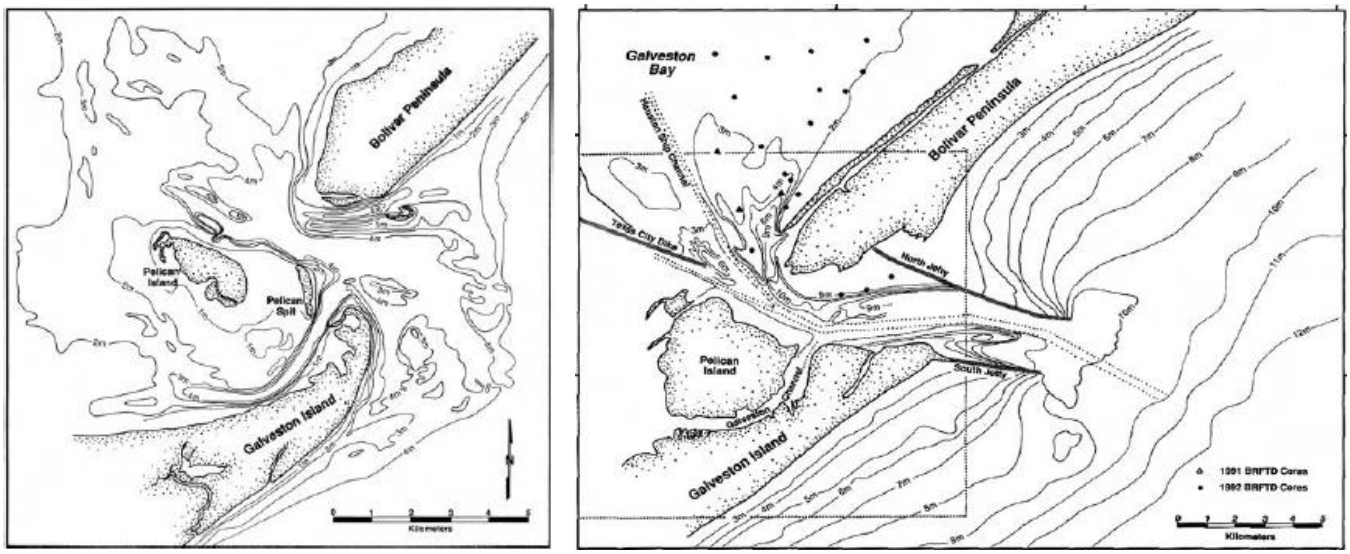

FIGURE 5.3.3. INTERVENTIONS AT GALVESTON ISLAND, AROUND 1856 (LEFT) AND 2007 (RIGHT), ADAPTED FROM ANDERSON, 2007

B.2. THE GALVESTON SEAWALL

Work began on the seawall in October 1902 and was completed in July 1904. The wall had an initial height of 5.2 m (17 ft.) above Mean Low Water and stretched from the South Jetty almost 5 kilometers (3 miles) long. It had a concave up, gravity-based design with a base of 5 m (16 ft.), gradual decreasing to a width of 1.5 m (5 ft.) at the top, as shown in Figure 5.32.1. The foundation consisted of wooden piles and were protected by a layer of rip rap in front of the curved cross-section. In the years thereafter the wall endured several storms and damages. Being rehabilitated several times, the current seawall begins from the tip of the east end of the island and has a current length of 16.6 km (10.3 miles), as shown in Figure 5.3.2. From this point on the rest of the island is not artificial protected (U.S. Army Corps of Engineers, 1981).

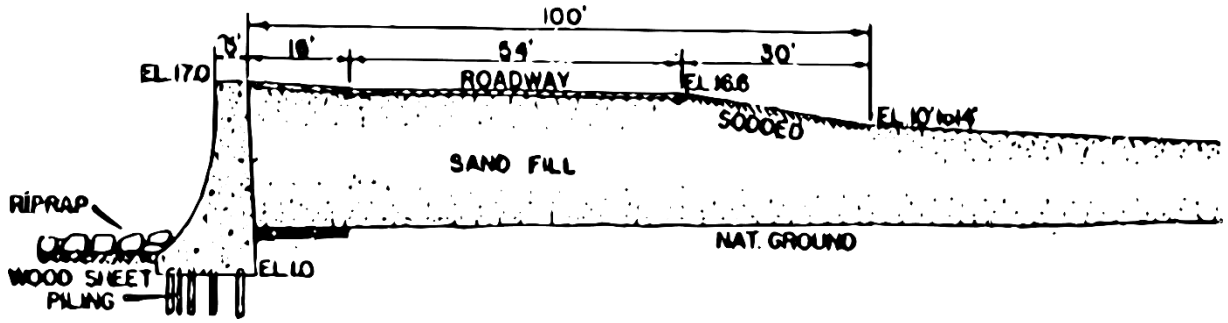

FIGURE 5.32.1. THE GALVESTON SEAWALL AS CONSTRUCTED IN 1904 (U.S. ARMY CORPS OF ENGINEERS, 1981)

The initial height was 5.2 m above MLW. However due to contributions such as sea level rise, subsidence of the soil and the heavy loads of the wall itself, the structure has been has been subsiding. To monitor this, several GPS tracking positions have been placed at specific places along the seawall top face (NOAA and NGS, 2017). A survey was done with data from several of these points, as shown in Table 5.3. and Figure 5.3.2. These values show that the average height of the seawall is 4.32 m +MSL. It should be mentioned that this elaborating only serves as a quick reference into the current height of the seawall and a more elaborate study should be done, as the amount of settlement could also spatially differ.

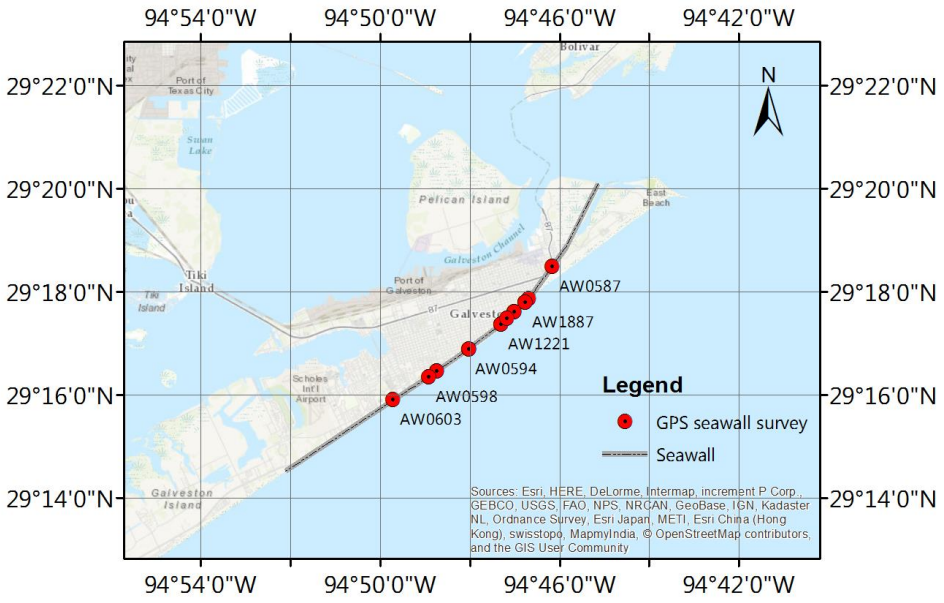

FIGURE 5.3.2. GPS SURVEY POINTS ALONG THE GSW

TABLE 5.3.1. SURVEY OF THE CURRENT HEIGHT OF THE GSW. THE DATA IS ACQUIRED AT OCT 2013 (NOAA NGS, 2017).

Station ID	Latitude	Longitude	Elevation w.r.t. NAVD88 [m]
AW0588	- 29 17 51.91	94 46 40.96	4.349
AW1887	- 29 17 47.82	94 46 46.29	4.341
AW1703	- 29 17 36.43	94 47 00.79	4.376
AW1221	- 29 17 22.56	94 47 18.54	4.369
AW0594	- 29 16 53.55	94 48 01.86	4.308
AW0596	- 29 16 27.84	94 48 44.88	4.282
AW0603	- 29 15 54.39	94 49 42.81	4.299
AW0587	- 29 18 29.79	94 46 10.14	4.203
AW0598	- 29 16 21.07	94 48 55.02	4.259
AW1247	- 29 17 28.56	94 47 10.86	4.388
		Average	**4.317**

APPENDIX C HYDRAULIC BOUNDARY CONDITIONS

In XBeach, varying water levels and wave climates are defined at the boundaries of the domain of the model. This study uses two boundary cases as input. One is the historic case of hurricane Ike, used for the validation of the model. The second case is a 1/100 year^{-1} design storm for the testing of the hybrid designs. In this section some background and the hydraulic boundary conditions for Hurricane Ike and the design storm will be elaborated.

C.1. HURRICANE IKE

The performance of the numerical model is validated by comparing the output with actual measurements during a historic event. For this study Hurricane Ike is used. In this section the origin and the used hydraulic conditions of Hurricane Ike will be elaborated.

C.1.1. ORIGIN

Ike originated from a significant tropical wave of the west coast of Africa on the 28 of August 2008. After passing the Cape Verde Islands, it gained enough convection to be a tropical depression. This tropical storm gradually intensified as it moved across the Atlantic. As Ike reached the Caribbean area, an eye became apparent and the storm intensified strongly. Some minor weakening occurred in the next couple of days together with a strong pull originating from mid-level high pressures, causing the hurricane to move in an unusual west-southwesterly motion on 6 September. This motion caused Ike to quickly return to a Category 4 status, making landfall at the Bahamas at 7 September, Cuba at 9 September and hitting Galveston Island at 0700 UTC 13 September. The hurricane moved further over land, reducing in strength as it crossed Texas, Arkansas, Missouri and finally being absorbed by another area of low pressure at region of Ontario & Québec, Canada by 15 September. (Berg, 2009)

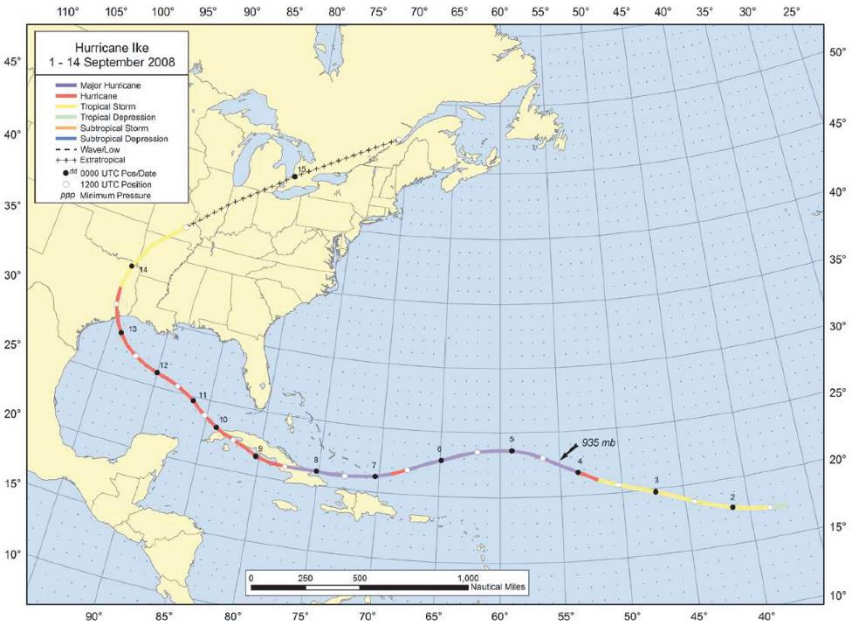

FIGURE 5.3.1. COARSE OF HURRICANE IKE FROM 1ST TO 14TH SEPTEMBER 2008, (BERG, 2009)

Prior to the landfall of Ike, a large unpredicted water level increase appeared in front of the Louisiana and Northern Texas coasts (LATEX). Residents in these coastal areas experienced widespread inundation, a full day before the storm made landfall. This forerunner surge was not a directly coupled to the primary coastal surge from Ike, which was driven by onshore directed winds. The explanation for this forerunner surge is that it was an effect of the Ekman setup. This large scale phenomenon is a large water setup due to an approximately geostrophic balance between the Coriolis force acting on the along-shelf current and the pressure gradient in the cross shore. Due to Ike's large wind field, a strong wind driven alongshore current was forced, going from east to west. With the LATEX relatively shallow shelf on the right hand side of this current, a large setup was created to compensate for the large force that was inflicted by the rotation of the Earth on this alongshore current. (Kennedy et al., 2011b).

After landfall, the surge propagated into the Galveston Bay. Since Galveston is only protected in front of the city by the seawall, mayor flooding and overwash occurred from the backside of the island, as shown in Figure 5.3.2. (Berg, 2009; SSPEED Center, 2010; Stoeten, 2013). This backwash of the surge is measured by several water gauges and stations, located at the backside of the island.

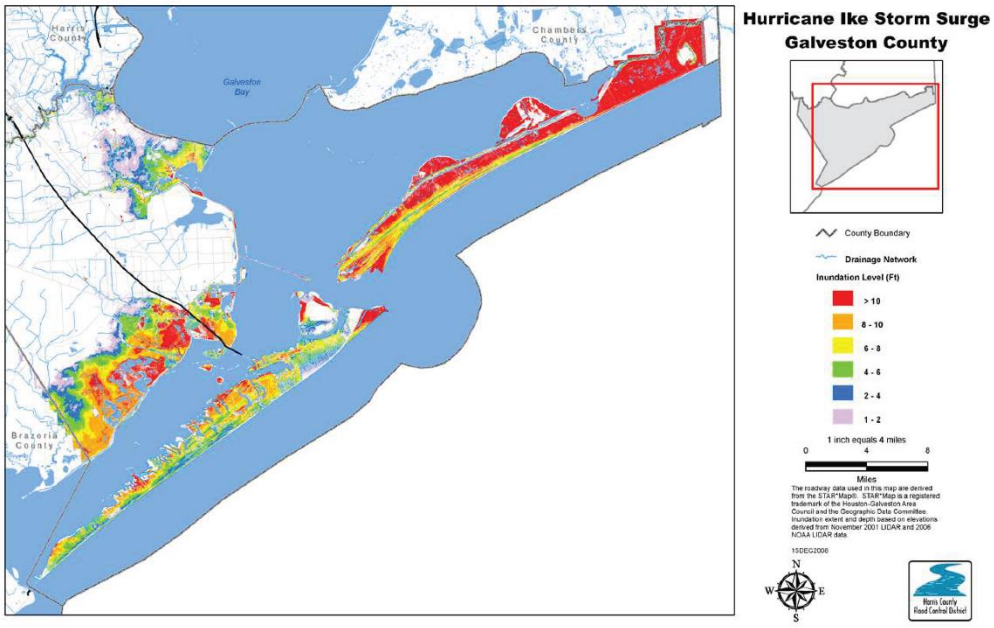

FIGURE 5.3.2. INUNDATION LEVELS OF GALVESTON ISLAND AND BOLIVAR PENINSULA. IT CAN BE SEEN THAT GALVESTON WAS SEVERELY INUNDATED DUE TO FLOODING FROM THE BACKSIDE OF THE ISLAND (BERG, 2009)

C.1.2. SURGE INPUT

A set of 8 rapid-deployed buoys were placed in front of the coast, 2 days prior to landfall. Together with the regular buoys the National Data Buoy Center (NDBC), these temporarily buoys measured the relative water levels in front of Galveston Island, Follet's Island and Bolivar peninsula (Kennedy et al., 2011a). From these measurements, the forerunner surge is clearly visible. At Galveston Island, the surge occurred around 15 hours prior to landfall, after which the water level decreased a bit and increased again when Ike made landfall.

For this research, use will be made of the measurements of the rapid deployed buoys, specifically "buoy X"(Kennedy et al., 2011b)(Kennedy et al. 2011)(Kennedy, Gravois, Zachry, et al., 2011). The offshore boundary of the domain of the model is therefore set at the location of this buoy. The input consist of the time series of the main and fore runner surge, starting 2 days prior to landfall. The model also incorporates the backwash of the surge, by defining a bayside boundary. The hydraulic input for this bayside boundary is based on measurements taken at the Pier 21, which is at the backside of the island. However, the measured data at Pier 21 proved to deviate from the measured data measured by land based gauges, deployed by the USGS. 4 of these gauges were deployed on Galveston, varying from front and backside locations. These land based gauges are used to validate the water levels during inundation in the model. However, during the validation process, it was found that the bayside water level deviated from the measured data at the backside of the island. Therefore, the measured water level at Pier 21 has been modified to resemble the measured data. This modification is shown in Figure 5.3.3. More on the results of this modification of the water level in section D.2.2.

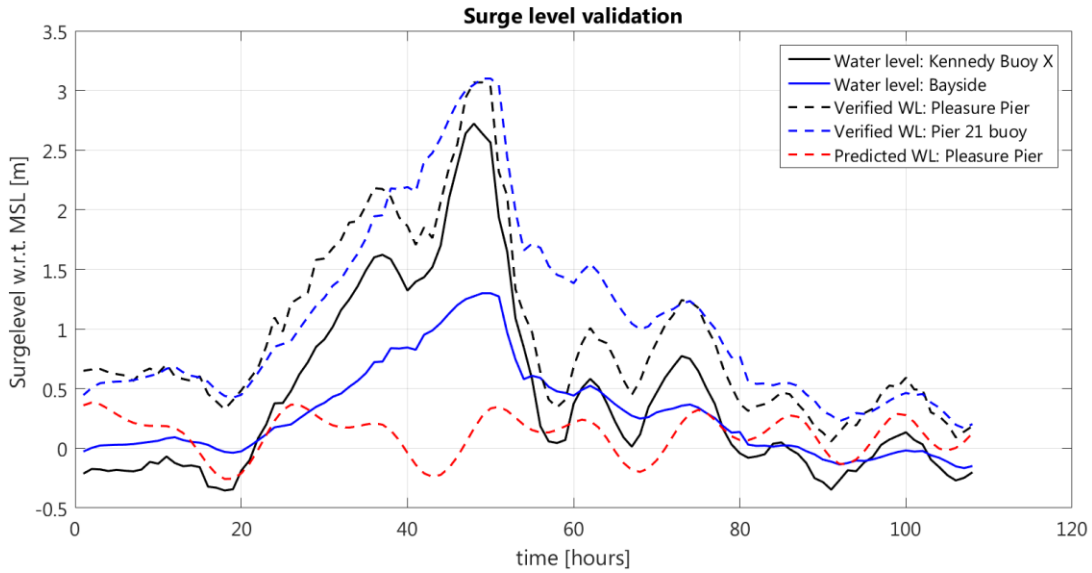

FIGURE 5.3.3. SURGE ELEVATIONS DURING HURRICANE IKE. THE MEASURED WATER LEVEL FROM KENNEDY BUOY X IS USED FOR THE GULF SIDE BOUNDARY (SOLID BLACK) AND THE DATA FROM PIER 21 (DASHED BLUE) IS MODIFIED FOR THE BAYSIDE BOUNDARY (SOLID BLUE). THE VERIFIED AND PREDICTED WATER LEVEL AT THE PLEASURE PIER AT THE FRONT OF THE ISLAND ARE GIVEN AS A REFERENCE (DASHED BLACK AND RED).

C.1.3. WAVE CLIMATE INPUT

Beside the water level, the buoys from Kennedy also measured the wave action. These were 1 Hz time series of the absolute pressure and were corrected to water pressure. The maximum significant wave height that was measured was 5.8 m around landfall at one of the buoys with a maximum error of 10 cm for all the measurements. Lot of measurements were limited due to the height to depth ratio. A study was performed on the observations with theoretical values form empirical formulations. These studies showed that the first maximum wave heights were dominated by remotely generated waves. Further into the storm the forerunner surge allowed bigger waves into the shallower depths. Also local winds appear to exert a much stronger control on nearshore wave heights during the peak of the hurricane. (Kennedy et al., 2011a)

The input for the wave heights will be extracted from the measurements at buoy X. The angle of incidence of the wave groups was not measured at these buoys and is therefore extracted from the measurements of the offshore buoy S42035 (NOAA, 2016c). After a comparison of the wave height and wave period measurements at both buoys it was deemed that the wave angle probably has not changed significantly between the two stations. This comparison can be seen in Figure 5.3.3.

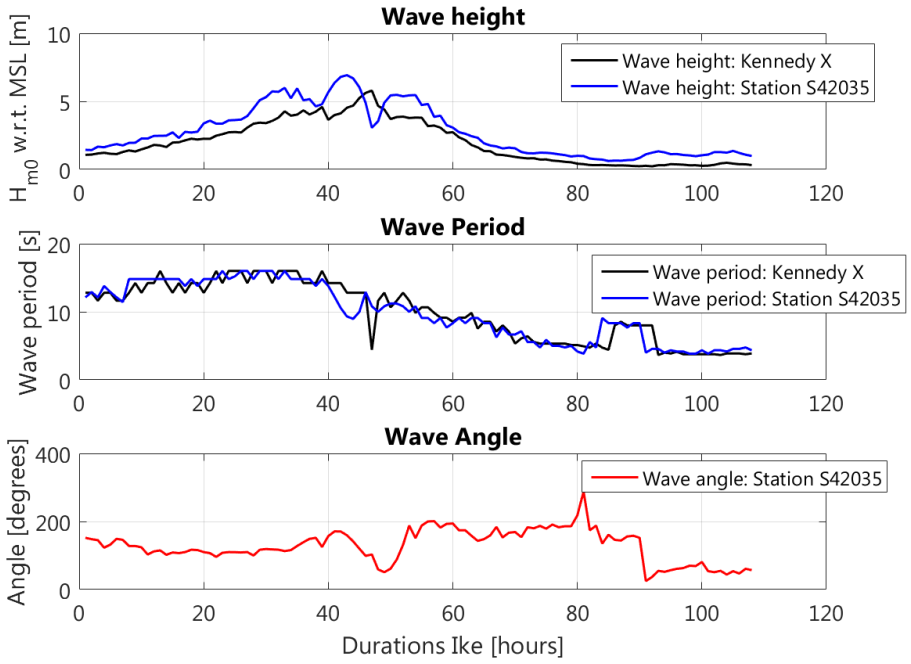

FIGURE 5.3.3. WAVE TIME SERIES AS MEASURED BY KENNEDY AND STATION S42035. IT CAN BE SEEN THAT AS WAVES PROPAGATED TOWARDS SHORE, THE WAVE HEIGHT WAS SLIGHTLY REDUCED. THE WAVE PERIOD DID NOT SHOW LARGE DEVIATIONS. IT IS ASSUMED THAT THE WAVE ANGLE USED AT THE MODELS BOUNDARY, DID NOT VARY TO MUCH FROM THE VALUES MEASURED AT STATION S42035, NEGLECTING POSSIBLE DIFFRACTION.

The time series will be parameterized into a JONSWAP in order to create a divers and random generated wave field for the simulation. Since JONSWAP was not designed to simulate hurricane spectra, this has to be taken into account during the simulation. However it has been found that one-dimensional and directional hurricane spectra still resembles a fetch-limited spectra such as JONSWAP, due to the effects of nonlinear interactions, which reshape the spectra. (Hu and Chen, 2011; Young, 2006, 1998)

C.2. DESIGN STORM

In recent evaluations it is stated that it is questionable if the GSW is still capable of providing sufficient protection for a 1/100 year^{-1} storm. (van Berchum et al., 2016; Jonkman et al., 2015). Transforming the GSW into a hybrid, e.g. reinforcing it with a dune cover, can enhance the resilience of the structure (Sutton-Grier et al., 2015). In order to simulate different hybrid designs, a 1/100 year^{-1} storm event has to be determined. Significant research is done on a design storm for design purposes. The design storm in this research is therefore composed from these values.

C.2.1. DESIGN STORM PROFILE

For all the hybrid designs, a single design storm is used. The duration and development over time is therefore of importance. Since no significant statistical analysis of a 1/100 year storm profile is available, the shape and duration of the design storm are therefore based on that of Hurricane Ike. The design values found in earlier work form the maxima of these profiles. The duration of the design storm is set at 90 hours. The average radius of a category 3 hurricane is 240 km. These storms have an average rate of movement of 20 km/hr. This gives a requirement of a minimal duration of 12 hours (Atlantic Oceanographic & Meteorological Laboratory, 2014; Keim et al., 2007). In order to allow for a gradual development of the storm and incorporate all the features such as the forerunner surge, the total duration is extended to 90 hours of simulation time.

C.2.2. WAVE CLIMATE

For the design wave height, use has been made by the most recent work. This contains a brief study by analyzing time series from an offshore buoy with an extreme value analysis, based on a Weibull distribution. These offshore wave heights were simulated towards shore, including hydrodynamic processes (Almarshed, 2015; van Berchum et al., 2016). Referencing these values with other work shows similar results and correspond with a category 3 storm. (Jin et al., 2010; NOAA, 2016a). The peak wave period was also derived by Almarshed and is used in this study. The development of the significant wave height and the wave period over time are shown in Figure 5.3.1. The angle of incidence of the waves can change during a storm. During Hurricane Ike, an offshore station measured an initial angle of incidence with respect to the shoreline. In this study the angle of incidence is chosen normal to the shore as no energy is lost due to refraction and along shore processes. This will form the strongest possible forcing on the shore. The used values in the wave input are stated in Table 5.3.1.

TABLE 5.3.1. WAVE CLIMATE FOR DESIGN STORM

Return period (years)	100
Maximum significant wave height H_{m0} (m), {ft}	4.59, {15.06}
Maximum Peak wave period, T_p (s)	12.88
Wave angle w.r.t coastline	0

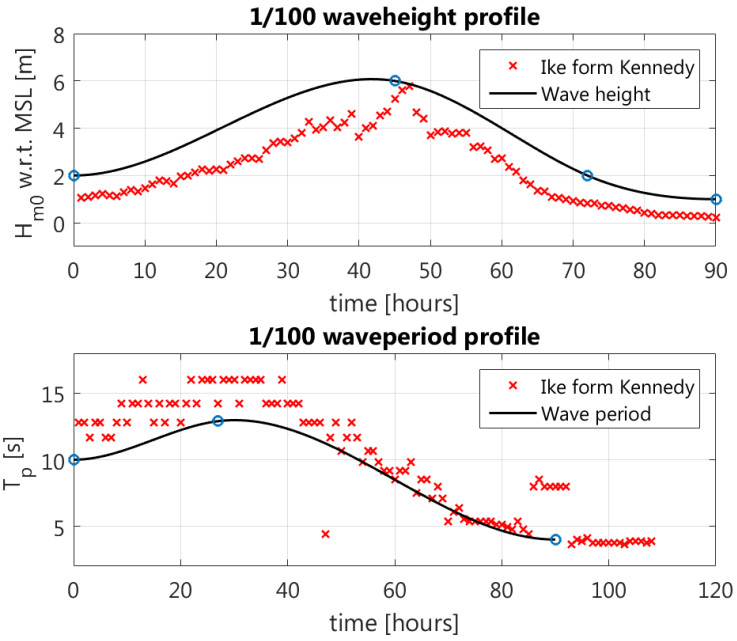

FIGURE 5.3.1. DEVELOPMENT OF THE SIGNIFICANT WAVE HEIGHT, H_{M0} AND THE PEAK WAVE PERIOD, T_P FOR THE DESIGN STORM. THE SAME QUANTITIES DURING HURRICANE IKE AT BUOY X FROM KENNEDY ARE GIVEN AS REFERENCE.

C.2.3. STORM SURGE AND FORERUNNER SURGE

The surge elevation for the design storm is compiled with found values from earlier elaborations. The main surge elevation for a 1/100 year^{-1} event has been adopted from an extreme value analysis (Almarshed, 2015). Other work has been carried out on determining the 1/100 surge level (Lendering et al., 2014; Rippi, 2014; Stoeten, 2013). These values corresponded well with used findings.

Due to the extreme metrological effects, such as pressure and wind velocities, a large setup can occur prior to the storm itself, as was the case with Ike and its forerunner surge. This early increase of water level also extends the depth at which waves tend to break towards the shore. Larger waves can therefore be expected in the nearshore. To include this phenomena, a forerunner surge has been included into the design surge. A study was performed to determine the design height of a forerunner surge for a 1/100 year^{-1} case by extrapolating historical water level data related to Hurricane Ike (Lendering et al., 2014). The outcome was a profile with a maximum height of 3 m, 6 hours prior to landfall. In this research these preliminary values will be adopted.

The maximum elevations of the individual components of the combined design storm are stated in Table 5.3.2. Sea level rise and other contributions to long term subsidence are included in the design storm. More about this components in the next section. The combination of these components and the resulting storm surge can be seen in Figure 5.3.2.

TABLE 5.3.2. MAXIMUM ELEVATIONS OF THE COMPONENTS OF THE DESIGN STORM SURGE.

Surge component	**Surge elevation for 1/100 year^{-1} [m]**	**[ft]**
Main surge	4.71	15.45
Fore runner	3	9.84
SLR and others	0.5	1.64

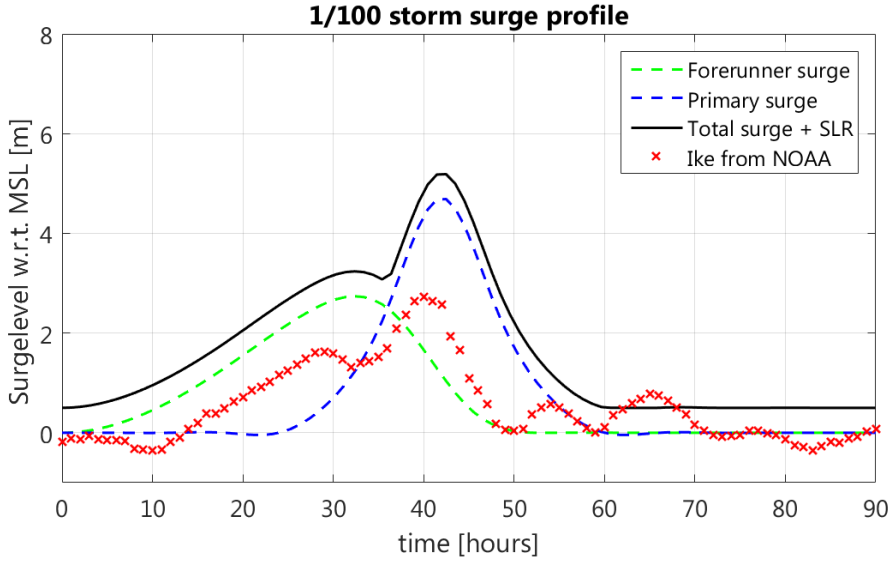

FIGURE 5.3.2. DEVELOPMENT OF THE TOTAL DESIGN STORM SURGE AND THE INDIVIDUAL COMPONENTS. THE STORM SURGE DURING HURRICANE IKE AT AN OFFSHORE BUOY ARE GIVEN AS REFERENCE.

C.2.4. RELATIVE SEA LEVEL RISE AND LAND SUBSIDENCE

The hybrid solution should provide Galveston protection for a 1/100 $year^{-1}$ storm. However, since the dune cover in the hybrid design is composed of sand or similar sediment, its dimensions are easily adaptable in the future. Therefore it is common to choose a lower lifetime for this type of structure (Arcadis, 2013).

The hybrid structure is designed with a lifetime of 50 years and is therefore simulated with a storm in the year 2066. Sea level rise for this year has to be incorporated. The effect of sea level rise is investigated in numerous studies for different locations at the Upper Texas Coast for design purposes. The current mean sea level rise in the case of Galveston is determined at 6.62 millimeters/year. (NOAA, 2016d)

Consolidation and extraction of resources leads to a lower surface level. The subsidence differs significantly per location, however a mean lowering of the ground level of 2.3 mm/ year is determined for the Galveston area (Paine, 1993).

These two effects give an mean sea level rise of approximately 0.5 m in the year 2066. This value corresponds with the trend with other found values for the mean sea level rise (de Vries, 2014).

C.2.5. LANDFALL LOCATION

Another variable that is of importance for the design storm is the location of landfall. Use is made of previous work that looked at the effect of different landfall locations on the hydraulic boundary conditions. Different combinations such as duration and the inclusion of a fore runner surge where simulated (Lendering et al., 2014). The variety in the hydraulic conditions due to the landfall location are not included into this study.

APPENDIX D XBEACH VALIDATION

D.1. METHOD

The validation was performed by comparing the modeled water levels and bed level change versus the measured values at specific areas. First, the simulated water levels were compared with measurements, in order to be assured that the hydrodynamics are simulated correctly. Secondly, bed level changes over 6 transects per selection are compared to assess the models ability to simulate erosion and accretion patterns.

For validation purposes it was required to make two selections of the DEM. The first selection focusses on the west end of the seawall. This area will be modeled to reproduce the collision, overwash and inundation regime as described by Sallenger, (Sallenger, 2000) in more depth. The second area is at the east end of the island and takes the entire seawall into account all the way up towards the west jetty at Bolivar Roads. This area will be used to validate the model for a second time, specifically looking at the dune formations in front of the seawall at East Beach. Both the west and east end selections takes the water level at the bayside of the island into account.

In the next sections the validation process of these two regions will be elaborated. First the selection and simplification of the bathymetry is explained. Secondly the validations of the results are shown for each section. The conditions at the boundaries of the validation models are based on measurements during Hurricane Ike and are already treated in Appendix C. The input file for XBeach with specific parameters are stated in Appendix F.

D.2. WEST END CASE

The West End selection covers the part of Galveston island where big open vegetated spaces are present, as indicated in Figure A.1.1. The GSW ends half way into the selection, creating an area where the coastline abruptly is not protected anymore. This selection is further characterized with scattered structures as standalone houses and apartments, road pavement, lakes, bayou's and the Termini-San Luis Pass Road runs across the island from East to West. Since this area is lower than the area behind the seawall, significant overwash and inundation took place during Ike. Some initial dune ridges were also eroded away in the storm. These events are an useful indication for the validation of the XBeach model setup.

D.2.1. BATHYMETRY

The bathymetry of the west end case is shown in Figure 5.3.. XBeach requires the offshore boundary to be located at the left side of the domain. To reduce the computational time, this selection was reduced using tools provided by Deltares (Deltares, 2016). These allowed to redefine the cross and alongshore grid to a more appropriate one to the bathymetry's information. The final grid resolution was reduced to $dx = 15\ to\ 30\ m$ and $dy = 20\ to\ 30\ m$. In Figure 5.3.2., the result of the coarsening of the grid in x and y-direction can be seen. Also some additional alterations were done to improve the bathymetry, such as cropping the selection even more.

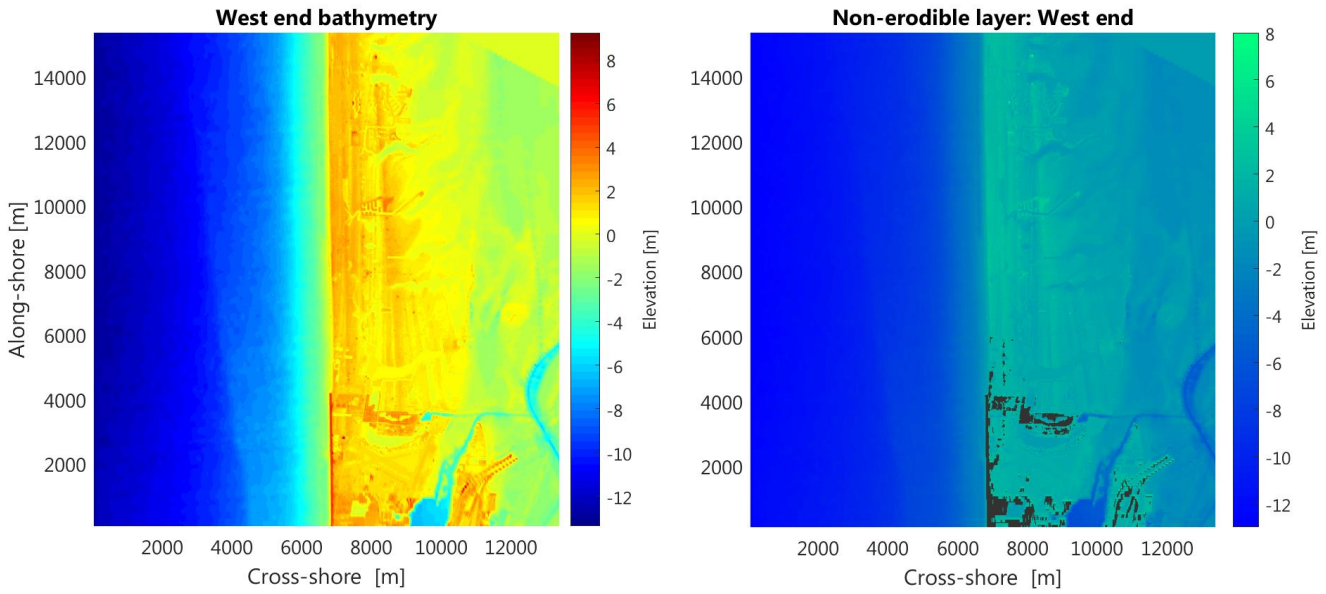

FIGURE 5.3.1. USED BATHYMETRY FOR THE WEST END CASE (LEFT PANEL) AND THE DEFINING NON-ERODIBLE LAYER (RIGTH PANEL). THE NON-ERODIBLE STRUCTURES ARE DISPLAYED IN BLACK.

Additionally to the bathymetry itself, XBeach allows for a non-erodible layer to be defined. In this case, these are objects such as the GSW, revetments or slopes and solid structures that were not taken out of the DEM. The definition of the non-erodible layer was done by applying a certain threshold in elevations. If a certain elevation is higher than this threshold, the area is regarded as a non-erodible structure. Since the GSW is typically 4.7 m with respect to MSL, this threshold is set at 3 m w.r.t. MSL. In Figure 5.3., the non-erodible layer for the west end case is shown.

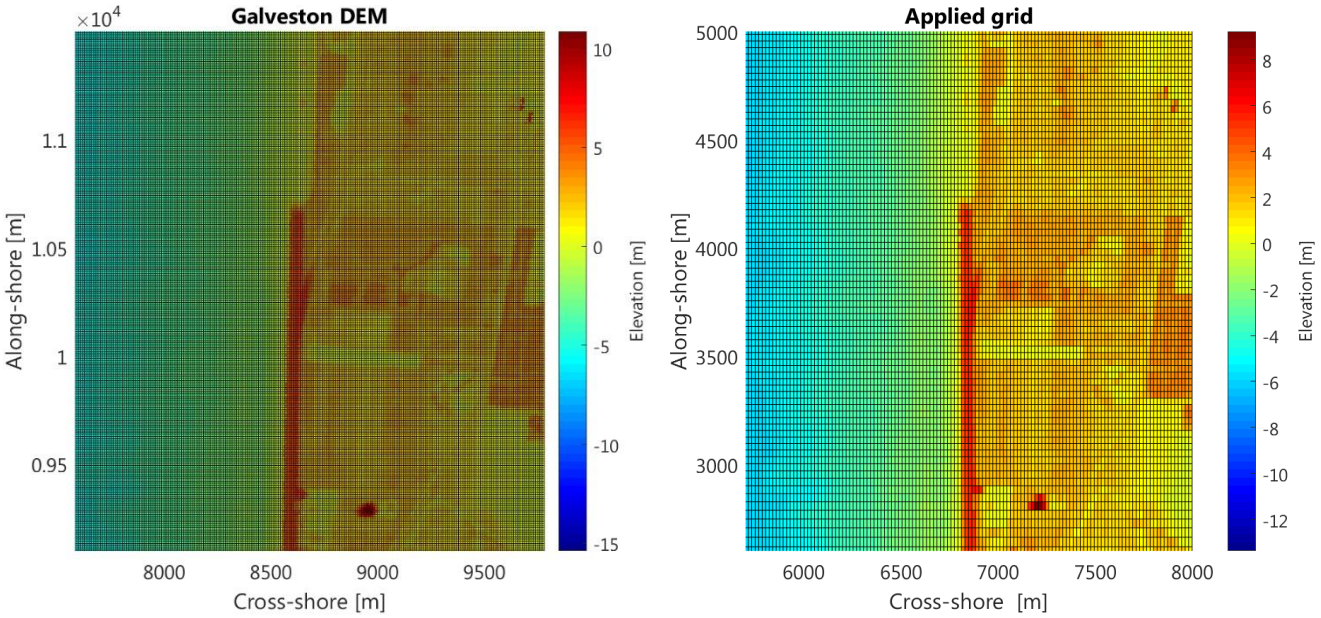

FIGURE 5.3.2. ADAPTATION OF THE BATHYMETRY BY REDEFINING THE GRID. LEFT THE ORIGINAL BATHYMETRY AS GIVEN BY THE DEM IS SHOWN. IN THE RIGHT PANEL THE SAME REGION AFTER THE ALTERATION IS DISPLAYED, SHOWING THE LOWER GRID RESOLUTION AND THUS REDUCING COMPUTATIONAL TIME.

D.2.2. WATERLEVEL VALIDATION

Two water gauges have been used: SSS-TX-GAL-010 and SSS-TX-GAL-011. These gauges are located at the east frontside corner and the west bayside corner of the barrier island selection respectively, as shown in Figure A.1.1. During the first validation runs, it was noticed that at a certain point after landfall, the high water level at the bayside of the domain caused a backwash of water over the island towards the lower level sea. This produced aberrant erosion and accretion in the cross shore profiles, as well in the water level measurements at the backside of the island. It has been estimated that the used bayside water level from Pier 21 gauge is not representative for the bayside boundary in the model. Therefore the backside surge has been adjusted, which offered better results as can be seen in Figure 5.3.3. Although the water levels after the peak surge diverges form the measurements, it is estimated that this effect is less of importance than the correct prediction of the maximum surge level and the development towards that moment.

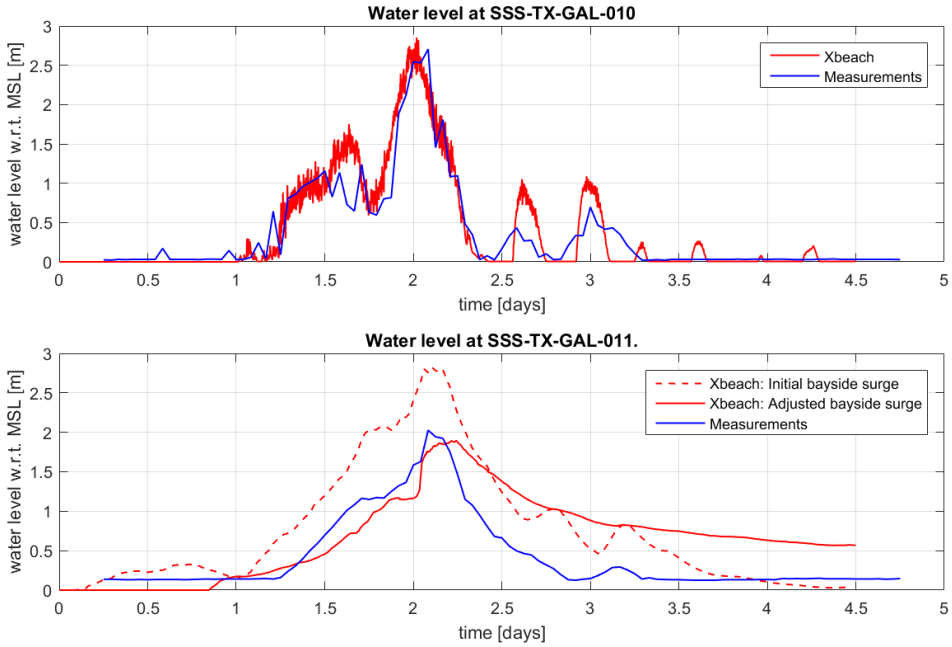

FIGURE 5.3.3. WATER LEVEL VALIDATION FOR THE WEST END CASE.. THE WATER LEVEL ELEVATION AS MEASURED AT THE LOCATIONS OF THE GAUGES IS PLOTTED WITH THE CORRESPONDING OUTPUT MODELED BY XBEACH.

AT THE LOCATION OF GAUGE SSS-TX-GAL-010 (TOP PANEL), THE MODELED WATER LEVEL (RED) MATCH THE MEASUREMENTS (BLUE) QUITE WELL. THE OUTPUT OF THE MODEL (RED) HAS A FINER TIMESTEP, SHOWING MORE FLUCTUATIONS THAN THE MEASUREMENTS. AT THE LOCATION OF GAUGE SSS-TX-GAL-011 (BOTTOM PANEL), THE INITIAL MODELED WATER LEVEL (DASHED RED) DIVERGE FROM THE MEASUREMENTS (BLUE) AT THAT LOCATION. AFTER THE ADAPTATION OF THE BAYSIDE SURGE LEVEL, THE MODELED WATER LEVEL (SOLID RED) MATCH THE WATER LEVEL RISE BETTER. HOWEVER, AFTER THE PEAK OF THE STORM THIS WATER LEVEL STILL DIVERGES.

D.2.3. BED LEVEL VALIDATION

With a validation of the water levels at the sea and bayside of the island, the modeled beach erosion/accretion is examined. Six transects (A till F) were made perpendicular to the coastline across the length of the selection, as shown in Figure 5.3.4. At these cross sections, data of the pre- and post LiDAR surveys were retrieved as well as the pre- and post-bed levels from the results of the model.

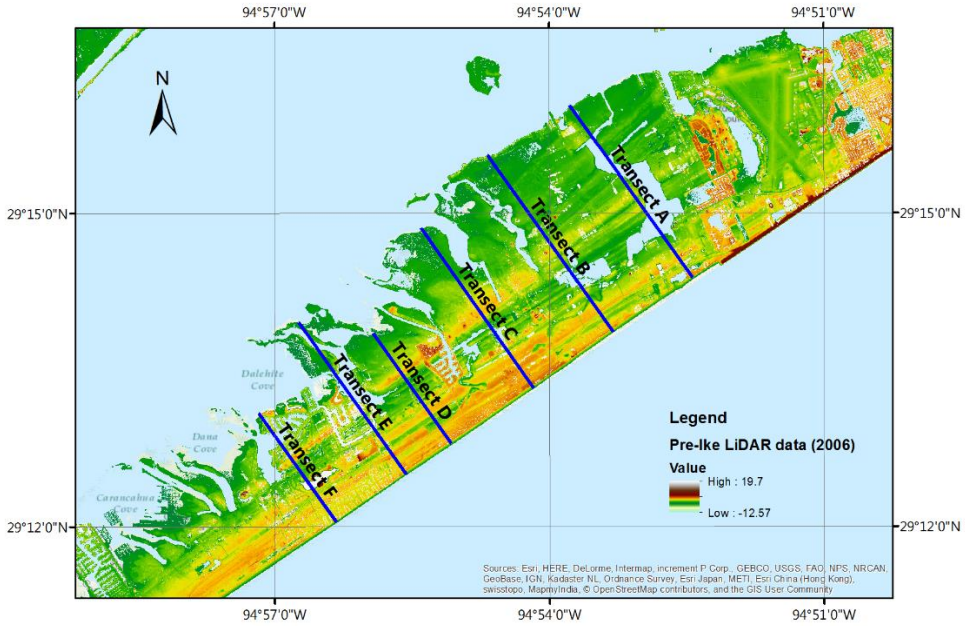

FIGURE 5.3.4. TRANSECTS MADE IN THE WEST END CASE SELECTION.

After examining all the transects in the west end case, it was found that the output from the model resembles the profile of the beach in pre and post-Ike conditions quite well. The model is sufficiently capable of approximating the slope of the beachfront. However, looking further along the transect, it can be seen that XBeach shows to much erosion. This can be associated with several factors.

First, the post-Ike measurements were performed in November 2009. This is a full year after the event and it could be possible that new ridges have been formed by nature or more realistic artificially. It is also possible to detect the Termini-San Luis Pass Road quite clearly in all the transects. This is due to the fact that XBeach is only given an input for the sediment and thus regards everything as sand, if not defined as non-erodible. Therefore, the profile of the road is completely vanished after the simulation in XBeach. The same holds for vegetational area's and scattered structures. In reality, these regions have a much higher resistance against the flow during overflow, than is incorporated in the model. XBeach offers the possibility to model vegetation or higher resistant areas. However, this option is not adopted in this research.

Another reason could be the alignment of the transects for the pre- and post-lidar data and the corresponding XBeach transects. In Figure D.2.5., the pre- and post-Ike lidar data are plotted together with the initial and simulated cross sections simulated by XBeach. Possible explanations for the diverging of the simulated results were looked into and are indicated in the same graphs, using results of other surveys and examinations (USGS, 2009). For instance, it was found that the divergence at transect A, was due to heavy reinforced plateau near the beach front which consisted of concrete, as shown in Figure 5.3.6.

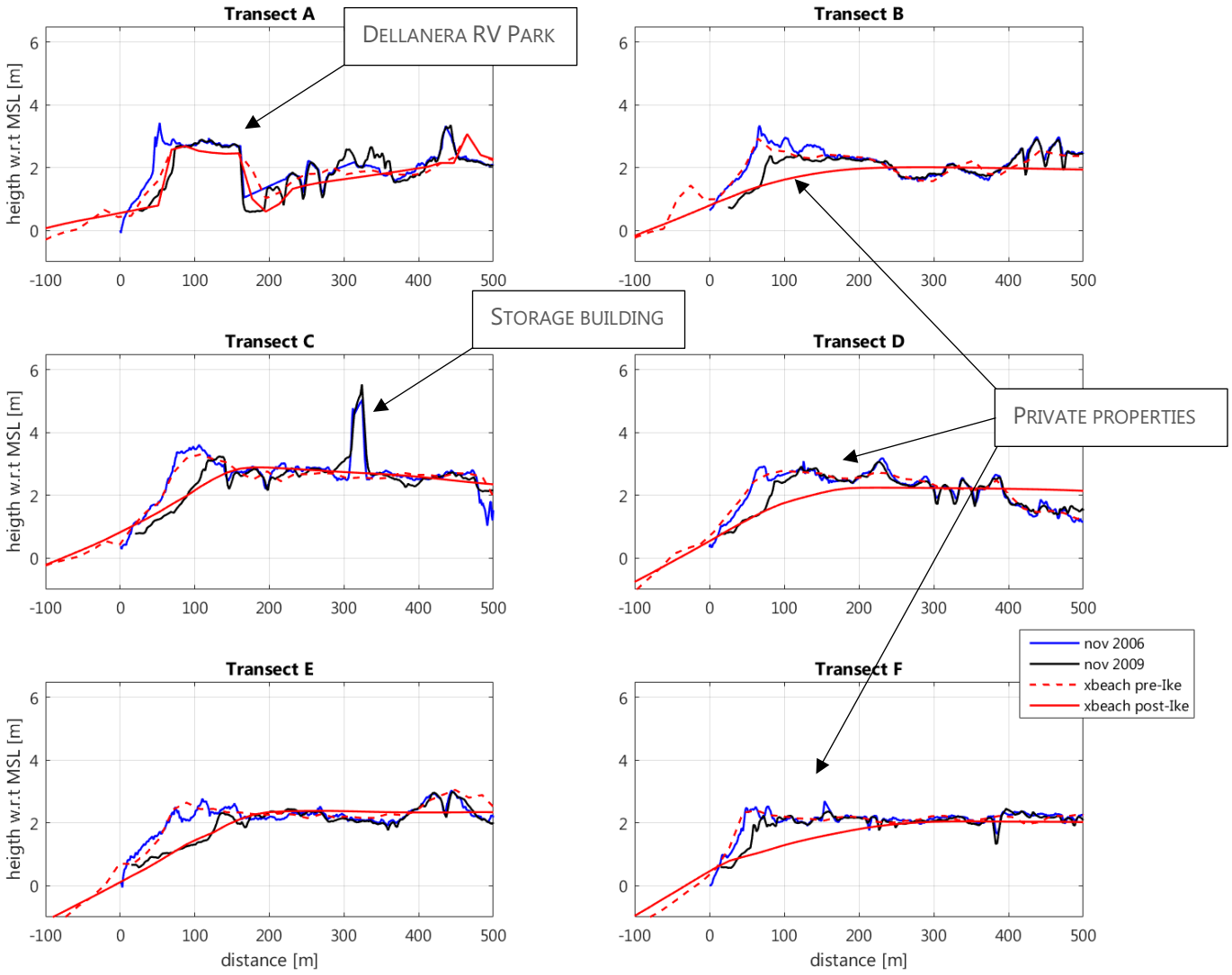

FIGURE 5.3.5. BED LEVEL VALIDATION OF THE WEST END CASE. AT EACH TRANSECT THE PRE-IKE LIDAR (BLUE) AND THE POST LIDAR DATA (BLACK) IS PLOTTED WITH THE INITIAL BATHYMETRY OF THE MODEL (DASHED RED) AND THE MODELED RESPONSE FROM THE MODEL (RED).

FIGURE 5.3.6. PRE- AND POST-IKE AERIAL PHOTOGRAPHS OF SECTIONS OF THE WEST END AREA. THE LEFT PANEL SHOWS THE AREA THAT CORRESPONDS WITH TRANSECT A. INDICATED WITH THE YELLOW ARROW IS THE DELLANERA RV PARK. IT IS CLEAR THAT AREA IS HEAVY REINFORCED AND DID NON ERODE DURING THE STORM. THE RIGHT PANEL SHOWS THE AREA THAT CORRESPONDS WITH TRANSECT B. THE SHORELINE HAS RETREATED DUE TO HEAVY EROSION WHEN IKE MADE LANDFALL. HOWEVER PRIVATE PROPERTIES PREVENTED FROM FURTHER EROSION (USGS, 2009).

D.3. EAST BEACH CASE

The East Beach case is the selection that starts at the South Jetty at Bolivar Roads all the way to the end of the seawall. This selection is shown in Figure A.1.1. This area is mostly characterized by the presence of the GSW at the shoreline. At the east end of the selection, a wide beach can be found. This formation is the reaction from the construction of the South Jetty, after which large amounts of sediments accreted in the 'shadow' zone of the jetty. In this area, dune ridges and vegetated surfaces are formed and run up to the seawall itself. The validation at this selection gives a good insight in the performance of the model to simulate the response of the beach in combination with the seawall, which is of interest in order to test the hybrid designs. Since the city of Galveston is higher than the low lying part in the West end case, no backwash occurred during Ike. Also, no inundation gauges were deployed at the backside of the city. The bayside water level is not of interest in this case.

D.3.1. BATHYMETRY

The bathymetry of the East beach case is shown in Figure 5.3.1. To reduce the computational time, the final grid was reduced similar to that of the West end case, which is a resolution of $dx = 15\ to\ 30\ m$ and $dy = 20\ to\ 30\ m$.

The GSW and the South Jetty are modeled as a stable and non-erodible layer. This is done in the same manner as explained in the West end case. The groins and revetment in front of the sea wall is not taken into account. At the bottom of the selection, the seawall moves from a coastline position more land inward. From this point, the erodible layers is present again up to the South Jetty. The non-erodible layer for East end is shown in the right panel of Figure D.3.1.

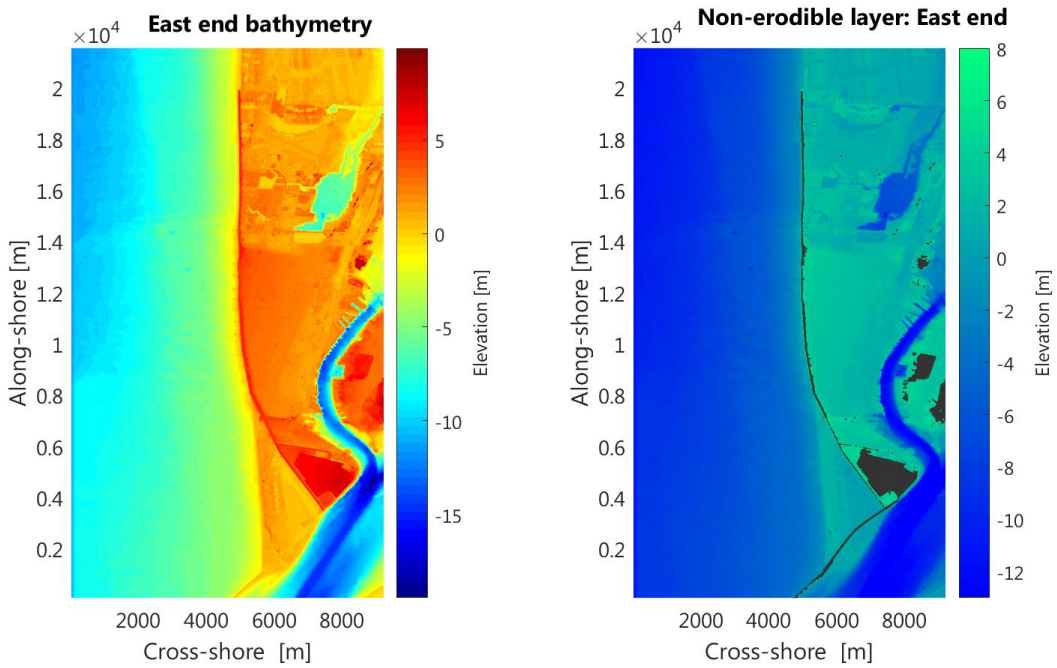

FIGURE 5.3.1. USED BATHYMETRY FOR THE EAST BEACH CASE (LEFT PANEL) AND THE DEFINING NON-ERODIBLE LAYER (RIGHT PANEL). THE NON-ERODIBLE STRUCTURES ARE DISPLAYED IN BLACK

D.3.2. WATERLEVEL VALIDATION

The validation of the water level is primarily done with the use of the station at Pleasure Pier, which is located in the middle of the selection. Additionally, SSS-TX-GAL-008 is located at the tip of the island just on the inner side of the South Jetty, which could be used as well. However, this station is also located in the courser defined edge of the grid domain.

The examination of the results show that in case of the modeled and measured water level at Pleasure Pier during Ike, the model is giving a good result. Not only is it able to give a good development of the surge, but also correctly predicts the local maximum of the forerunner surge and the peak surge.

At the buoy, SSS-TX-GAL-008, it is clear to see that the here the water levels are not predicted that well. The moment of inundation start roughly a half day later than according to the measurements. However, the measured peak surge level is correctly simulated by the model. After the peak of the storm, the water level slowly decreases again, deviating quite some from the measured data. This deviation can be explained due to boundary issues. The end of the model is close to the bolivar roads where water has to propagate into the bay. In the model however the South Jetty crosses this boundary, making it impossible for flow from offshore into the bay. This cause pile up of water at the backside of the bay and can be seen after the peak of the storm in Figure 5.3.. Also the schematization the South Jetty deviates some of the actual structure. This could also be a reason, since it implicates that the boundary is not good described. However, examination of the results from the Pleasure Pier, gives enough confidence for the examination of the erosion/accretion response of the model.

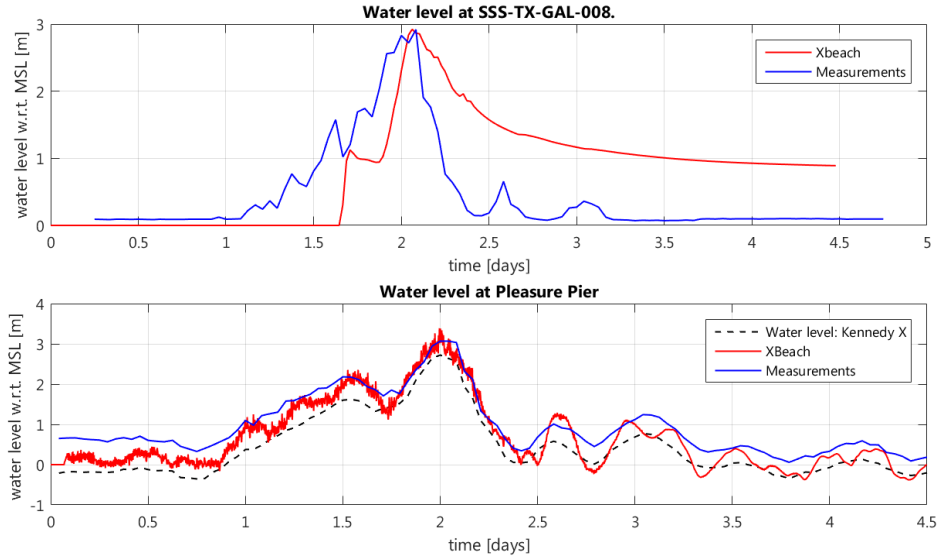

FIGURE 5.3.2. WATER LEVEL VALIDATION FOR THE EAST BEACH CASE. THE WATER LEVEL ELEVATION AS MEASURED AT THE LOCATIONS OF THE GAUGES (BLUE) IS PLOTTED WITH THE CORRESPONDING OUTPUT MODELED BY XBEACH (RED). THE WATER LEVEL AS MEASURED BY KENNEDY IS GIVEN AS A REFERENCE (DASHED BLACK)

D.3.3. BED LEVEL VALIDATION

In the East beach selection, the seawall is situated more inland instead of at the beachfront. In combination with the aggregated material due to the jetty, a vast area of beach, dune ridges and vegetation can be found. In contrast to West end selection, only a few structures and buildings are present in this area. During Ike, significant inundation occurred at this location and was eventually stopped by the GSW itself. Since the seawall is defined as a non-erodible layer, this natural region in front of the seawall is of interest for validation. Six transects have been made (A to F) , as indicated on Figure 5.3.3. On these transects the pre- and post Ike LiDAR measurements are compared to the initial and final bed level from the model.

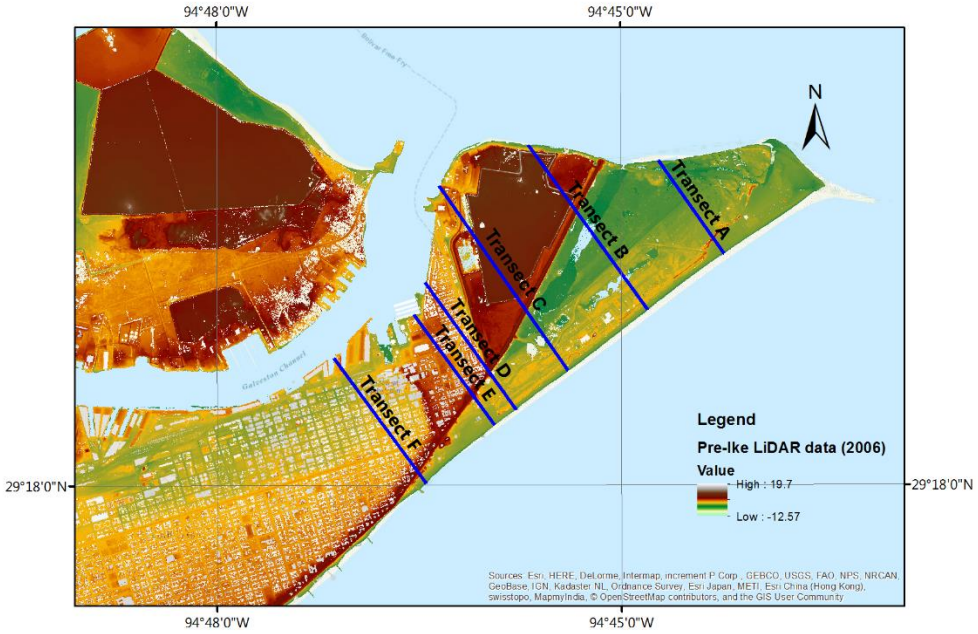

FIGURE 5.3.3. TRANSECTS MADE IN THE EAST BEACH CASE SELECTION.

FIGURE 5.3.4. PRE- AND POST-IKE AERIAL PHOTOGRAPHS OF SECTIONS OF THE EAST BEACH AREA. THE PHOTO SHOWS THE PALISADE PALMS AND THE COASTLINE REGRESSION AFTER IKE. THIS REGION LIES BETWEEN TRANSECT B & C. (USGS, 2009).

The overall results show a good match between the initial surface elevation of the model and the measured data from the survey. Similar to the West end case, the model is capable of simulating the beach profile in the first 100 to 200 m quite well. In some cases it was found that new dune ridges were already formed in the post-Ike measurements. This is due to the fact that the latter survey is performed in November 2009, which is a full year after the event. Also some ridges were found in the post-Ike results of the model. These ridges, however, are not found in the measured bathymetry. This can be related to the sediment that has been eroded at the beach front, being transported on to shore, during the peak of the storm. However, the seawall becomes present at these locations and possibly stopped the flow from transporting the sediment further. Hereby depositing this in front of the seawall. Also an error is found at transect A, where due to the definition of the non-erodible layer via a certain threshold, a erodible dune ridge was regarded as a non-erodible structure. Therefore, this ridge was not available for erosion and is still present in the post-Ike modeled results. Similar to the West end case, some deviation between the measured and the modeled bathymetry is due to the alignment of the transects for the pre- and post-lidar data and the corresponding XBeach transects. In Figure D.3.5., the pre- and post-Ike lidar data are plotted together with the initial and simulated cross sections simulated by XBeach. Additional referencing was done by using the results of other surveys and examinations (USGS, 2009). For instance, the on land erosion modeled at transect B & C corresponds in the same order of magnitude (around 100 m of beach front has been flatten out) with the visual coastline regression from the aerial inspection, as shown in Figure 5.3.4.

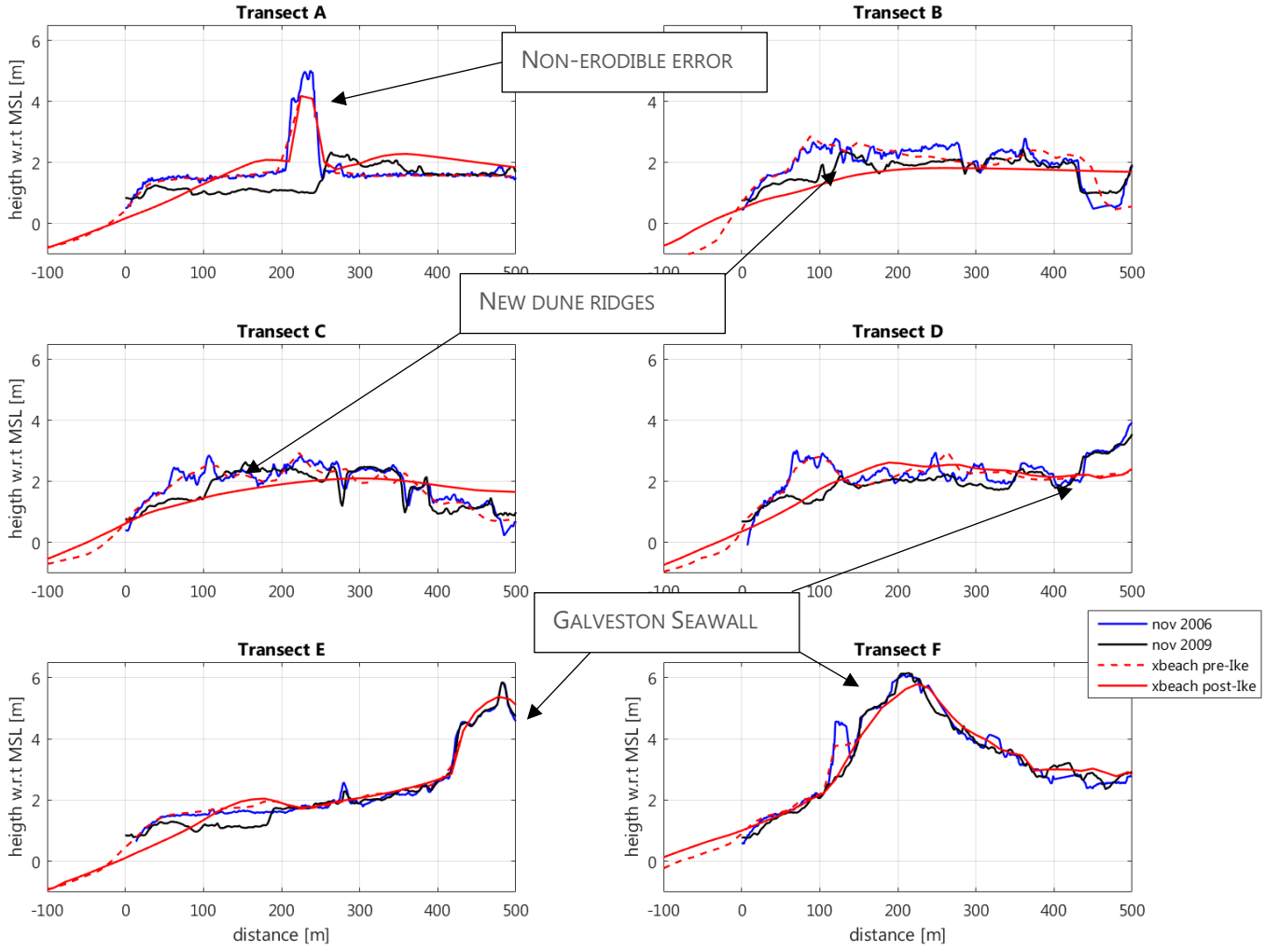

FIGURE 5.3.5. BED LEVEL VALIDATION OF THE WEST END CASE. AT EACH TRANSECT THE PRE-IKE LIDAR (BLUE) AND THE POST LIDAR DATA (BLACK) IS PLOTTED WITH THE INITIAL BATHYMETRY OF THE MODEL (DASHED RED) AND THE MODELED RESPONSE FROM THE MODEL (RED).

D.4. PERFORMANCE

In order to use the XBeach model setup for the simulation of the hybrid designs, the overall performance of the model has to be assessed. In order to give an indication of the correct modulation of the actual response of Galveston Island during Ike, the modeled bed level change is projected against the measured bed level change, as can be seen in Figure 5.3.1. It can be seen that the scatter gives a big diversity of points, however an overall trend with roughly the same modeled as measured bed level change can be observed.

The performance is qualified by calculating its skill and bias. The procedure is similar as earlier work has performed it on XBeach results (Harter, 2015; McCall et al., 2010).

The skill is a representation on the ability of the model to predict the bed level change. The simulated error in bed level change is compared to the variance of the measured bed level change at all the locations in the total of 12 transects.

The skill is defined as:

$$Skill = 1 - \frac{\sum_i^N \left(d_{zb,Measured,i} - d_{zb,Modeled,i} \right)^2}{\sum_{i=1}^N \left(d_{zb,Measured,i} \right)^2} \qquad \text{D.1}$$

Where N is the total number of measured points from the LiDAR data, $d_{zb,Measured,i}$ is the measured bed level change according to the LiDAR data at location i, $d_{zb,Modeled,i}$ is the modeled bed level change according to XBeach at location i. If the skill is 1, the simulation correlates one-to-one with the reality. If the skill is zero, the simulation is no better than simulating no bed level change. If the skill is lower than zero, the simulation is worse than predicting zero bed level change.

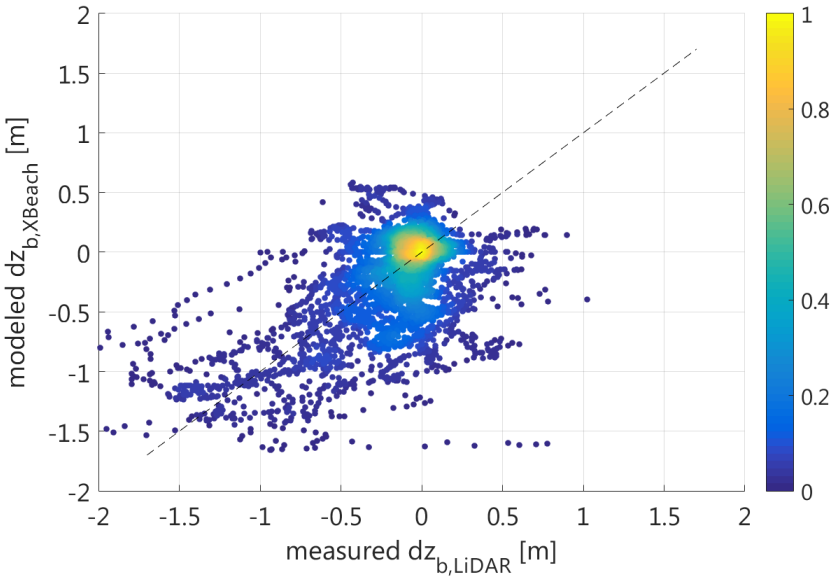

FIGURE 5.3.1. DENSITY SCATTER PLOT OF THE MODELED VERSUS THE MEASURED VALUES PER POINT.

Apart from the predictive skill of the model, the errors of the model are of interest. This error consist of random components and a persistent bias. This bias describes the mean error and is calculated as follows:

$$Bias = \frac{1}{N}\sum_{i=1}^{N}\left(z_{b,post-storm,Modeled,i} - z_{b,post-storm,Measured,i}\right) \quad \text{D.2.}$$

The results of the skill and bias, are stated in Table 5.3.. In this case, the XBeach model has a relative low skill, indicating that the model is only as good as modeling zero bed level change. However, this number has to be reconsidered giving the fact that a lot of the barrier island is covered by vegetation, bayous and road pavements. Also, this method is generally applied for entire point clouds of measured and modeled bed levels, instead of selected transects. The XBeach model predicts on average a 0.10 m lower bed level than was measured from the LiDAR data. For the purpose of this research this result is deemed sufficient enough to test the different hybrid designs.

TABLE 5.3.1. SKILL AND THE BIAS OF THE MODEL VALIDATION

Skill	0.1732
Bias	-0.0818

APPENDIX E HYBRID DESIGNS DIMENSIONS

TABLE E.1.1. HYBRID DESIGNS PARAMETERS

Variant ID	seawall height	dune height	dune width	dune slope	beach width	Beach height	
1.1	4.4	-	-	-	Original	-	Pre-hybrid
1.2	7.8	-	-	-	Original	-	Extended seawall
2.1	5.8	5.9	10	1 : 6	90	-	
2.2	6.5	6.6	20	1 : 5.5	80	-	
2.3	6.5	6.6	30	1 : 5.5	70	-	
2.4	6.5	6.6	40	1 : 5.5	80	-	
2.5	6.5	6.6	20	1 : 8	65	-	
2.6	6.5	6.6	20	1 : 10	55	-	
2.7	6.5	6.6	20	1 : 3.5	90	-	
2.8	6.5	6.6	20	1 : 5.5	90	-	
2.9	6.5	6.6	20	1 : 5.5	110	-	
2.10	6.5	6.6	20	1 : 5.5	130	-	
2.11	6.5	6.6	10	1 : 5.5	110	-	
2.12	6.5	6.6	0	1 : 5.5	110	-	
2.13	6.5	6.6	10	1 : 3.5	110	-	
2.14	6.5	6.6	10	1 : 5.5	110	-	
2.15	6.5	6.6	20	1 : 5.5	110	-	
2.16	6.5	6.6	10	1 : 8	110	-	
2.17	6.5	6.6	40	1 : 3.5	110	-	
2.18	7.0	7.1	40	1 : 3.5	110	-	
2.19	7.5	7.6	20	1 : 3.5	110	-	
2.20	7.0	7.1	10	1 : 3.5	110	-	
2.21	7.5	7.6	60	1 : 3.5	130	-	
2.22	7.0	7.1	20	1 : 5.5	110	-	Dike core (1:5)
2.23	6.5	6.6	20	1 : 5	80	2.5	
2.24	6.5	6.6	10	1 : 3.5	95	2.5	
2.25	6.5	6.6	10	1 : 5.5	130	3.0	
2.26	6.5	6.6	20	1 : 6	150	3.5	
2.27	6.5	6.6	10	1 : 5.5	130	3.0	Dike core (1:5)
2.28	6.5	6.60	5	1 : 8	130	3.5	
2.29	6.5	6.60	5	1 : 8	110	3.0	beach berm 20 m
2.30	6.5	6.60	-	-	130	3.5	beach berm to SW
2.31	6.5	6.60	20	1 : 8	130	3.5	
2.32	6.5	6.6	30	1 : 5.5	90	-	
2.33	6.5	6.6	5	1 : 8	110	4.0	Dike core (1:5)

APPENDIX F INPUT FILES

F.1. PARAMS.TXT

```
%%%%%%%%%%%%%%%%%%%%%%%%%%%%%%%%%%%%%%%%%%%%%%%%%%%%%%%%%%%%%%%%%%%%%%%%%%%%%%%
%%% XBeach parameter settings input file
%%%
%%%
%%%
%%% date:     04-Nov-2016 01:05:56
%%%
%%% function: xb_write_params
%%%
%%%%%%%%%%%%%%%%%%%%%%%%%%%%%%%%%%%%%%%%%%%%%%%%%%%%%%%%%%%%%%%%%%%%%%%%%%%%%%%

%%% Physical processes %%%%%%%%%%%%%%%%%%%%%%%%%%%%%%%%%%%%%%%%%%%%%%%%%%%%%%%%

-

%%% Grid parameters %%%%%%%%%%%%%%%%%%%%%%%%%%%%%%%%%%%%%%%%%%%%%%%%%%%%%%%%%%%

depfile      = var2.17_bed.dep
posdwn       = 0
nx           = 634
ny           = 413
alfa         = 0
vardx        = 1
xfile        = var2.17_x.grd
yfile        = var2.17_y.grd
thetamin     = -90
thetamax     = 90
dtheta       = 15
thetanaut    = 0

%%% Time management %%%%%%%%%%%%%%%%%%%%%%%%%%%%%%%%%%%%%%%%%%%%%%%%%%%%%%%%%%

tstart       = 100
tstop        = 324000
tintp        = 60
tintg        = 1200
CFL          = 0.7

%%% Wave breaking parameters %%%%%%%%%%%%%%%%%%%%%%%%%%%%%%%%%%%%%%%%%%%%%%%%%%

break        = baldock
gamma        = 0.7
n            = 10
```

```
%%% Wave boundary condition parameters %%%%%%%%%%%%%%%%%%%%%%%%%%%%%%%%%%%%

instat       = stat_table
bcfile       = 100waves.txt
rt           = 324000
dtbc         = 1

%%% Flow parameters %%%%%%%%%%%%%%%%%%%%%%%%%%%%%%%%%%%%%%%%%%%%%%%%%%%%%%%

C            = 55

%%% Flow boundary condition %%%%%%%%%%%%%%%%%%%%%%%%%%%%%%%%%%%%%%%%%%%%%%

front        = abs_2d
back         = abs_2d

%%% Tide boundary conditions %%%%%%%%%%%%%%%%%%%%%%%%%%%%%%%%%%%%%%%%%%%%%

zs0file      = 100tide.txt
tideloc      = 2
paulrevere   = 0

%%% Limiters %%%%%%%%%%%%%%%%%%%%%%%%%%%%%%%%%%%%%%%%%%%%%%%%%%%%%%%%%%%%%

gammax

%%% Sediment transport parameters %%%%%%%%%%%%%%%%%%%%%%%%%%%%%%%%%%%%%%%%

rhos         = 2650
D50          = 0.000150
D90          = 0.000187
struct       = 1
ne_layer     = var2.17_nebed.dep

%%% Morphology parameters %%%%%%%%%%%%%%%%%%%%%%%%%%%%%%%%%%%%%%%%%%%%%%%%

morfac       = 10
morstart     = 3600

%%% MPI Parameters %%%%%%%%%%%%%%%%%%%%%%%%%%%%%%%%%%%%%%%%%%%%%%%%%%%%%%%

mpiboundary     = x
```

```
%%% Output variables %%%%%%%%%%%%%%%%%%%%%%%%%%%%%%%%%%%%%%%%%%%%%%%%%%%%%%%%%%%%

outputformat = netcdf
tunits       = seconds since 2016-12-01 +0
nglobalvar   = 14
H
hh
zs
zb
u
DR
D
Dc
E
Fx
Subg
Susg
Sutot
runup
```